GEOLOGICAL SURVEY OF CANADA
COMMISSION GÉOLOGIQUE DU CANADA

## CURRENT RESEARCH 1996-B
# INTERIOR PLAINS AND ARCTIC CANADA

## RECHERCHES EN COURS 1996-B
# PLAINES INTÉRIEURES ET RÉGION ARCTIQUE DU CANADA

**1996**

Natural Resources
Canada

Ressources naturelles
Canada

Canada

## NOTICE TO LIBRARIANS AND INDEXERS

The Geological Survey's Current Research series contains many reports comparable in scope and subject matter to those appearing in scientific journals and other serials. Most contributions to Current Research include an abstract and bibliographic citation. It is hoped that these will assist you in cataloguing and indexing these reports and that this will result in a still wider dissemination of the results of the Geological Survey's research activities.

## AVIS AUX BIBLIOTHÉCAIRES ET PRÉPARATEURS D'INDEX

La série Recherches en cours de la Commission géologique contient plusieurs rapports dont la portée et la nature sont comparables à ceux qui paraissent dans les revues scientifiques et autres périodiques. La plupart des articles publiés dans Recherches en cours sont accompagnés d'un résumé et d'une bibliographie, ce qui vous permettra, on l'espère, de cataloguer et d'indexer ces rapports, d'où une meilleure diffusion des résultats de recherche de la Commission géologique.

GEOLOGICAL SURVEY OF CANADA
COMMISSION GÉOLOGIQUE DU CANADA

# CURRENT RESEARCH 1996-B

# INTERIOR PLAINS AND ARCTIC CANADA

# RECHERCHES EN COURS 1996-B

# PLAINES INTÉRIEURES ET RÉGION ARCTIQUE DU CANADA

## 1996

**Cover description**

Brecciated crinoidal and petroliferous dolowackestone of the lower Blue Fiord Formation (Emsian) with vein and replacement yellow sphalerite, calcite, dolomite, lesser marcasite, galena, and migrated bitumen. The sample was collected in 1995 during regional scale bedrock mapping by the Geological Survey of Canada on coastal southeastern Bathurst Island. This area features several previously undocumented Mississippi Valley-type lead-zinc showings that are described in a paper by J.C. Harrison and T. de Freitas, this volume. ISPG 4522-19

Dolowackestone à crinoïdes bréchifié, contenant du pétrole (partie inférieure de la Formation de Blue Fiord de l'Emsien); on y observe, sous forme de filons et d'amas de remplacement, de la sphalérite jaune, de la calcite et de la dolomite, de même que, en moindres quantités, de la marcasite, de la galène et du bitume migré. La roche a été échantillonnée en 1995, dans le cadre de travaux de cartographie régionale du substratum menés par la Commission géologique du Canada sur la côte sud-est de l'île Bathurst. Dans cette région, il existe plusieurs indices de plomb-zinc de type Mississippi-Valley, lesquels indices n'ont jamais fait l'objet de publications et sont décrits dans l'article de J.C. Harrison et de T. de Freitas du présent volume de «Recherches en cours». (ISPG 4522-19)

## Separates

A limited number of separates of the papers that appear in this volume are available by direct request to the individual authors. The addresses of the Geological Survey of Canada offices follow:

Geological Survey of Canada
601 Booth Street
OTTAWA, Ontario
K1A 0E8
(FAX: 613-996-9990)

Geological Survey of Canada (Calgary)
3303-33rd Street N.W.
CALGARY, Alberta
T2L 2A7
(FAX: 403-292-5377)

Geological Survey of Canada (Victoria)
100 West Pender Street
VANCOUVER, B.C.
V6B 1R8
(FAX: 604-666-1124)

Geological Survey of Canada (Victoria)
P.O. Box 6000
9860 Saanich Road
SIDNEY, B.C.
V8L 4B2
(Fax: 604-363-6565)

Geological Survey of Canada (Atlantic)
Bedford Institute of Oceanography
P.O. Box 1006
DARTMOUTH, N.S.
B2Y 4A2
(FAX: 902-426-2256)

Quebec Geoscience Centre/INRS
2535, boulevard Laurier
C.P. 7500
Sainte-Foy (Québec)
G1V 4C7
(FAX: 418-654-2615)

## Tirés à part

On peut obtenir un nombre limité de «tirés à part» des articles qui paraissent dans cette publication en s'adressant directement à chaque auteur. Les adresses des différents bureaux de la Commission géologique du Canada sont les suivantes :

Commission géologique du Canada
601, rue Booth
OTTAWA, Ontario
K1A 0E8
(facsimilé : 613-996-9990)

Commission géologique du Canada (Calgary)
3303-33rd St. N.W.,
CALGARY, Alberta
T2L 2A7
(facsimilé : 403-292-5377)

Commission géologique du Canada (Victoria)
100 West Pender Street
VANCOUVER, British Columbia
V6B 1R8
(facsimilé : 604-666-1124)

Commission géologique du Canada (Victoria)
P.O. Box 6000
9860 Saanich Road
SIDNEY, British Columbia
V8L 4B2
(facsimilé : 604-363-6565)

Commission géologique du Canada (Atlantique)
Institut océanographique Bedford
P.O. Box 1006
DARTMOUTH, Nova Scotia
B2Y 4A2
(facsimilé : 418-654-2615)

Centre géoscientifique de Québec/INRS
2535, boulevard Laurier
C.P. 7500
Sainte-Foy (Québec)
G1V 4C7

# CONTENTS

# Deformation history of the Moose Mountain structure, southwestern Alberta, based on mesostructures: a progress report

S. Feinstein[1], Y. Eyal[1], and J.S. Bell
GSC Calgary, Calgary

**Abstract:** In July 1995, we carried out a field study of mesostructures in the thrust-faulted Moose Mountain structure of the southern Canadian Rocky Mountains. Small-scale structural features were measured at 16 sites. Reported here are preliminary analyses and results from two sites that encompass 84 measurements of fault plane striations, veins, and fold axes. Preliminary analyses suggest that these mesostructures originated in two different paleostress regimes: in one, $S_{Hmax}$ was oriented approximately north-south; in the other, $S_{Hmax}$ was oriented approximately northeast-southwest. The latter regime is genetically compatible with the large-scale geometry of the Moose Mountain structure and with regional thrust fault networks; the former regime is discordant with such structures. The timing of the two inferred events has not yet been determined, nor have we addressed their implications for the overall kinematic evolution of the area.

**Résumé :** En juillet 1995, les mésostructures observées dans la structure de Moose Mountain de la partie sud des Rocheuses canadiennes ont fait l'objet de travaux sur le terrain. Les structures à petite échelle ont été mesurées à 16 sites. Sont présentées ici les analyses et les résultats préliminaires de 84 mesures de stries de plans de faille, de filons et d'axes de pli prises à deux sites. Selon les analyses, ces mésostructures dérivent de deux régimes différents de paléocontraintes : dans l'un, $S_{Hmax}$ était à peu près d'orientation nord-sud; dans l'autre, $S_{Hmax}$ était plutôt d'orientation nord-est-sud-ouest. Ce dernier régime est génétiquement compatible avec la géométrie à grande échelle de la structure de Moose Mountain et avec les réseaux de failles de chevauchement à l'échelle régionale; le premier régime est cependant discordant par rapport à ces structures. La chronologie de ces deux événements, établie par inférence, n'a pas encore été déterminée, non plus que leurs répercussions sur l'évolution cinématique globale de la région.

---

[1] Department of Geology, Ben Gurion University of the Negev, Beer Sheva 84105, Israel

## PURPOSE OF STUDY

This reconnaissance study of mesostructures in rocks exposed in the core and flanks of the Moose Mountain structure was designed to determine whether this type of analysis would help document, in detail, the kinematic evolution of the structure. Like many such features in the Rocky Mountain Foothills west of Calgary, the axis of the Moose Mountain structure trends northwest, parallel to the surface traces of associated and adjacent thrust faults. There is no doubt that the large scale structure is due to a major component of lateral compression being directed approximately perpendicular to the axis of the anticlinal structure. However, its kinematic history has not been documented in detail; we do not know what discrete tectonic events the rocks may have experienced or, indeed, whether their final compressional shortening occurred obliquely or normal to the present structural axis. We hoped that the analysis of "small scale" mesostructures would throw light on these matters, and that reconnaissance fieldwork in the Moose Mountain area would show whether more extensive regional mesostructural studies are likely to be productive.

## LOCATION AND GEOLOGICAL SETTING

The Moose Mountain structure is located some 50 km west-southwest of Calgary in the foothills of the Rocky Mountains of western Canada. At the surface, it outcrops as a faulted anticline rimmed by Mesozoic clastic rocks and cored by Paleozoic carbonates (McMechan, 1995). Exploration and production wells drilled on and around the structure have shown that what appears to be a relatively simple faulted anticline at ground level is actually a complexly faulted anticline, cored and uplifted by an imbricate stack of thrust sheets (Jones, 1971; Gordy et al., 1975a). As Figure 1 illustrates, the Moose Mountain structure has a northeastern vergence and is an integral part of the overthrust terrane that fronts the Western Cordillera. It is located in the westernmost

part of the Foothills Belt, immediately east of the McConnell Thrust, which defines the eastern limit of the Front Ranges of the Rocky Mountains (Fig. 1).

## FIELD MEASUREMENTS AND DATA PROCESSING

A general review of the data gathering and analytical techniques used in this study is given by Eyal and Reches (1983) and Eyal and Ron (1995). We measured the dips and strikes of the planes of mesofaults and veins, and the trends and plunges of fold axes and of striations on fault planes. The mesofaults are features of outcrop scale or smaller and the offsets on most of them range in the order of millimetres to tens of centimetres. Their faces are marked by striae which demonstrate that displacement has occurred. The sense of fault slip was determined in the field from striation plunges and secondary mineralization within small pull-apart cavities and/or slickolites associated with fault-plane striations and/or stratigraphic offsets (Fig. 2). Furthermore, crosscutting inter-relationships between mesostructures were documented where possible to determine the relative timing of different events.

The data for each site were classified into distinct groups based on fault dip, fault strike, and the sense of displacement. Faults were classified in two stages. First of all, the sense of slip was noted for those fault planes where this was readily apparent, and groups were defined for faults with common slip vectors. Next, faults for which a sense of displacement could not be determined were assigned to a specific group on the basis of similarity of orientations, on the assumption that faults with similar strikes and striation trends most probably form a natural population. At site 8, the sense of slip was directly determined from field observation for 11 of the 19 right-lateral faults, and for 14 of the 21 left-lateral faults.

The maximum and minimum horizontal stress directions ($S_{Hmax}$ and $S_{Hmin}$ respectively) for each locality were inferred from the mean strike of the various groups of a site, their type,
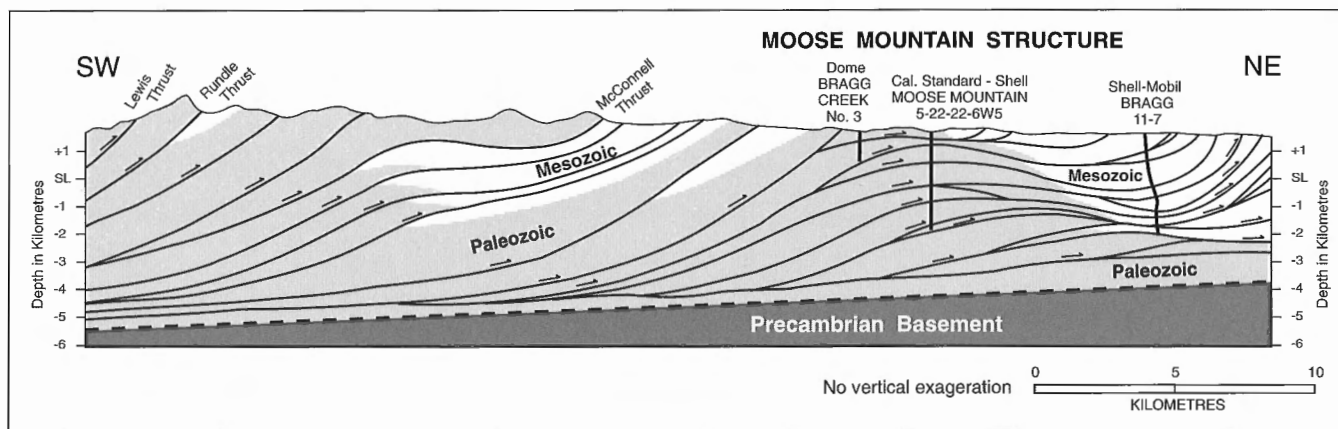


**Figure 1.** *Regional cross-section showing the relationship of the Moose Mountain structure to Rocky Mountain and Foothills thrust faulting (after Gordy et al., 1975b). White units are Mesozoic, light grey units are Paleozoic, and the dark grey corresponds to Precambrian basement.*

and the mean striation trend. For strike-slip faults, we assumed that $S_{Hmax}$ would be oriented at an acute angle of 30° to the fault strike, provided that the inferred orientation was consistent with the observed slip. For normal faults, we assumed that $S_{Hmin}$ would be perpendicular to the fault strike and parallel to the trend of folding.

We used Allmendinger's (1992) stereonet program for data processing and determining the paleostress axes. The results were compared and tested for internal consistency.

## RESULTS

In the present study we measured more than 900 mesostructures from 16 sites located across the Moose Mountain structure (Fig. 3). The sites studied are located at a variety of stratigraphic levels and their spatial and vertical distribution provide good three-dimensional control within the upper part of the Moose Mountain structure. We present here a preliminary assessment of data from two sites. At site 7, we recovered mesostructural data from a roadcut exposing Lower Cretaceous Blairmore Group clastics on the eastern flank of the Moose Mountain structure (Fig. 3). At site 8, measurements were made along the upper part of the Canyon Creek in Middle Paleozoic carbonates in the core of the structure.

The data obtained for sites 7 and 8 are summarized in Table 1 and on Figure 4. They comprise measurements from 50 fault planes, 26 veins, and 18 fold axes. Figure 4 presents a stereographic projection of the measurements obtained for



***Figure 2.*** *Striated surface of a microfault (to left of quarter). Striations are approximately parallel to bedding and the displacement is right-lateral according to the calcite infilling.*

sites 8 (a-e) and 7 (f). We plotted poles of planes as points on the stereonets so as to achieve a uniform presentation format for a variety of different planar features (e.g. faults, veins).

### Site 7

Figure 4f presents a stereographic projection of the plunge axes obtained for small-scale folds (18) in the Blairmore Group sandstone, shale, and coal interlayers in site 7. The mean dip and plunge azimuth of the fold axes is 12°/136°, so they are parallel to the traces of thrust faults and the axes of larger folds (Fig. 3).

### Site 8

Figure 4a shows a plot of poles for all fault planes (50) measured in site 8. This plot shows a relatively high angle dip for most of the faults and a triaxial cluster of their dip directions. Figure 4b presents measurements obtained for striations on fault planes. Examination of the sense of displacement along the faults reveals that each trend of the triaxial cluster in Figure 4a represents a different category of faulting: left-lateral (Fig. 4c), right-lateral (Fig. 4d), and normal faults. The great circles in Figures 4c, d, and e represent the mean fault or vein planes; the asterisks represent the mean trend of striations and the arrows indicate sense of displacement. Normal slip could be clearly defined only for a few faults (4), and therefore no specific plot is presented here for the normal faults shown in Figure 4a. The distribution of striations compared to fault orientation (cf. Fig. 4b with Fig. 4a, c, d) indicates that the majority of them were formed by lateral rather than by normal slip. The left-lateral faults strike northeast to east-northeast and their mean trend is 71°/144° (dip/dip trend); the right-lateral faults strike northwest to north-northwest and their mean trend is 72°/052°; and the normal faults strike north. The veins strike northeast to east-northeast and their mean trend is 77°/146°.

## DISCUSSION

The small-scale folds at site 7 reflect the large-scale structures in the area (Fig. 3), and imply a northeast-southwest compression axis, which is not new kinematic information. On the other hand, the mesostructural data at site 8 allow us to make inferences that are not obvious from the large-scale structures. These measurements represent a coherent data set for two populations of fault planes and senses of slip. Moreover, the vein orientations are consistent with one population.

The mesostructures recorded in sites 8 and 7 (Table 1; Fig. 4) delineate two distinct paleostress fields. The general southeast trend of the fold axes (Fig. 4f) is diagnostic of a paleostress field in which $S_{Hmax}$ is oriented northeast-southwest. This $S_{Hmax}$ orientation is also consistent with the strike of the veins (Fig. 4e). However, the northeast-trending faults with left-lateral offsets and the northwest-trending faults with right-lateral offsets favour a paleostress field where $S_{Hmax}$ is oriented north-south to north-northeast-south-southwest (Fig. 4c, d).
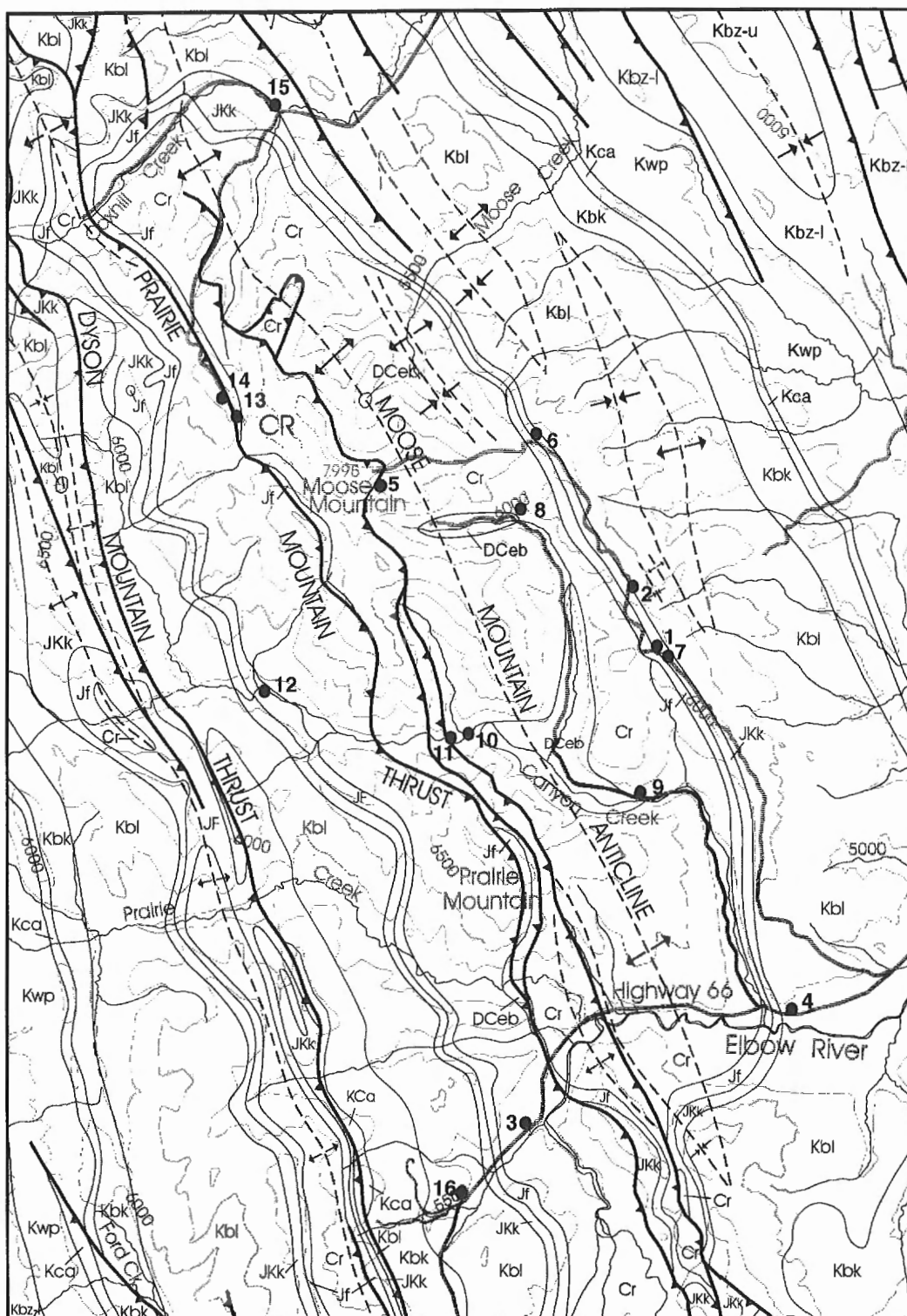
**Figure 3.** *Geological map of the Moose Mountain structure (after McMechan, 1995) showing locations of 16 sites where mesostructural features were identified and measured. Geological symbols correspond to those on GSC Map 1865A (McMechan, 1995). Formations are identified as follows: Kbz-u, Brazeau Formation, upper part; Kbz-l, Brazeau Formation, lower part; Kwp, Wapiabi Formation; Kca, Cardium Formation; Kbk, Blackstone Formation; Kbl, Cadomin, Gladstone, Beaver Mines, and Mill Creek formations (undivided); JKk, Kootenay Group; Jf, Fernie Formation; Cr, Rundle Group; DCeb, Exshaw and Banff formations. Prefixes: K, Cretaceous; J, Jurassic; C, Carboniferous; D, Devonian.*

**Table 1.** Data summary for mesostructural measurements in sites 7 and 8. N/n is the number of measurements taken versus the number of readings used in calculations. Column H, ∝95, signifies the 95% confidence level: the upper number is the apical angle of the cone of confidence for the attitudes of the faults; the lower number is the apical angle of the cone of confidence for the plunges of the striations. Measurements listed in columns F, G, and H are in degrees.

| A | B | C | D | E | F | G | H | I | J | K |
|---|---|---|---|---|---|---|---|---|---|---|
| Site | N/n | Group | No. of readings | Structure type | Mean plane dip | Mean striae/axes plunge | ∝95 | Estimated paleo $S_{Hmax}$ | Estimated paleo $S_{Hmax}$ | Rock Unit/Age |
| 7 | 18/18 | a | 18 | Fold axes | | 12/136 | 9 | NE-SW | NW-SE | Blairmore Fm./ Cretaceous |
| 8 | 77/66 | a | 21 21 | left-lateral fault | 71/144 | 20/334 | 9 12 | N-S to NNE-SSW | E-W to ESE-WNW | Rundle Group/ Carboniferous |
| | | b | 19 19 | right-lateral fault | 72/052 | 21/334 | 11 13 | N-S to NNE-SSW | E-W to ESE-WNW | |
| | | c | 26 | veins | 77/146 | | 7 | NW-SE to NNW-SSE | NW-SE to NNW-SSE | |



**(a)** Site 8 · All Poles N = 50
**(b)** Site 8 · All Striations N = 50
**(c)** Site 8 · Left Lateral Faults N = 21
**(d)** Site 8 · Right Lateral Faults N = 19
**(e)** Site 8 · Veins N = 26
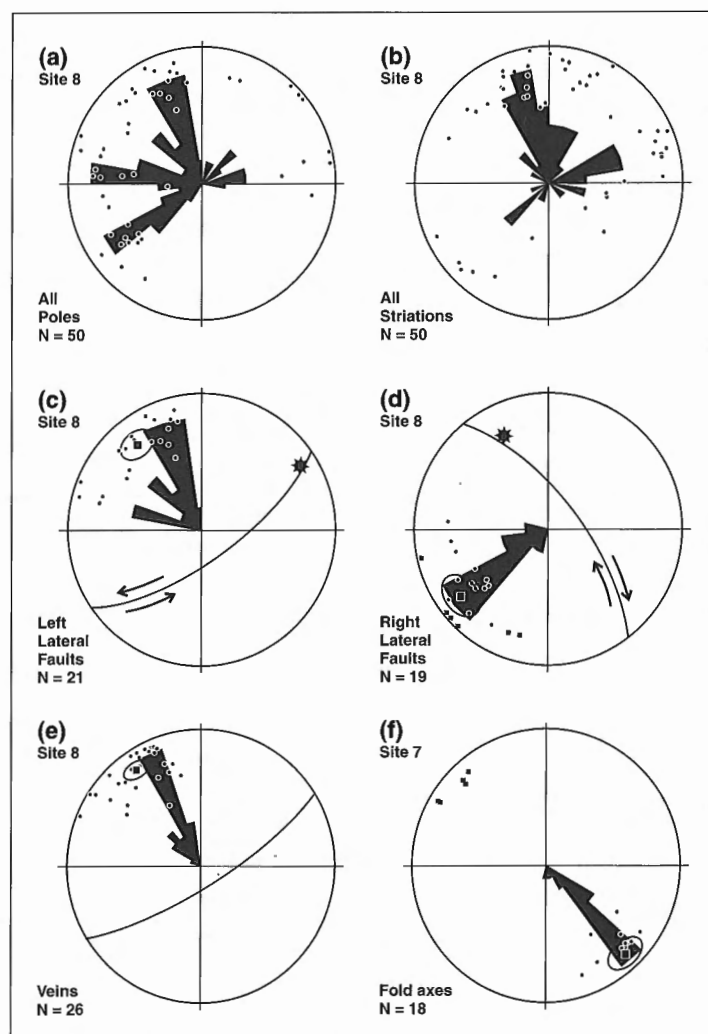**(f)** Site 7 · Fold axes N = 18

*Figure 4.*

*Stereographic projections of mesostructural data, as explained in the text. Site 8: **a)** Poles for all fault-planes. **b)** All striations measured. **c)** Poles for right-lateral faults. **d)** Poles for left-lateral faults. **e)** Poles for calcite veins; Site 7: **f)** Plunges of fold axes.*

The apparent impression from Figure 4 is that the dominant paleostress field is that in which $S_{Hmax}$ is oriented north-south. However, it should be remembered that the displayed data represent only a small fraction of the total measurements taken during this study, so such a conclusion is premature. The northeast-southwest $S_{Hmax}$ paleostress orientation is perpendicular to the axis of the Moose Mountain structure and with the regional thrust belt (Ower, 1975; McMechan and Thompson, 1989; Monger, 1989; McMechan, 1995). It is therefore pertinent to question why only the veins record a paleostress field at site 8 that is concordant with the large-scale deformation, whereas the majority of the microfaults are not related to the paleostress field under which the Moose Mountain structure was deformed. The mesostructures reported for site 7 record the northeast-southwest $S_{Hmax}$, with no apparent indication of the north-south $S_{Hmax}$. However, this situation could be due to the fact that only a single class of mesostructures (fold axes) has so far been processed.

The north-south to north-northeast-south-southwest $S_{Hmax}$ paleostress orientation derived from the strike slip faults (Fig. 4c, d) is discordant to the main Rocky Mountain thrust and fold belt structural pattern and its delineation by the mesostructures was not anticipated. At this time, the significance of these data is not clear and future work will assess this as well as investigate possible relationships to dextral shear zones in the Canadian Cordillera (Price and Carmichael, 1986).

## ACKNOWLEDGMENTS

## REFERENCES

**Allmendinger, R.W.**
1992:   Stereonet 4.5 application program; Department of Geological Sciences, Cornell University, Ithaca, New York.
**Eyal, Y. and Reches, Z.**
1983:   Tectonic analysis of the Dead Sea Rift region since Late Cretaceous based on mesostructures; Tectonics, v. 2, p. 167-185.
**Eyal, Y. and Ron, H.**
1995:   Late Cenozoic crustal deformation of the north-central Basin and Range Province, Western U.S; Tectonophysics, v. 246, p. 211-224.
**Gordy, P.L., Frey, F.R., and Ollerenshaw, N.C.**
1975a:  Road log Calgary, Turner Valley, Jumping Pound, Seebe; in Structural Geology of the Foothills Between Savanna Creek and Panther River, S.W. Alberta, Canada, (ed.) H.J. Evers and J.E. Thorpe; Guidebook published by Canadian Society of Petroleum Geologists and Canadian Society of Exploration Geophysicists, Calgary, p. 37-61.
**Gordy, P.L., Stewart, G., and Frey, F.R.**
1975b:  Geological cross-section through the Foothills; in Structural Geology of the Foothills Between Savanna Creek and Panther River, S.W. Alberta, Canada, (ed.) H.J. Evers and J.E. Thorpe; Guidebook published by Canadian Society of Petroleum Geologists and Canadian Society of Exploration Geophysicists, Calgary, Plate 2.
**Jones, P.B.**
1971:   Folded faults and sequence of thrusting in Alberta Foothills; American Association of Petroleum Geologists Bulletin, v. 55, p. 292-306.
**McMechan, M.E.**
1995:   Geology, Rocky Mountain Foothills and Front Ranges in Kananaskis Country, Alberta; Geological Survey of Canada, Map 1865A, scale 1:100 000.
**McMechan, M.E. and Thompson, R.I.**
1989:   Structural style and history of the Rocky Mountain fold and thrust belt; in Western Canada Sedimentary Basins, (ed.) B. Ricketts; Canadian Society of Petroleum Geologists, Calgary, p. 47-71.
**Monger, J.W.H.**
1989:   Overview of Cordilleran Geology; in Western Canada Sedimentary Basins, (ed.) B. Ricketts; Canadian Society of Petroleum Geologists, Calgary, p. 9-32.
**Ower, J.**
1975:   The Moose Mountain structure, birth and death of folded fault play; in Structural Geology of the Foothills Between Savanna Creek and Panther River, S.W. Alberta, Canada, (ed.) H.J. Evers and J.E. Thorpe; Guidebook published by Canadian Society of Petroleum Geologists and Canadian Society of Exploration Geophysicists, Calgary, p. 22-29.
**Price, R.A. and Carmichael, D.M.**
1986:   Geometric test for Late Cretaceous-Paleogene intracontinental transform faulting in the Canadian Cordillera; Geology, v. 14, p. 468-471.

# Impacts of landsliding in the western Cypress Hills, Saskatchewan and Alberta[1]

## D.J. Sauchyn[2] and D.S. Lemmen
### Terrain Sciences Division, Calgary

**Abstract:** Landsliding on the Canadian prairies often produces downstream impacts on water quality, reservoir capacity, and fish habitat that represent more significant hazards than the destruction caused by the slide itself. Erosion measurements of Police Point landslide in the western Cypress Hills, which occurred in 1967 and remains highly unstable, document the importance of groundwater in controlling landslide activity and the futility of conventional remedial activities in limiting downstream impacts. Runoff from the landslide inputs large volumes of sediment to adjacent Battle Creek, with suspended sediment concentrations (up to 438 mg·L$^{-1}$)downstream of the landslide being two to three orders of magnitude greater than occur upstream.

Chronological data are available for only a few sites, all indicting landslide activity in the Late Holocene. Higher regional groundwater tables associated with wetter and cooler climates at this time may have provided antecedent conditions promoting reactivation of slopes in response to extreme hydroclimatic events.

**Résumé :** Dans les Prairies canadiennes, les glissements de terrain ont souvent des répercussions en aval, soit sur la qualité de l'eau, la capacité des réservoirs et les habitats des poissons, répercussions qui représentent des dangers plus significatifs que la destruction causée par le glissement lui-même. Des mesures de l'érosion au site du glissement de la pointe Police, survenu en 1967 dans l'ouest des collines Cypress et dont la surface est encore très instable, mettent en évidence l'importance des eaux souterraines dans la mitigation des glissements et l'inefficacité des mesures de correction classiques pour limiter les répercussions en aval. Les eaux de ruissellement provenant du glissement entraînent de grandes quantités de sédiments vers le ruisseau Battle adjacent, comme en témoignent les concentrations de sédiments en suspension en aval du glissement de terrain (atteignant 438 mg·L$^{-1}$), qui sont de dix à cent fois plus importantes qu'en amont.

Il n'existe des données chronologiques que pour quelques sites et toutes associent le glissement à l'Holocène tardif. La remontée des nappes d'eau souterraine régionales causée par des climats plus humides et plus froids à cette époque ont pu contribuer à la mise en place des conditions favorisant la réactivation des versants en réponse à des événements hydroclimatiques extrêmes.

---

## INTRODUCTION

Evidence of landsliding is ubiquitous along the numerous meltwater channels and incised river valleys on the southern Canadian prairies. The geological setting and geomorphic history of these valleys strongly favours instability in both the hillslope and fluvial systems. Channel incision was rapid and often catastrophic (e.g. Kehew and Lord, 1986), eroding through unconsolidated Pleistocene deposits (dominantly till and glaciolacustine sediments) and Upper Cretaceous sediments of inherently low shear strength. Erosion also produced stress relief in the over-consolidated Cretaceous clays, resulting in local deformation and further loss of strength. Slope response to the resultant instability was landsliding, the dominant process of valley widening on the prairies (Thomson and Morgenstern, 1978). For example, the Frenchman River valley (Fig. 1) is 80 m less deep and almost three times wider than the original meltwater channel, with the basal valley fill largely composed of landslide debris (Christiansen and Sauer, 1988).

Landsliding impacts not only hillslopes but also adjacent fluvial systems. Along through-flowing rivers, such as the South Saskatchewan and its major tributaries (the Oldman, Bow, and Red Deer rivers; Fig. 1), fluvial erosion of the basal slope is the most common trigger of landsliding (e.g. Thomson and Morgenstern, 1977). These rivers, fed by glaciers and snowfields of the Rocky Mountains, have the capacity to transport the sediment delivered from valley sides and low-order watersheds. In contrast, landslides along the numerous valleys occupied by underfit streams, with a limited capacity to undermine valley sides, more likely relate to hydroclimatic conditions than stream action. Such underfit streams that head in uplands on the plains (e.g. Frenchman River and Swift Current Creek, Fig. 1), have a limited capacity to transport large influxes of sediment. Landslides adjacent to these streams can have significant impacts on the fluvial system both up- and down-stream of the slide lasting for many years (decades to millennia). Despite the fact that high quality surface water is a scarce resource in the southern prairies, the impact of landslides on water quality has been little studied.

This paper focuses on a recent landslide in the western Cypress Hills and its impact upon the adjacent underfit stream. Police Point landslide (>1.5 Mm$^3$, Fig. 1 and 2) occurred in May 1967, after 1.5 m of snow fell and then melted within a few days (Janz and Treffry, 1968). This modern analogue along with absolute and relative chronological data of past landslide activity provide insight into the late Holocene evolution of the valley. This study is part of the
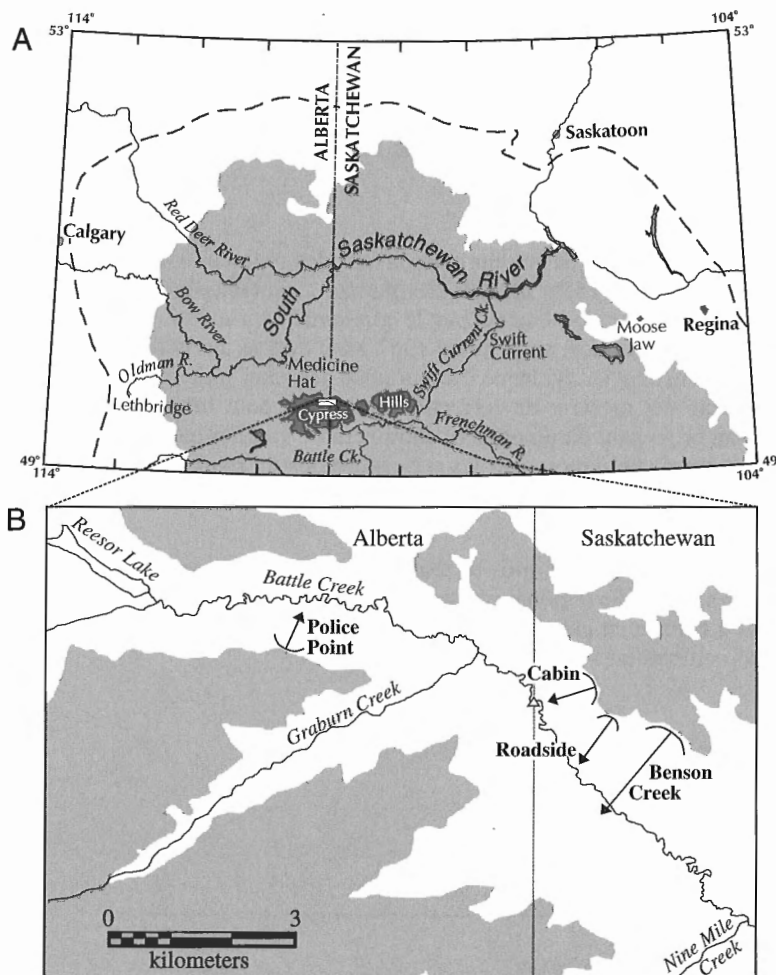


**Figure 1.**

*A) Regional location map showing west, central, and east blocks of the Cypress Hills (shaded dark) within the Brown Soil Zone (shaded light), considered the core of the Palliser Triangle. Dashed line denotes "Triangle" as originally defined by Capt. Palliser. B) Study area within upper Battle Creek basin. Upper plateau surfaces are shaded, local relief is about 200 m. Landslides are ubiquitous along the steep valley walls and only those discussed in text are depicted. Open triangle shows location of Water Survey of Canada hydrometric station.*

Palliser Triangle IRMA (Lemmen et al., 1993; Fig. 1), and compliments research on regional paleoclimatic reconstruction (e.g. Vance and Last, 1994) and other Holocene geomorphic systems (e.g. Wolfe et al., 1995).

## STUDY AREA AND APPROACH

The three blocks of the Cypress Hills are remnants of the late Tertiary erosion that lowered the bedrock surface of the northern Great Plains to its present level (Sauchyn, 1993). The upper surface of the West Block forms the Cypress Plain (Collier and Thom, 1918), rising from an elevation of 1310 m in Saskatchewan to 1465 m in Alberta, the highest point in southern Canada between the Appalachian and Rocky mountains. The oldest rocks that outcrop in the Cypress Hills region are Upper Cretaceous clay, silt, clay shale, and sand of the Bearpaw, Eastend, Whitemud, Battle, and Frenchman formations. These are overlain by a sequence of Tertiary sediments 85-145 m thick (Furnival, 1950), composed of the Paleocene Ravenscrag Formation (predominantly fine grained sandstone) and capped by sands, gravels, and conglomerate of the Eocene to Miocene Cypress Hills Formation (Leckie and Cheel, 1989). The highest surfaces of the hills were never glaciated, and only scattered glacial erratics, possibly ice-rafted, occur above 1250 m a.s.l. (Klassen, 1994; Vreeken, 1990). The absence of significant drift deposits allows rain and snowmelt to readily permeate the coarse sediments of the caprock, limiting the effectiveness of fluvial processes on the plateau but creating instability in the underlying Upper Cretaceous and Paleocene sediments (Sauchyn, 1993). Seeps and springs are common on the valley sides, particularly on landslide scarps. The Cypress Hills serve as a critical regional groundwater recharge area, strongly influencing surface water resources on the surrounding semiarid plains of southwestern Saskatchewan and southeastern Alberta. Therefore natural events in this region, as well as soil and water management practices, influence water quantity and quality for a large area.

The present study focuses on a 12 km section of the Battle Creek valley straddling the Alberta-Saskatchewan boundary, between Reesor Lake in Alberta and Nine Mile Creek in Saskatchewan (Fig. 1). The creek occupies a preglacial valley up to 4 km wide and 200 m deep. The valley floor drops about 45 m over the 12 km. The area was chosen because it includes the recent Police Point landslide, a hydrometric station at the Alberta-Saskatchewan border, and the availability of proxy paleoclimatic data from trees and permanent lakes (e.g. Sauchyn and Sauchyn, 1991). Fieldwork consisted of i) erosion measurements on the Police Point landslide, ii) measurement of suspended sediments loads and hydraulic geometry of Battle Creek, and iii) excavation of dormant landslides to add to existing data on regional landsliding chronology.

## EROSION MEASUREMENTS

The Police Point landslide remains largely unvegetated 28 years after initial failure, and is a major source of suspended sediment to Battle Creek (Fig. 2 and 3). Erosion



*Figure 2. Stereo-pair of Police Point landslide, south side of Battle Creek. 1) upper plateau surface; 2) upper scarp exposing Cypress Hills Formation; 3) rotated slump blocks; 4) gully erosion within Cretaceous sediments; and 5) sediment washed from landslide into the forest. Airphotos AFL W AS2343-249, 250. See Figure 3 for ground photographs.*

measurements on the lower slopes of the landslide was initiated to attempt to quantify present slope activity and sediment influx to the creek. On October 27, 1994, 101 erosion pins were installed along 10 transects oriented across the lower half of the landslide. The pins were driven to a depth of about one metre and resurveyed in early May, 1995, at which time an additional 24 pins were placed in newly formed gullies. All pins were then measured after each of nine storms in May-June (see below concerning lost pins). The rate of sediment input to Battle Creek was estimated in five gullies emanating from the landslide during a rainstorm on June 4.

Net erosion occurred at 78% of the pins, net deposition at 16%. The maximum erosion at one pin in response to a single storm event was 49 cm, maximum deposition was 12 cm. The average change in surface elevation at each pin along the transects was -2.9 cm, contrasted with an average of -19.3 cm in less than two months for each of the 24 pins located in gullies (negative value indicates erosion). Ten pins could not be located during the survey of 28 June, three more were lost by 23 September. The lost pins were either buried by debris flows or undermined by more than 1 m of erosion. In either case, these observations qualitatively illustrate the unstable
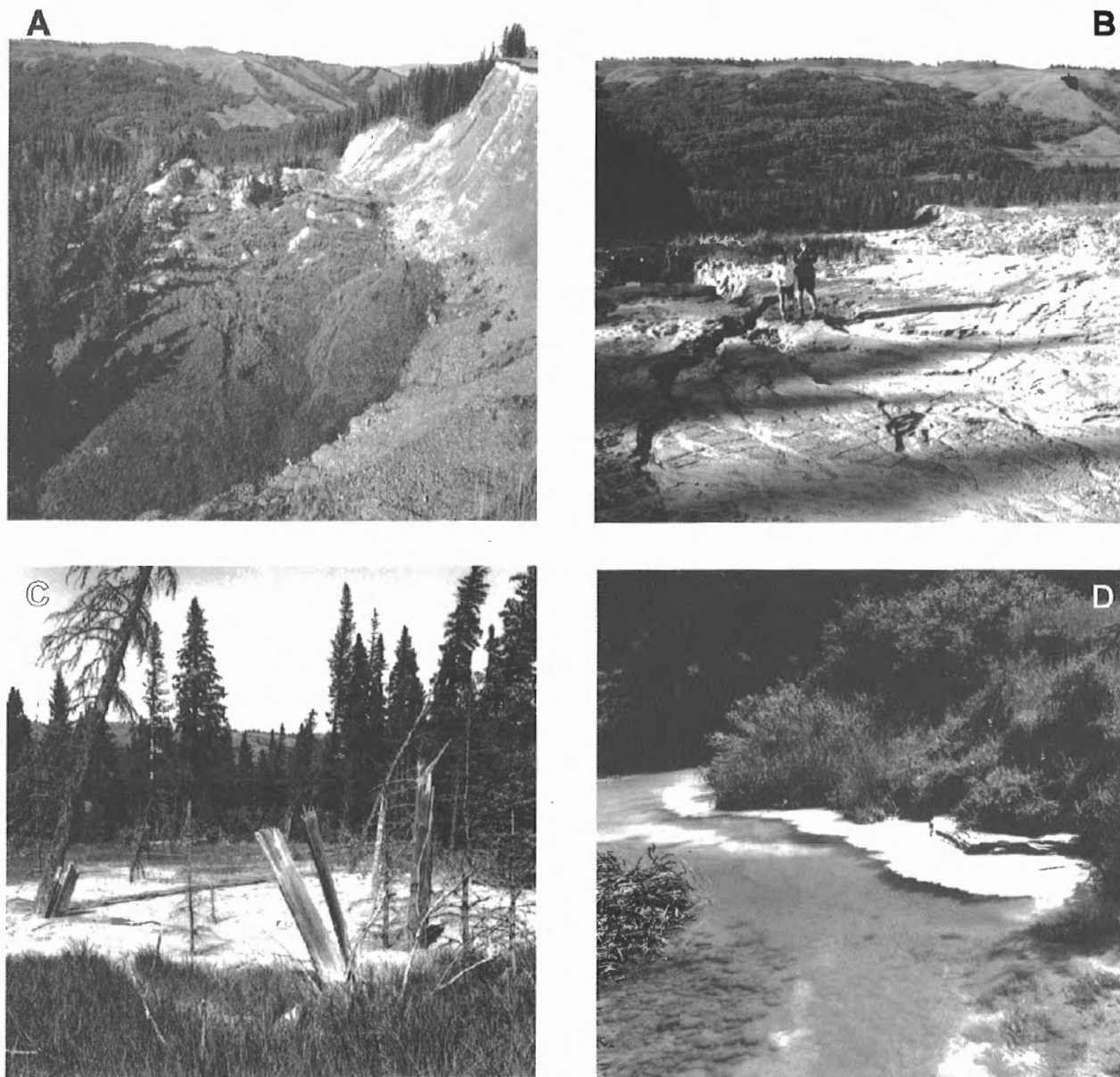


**Figure 3. A)** *Upper scarp of Police Point landslide exposing the Cypress Hills Formation. Note rotated slump blocks below the scarp.* **B)** *Gully erosion and tensional failure of the Cretaceous sediments exposed on the lower part of the landslide.* **C)** *Sediment-filled depression between the landslide and Battle Creek.* **D)** *Highly turbid sediment plume entering Battle Creek downslope of the landslide following major rain storm.*

nature of the landslide surface. Only one pin was found to be on a stable surface, with neither erosion or deposition observed at any time during the season. These observations also indicate that gully erosion is the dominant process of sediment loss on the landslide, as opposed to sheet erosion by overland flow (cf. Clements et al., 1970). Channelized runoff from the landslide into Battle Creek during storm events was extremely turbid, with peak suspended sediment concentrations exceeding $1.9 \times 10^5$ mg·L$^{-1}$. Suspended sediment load entering the creek via the five gullies is estimated to have been almost 1900 g·s$^{-1}$. Although significant erosion occurred during every rainstorm, each was unique in terms of effects on the landslide according to factors such as antecedent soil moisture and precipitation intensity. Considerably more monitoring of weather, erosion, and sediment transport is required to establish relationships among these parameters and hydroclimatic controls on erosion, and sediment production.

## STREAM DATA

Concurrent with erosion measurements on Police Point landslide (May-June, 1995), suspended sediment transport in Battle Creek was monitored using a DH-48 depth integrating sampler. Sixty-three water samples were collected during runoff events at the Water Survey of Canada (WSC) provincial boundary station (Fig. 1), with another 17 samples collected farther upstream. Suspended and dissolved sediment concentrations were determined by the WSC Sediment Laboratory.

Minimum suspended sediment concentrations of 2 mg·L$^{-1}$ were measured on May 1 upstream of Police Point landslide near Reesor Lake. Maximum concentrations of 438 mg·L$^{-1}$ were measured at the Boundary station following peak discharge associated with runoff from the June 4 rainstorm (Fig. 4). In general, suspended sediment concentrations

downstream of the landslide were 1-2 orders of magnitude greater than above the landslide (near Reesor Lake). Peak values occur immediately downstream of the landslide, but these are still three orders of magnitude less than occur in the landslide runoff due to rapid dilution. Concentrations generally decrease downstream of the landslide, particularly downstream of Graburn Creek (Fig. 1). These observations quantitatively substantiate the significance of Police Point landslide as the overwhelming source of suspended sediments in the upper Battle Creek watershed. In contrast to suspended sediment concentration, dissolved sediment concentration shows little variability with either downstream position or discharge (Fig. 4), confirming the significance of groundwater in the geomorphology and hydrology of the Cypress Hills (Spence, 1993).

In addition to impacting water quality, landsliding can also have a profound impact upon the hydraulic geometry of streams, locally effecting rates of erosion and sediment transport. This is particularly true where a landslide blocks a valley, necessitating channel incision of the landslide dam and involving significant local adjustments of the stream longitudinal profile and plan geometry (Cruden et al., 1993). Benson Creek landslide (Fig. 1 and 5) exemplifies these impacts within the study area. This large slide moved across the floor of Battle Creek valley between ca. 1500 and 1700 BP (Sauchyn, 1990; Table 1). The longitudinal stream profile (Fig. 5B) demonstrates a relatively steep gradient and low sinuosity (Fig. 1) where Battle Creek has deeply incised the toe of the landslide. Immediately upvalley, a meandering Battle Creek is incised in a broad flat plain, interpreted as the bottom of a short-lived lake created when the landslide blocked the creek. Measurements of channel bankfull width and meander wavelength indicate that the hydraulic geometry is uncharacteristic of a third order stream with a mean annual discharge of 0.364 m$^3$·s$^{-1}$ (1975-1991). After almost two millennia of disequilibrium, Battle Creek is apparently still responding to Benson Creek landslide.
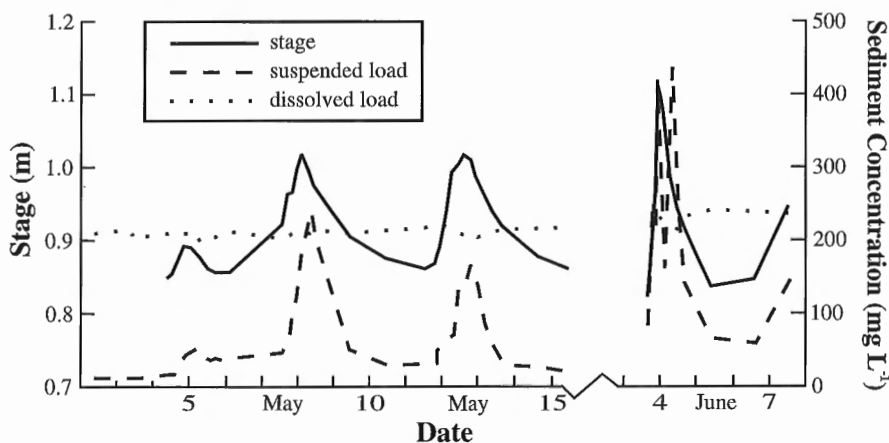


***Figure 4.*** *Stream flow characteristics for Battle Creek as measured at the provincial boundary hydrometric station (Fig. 1), May 2-15 and June 3-7, 1995. Note strong correlation between suspended sediment concentration and rainfall generated peak flows.*
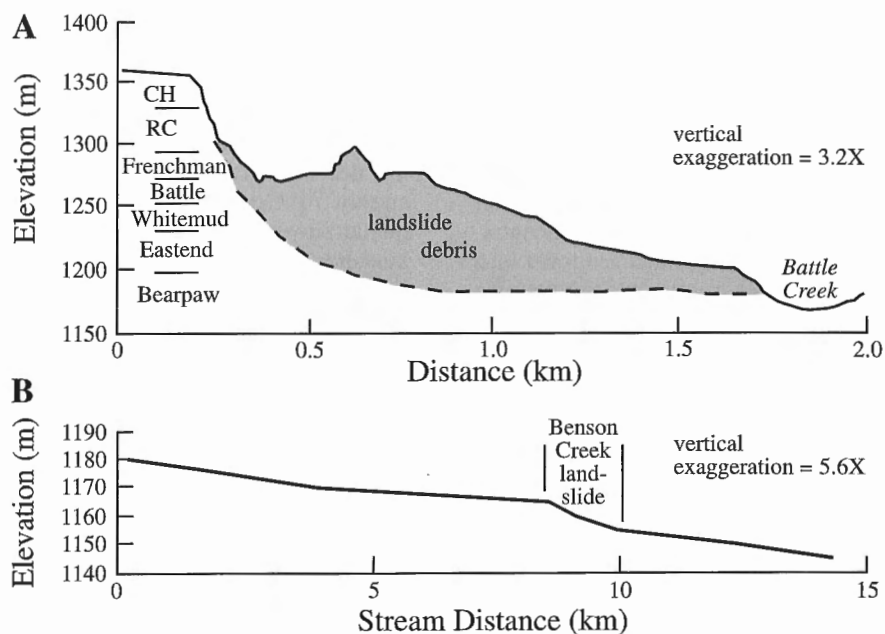
**Figure 5. A)** *Topographic and bedrock cross-section of Benson Creek landslide, running perpendicular to main axis of landslide as indicated by symbol on Figure 1. Formation abbreviations: CH = Cypress Hills and RC = Ravenscrag.* **B)** *Longitudinal stream profile of Battle Creek between Graburn and Nine Mile creeks (Fig. 1), showing the effect of Benson Creek landslide on the hydraulic geometry.*

**Table 1.** Absolute dating control on landslides from the west block of the Cypress Hill, Saskatchewan and Alberta.

| Site | Lab. No. | Material | Date[1] | Max. or Min.[2] | Stratigraphy | Lat. | Long. | Technique |
|------|----------|----------|---------|-----------------|--------------|------|-------|-----------|
| Police Point[3] | NA | NA | AD 1967 | NA | NA | 49°39.0' | 110°03.7' | Historic |
| Nine Mile | NA | tree rings | AD 1915 ± 3 years | Min | NA | 49°35.7' | 109°58.8' | Dendrochonology |
| Underdahl Ck.[3] | S-2631 | organic soil | 1235±100 | Min | base of depression fill on landslide surface | 49°32.0' | 109°55.0' | conventional $^{14}$C |
| Benson Creek | S-2907 | basal pond sediment | 1445±320 | Min | organic mud over slid Cretaceous bedrock | 49°38.0' | 109°58.3' | conventional $^{14}$C |
| | S-2772 | bone | 1745±85 | Max | alluvium under slid Cretaceous bedrock | 49°38.0' | 109°58.3' | conventional $^{14}$C |
| Green Lake[3] | S-2630 | organic soil | 1635±105 | Min | base of depression fill on landslide surface | 49°28.0' | 109°55.0' | conventional $^{14}$C |
| Cabin | TO-4479 | gastropod fragments | 2410±120 | Max | alluvium under slid Cretaceous bedrock | 49°38.5' | 109°59.8' | AMS |
| Roadside | TO-4480 | gastropod fragments | 2240±70 | Max | alluvium under slid Cretaceous bedrock | 49°38.0' | 109°59.0' | AMS |
| Harris Lake[3] | NA | NA | ca. 4000 | NA | NA | 49°40.0' | 109°55.0' | Estimate from lake record[4] |

NA - not applicable
1 - all dates BP unless otherwise indicated
2 - maximum or minimum age estimate on age of landslide
3 - relative age data for site included in Fig. 2.
4 - see Last and Sauchyn (1993) for details

## LANDSLIDE CHRONOLOGY

A backhoe was used to trench the toes of four landslides in the Battle Creek valley at the break in slope between the landslide debris and the adjacent valley floor. Sites were located away from the present creek or paleochannels, excluded reactivation by stream erosion as the origin of the trenched lobes. Trenching extended below the adjacent surface to uncover the contact between landslide deposits and underlying valley floor deposits. In section the alluvial deposits were dominantly silt and clay with local concentrations of sand. Dark organic-rich bands near the contact suggested formerly vegetated surfaces buried by landsliding, although at only one site was a well developed buried soil observed.

Two samples of buried valley floor deposits contained gastropod fragments suitable for radiocarbon dating by accelerator mass spectrometry. The dates, 2410 ± 120 BP (TO-4479) and 2240 ± 70 BP (TO-4480), represent maximum age estimates for Cabin and Roadside landslides respectively (Fig. 1, Table 1). The other samples were devoid of discrete identifiable macrofossils. Conventional radiocarbon dating of the bulk organics was not attempted given the sources of older carbon in the Cretaceous bedrock from which the local soil is derived.

These two new radiocarbon dates conform to the existing landslide chronology for the western Cypress Hills (Goulden and Sauchyn, 1986; Sauchyn, 1990, 1993). Absolute and/or relative ages are now available for 21 landslides in the region (Fig. 6, Table 1) and all fall within the Late Holocene. As landslide movement is progressive, showing multiple phases
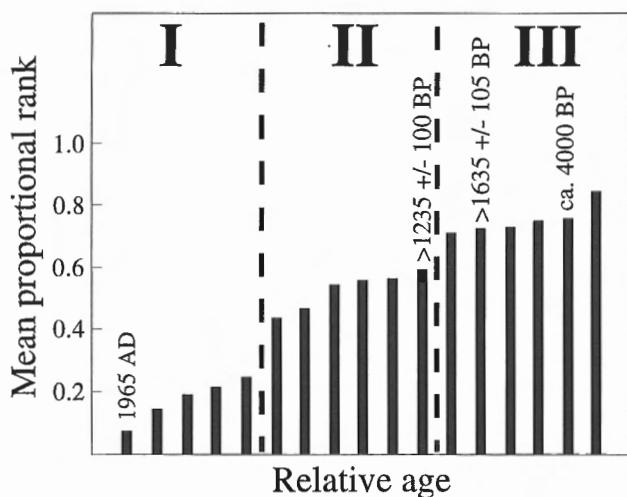


***Figure 6.*** *Relative ages of 17 landslides in the western Cypress Hills with corresponding absolute ages where available. Mean proportional rank refers to an index of relative age indicators; I, II, and III are distinct groups of landslides identified by cluster analysis (for details* see *Goulden and Sauchyn, 1986). Complete data on absolute dates is presented in Table 1.*

of activity, these dates simply document the most recent period of slope movement. Nonetheless they do suggest that the impacts imposed on Battle Creek at present by Police Point landslide are likely typical of late Holocene conditions.

## DISCUSSION

Police Point landslide illustrates the persistent impacts of a single high-magnitude event, providing a valuable analogue of both how past landslides have effected Battle Creek and how future landsliding will impact the adjacent watershed. The low residual strength and fine texture of the Cretaceous bedrock results in prolonged erosion and instability of landslides, inhibiting colonization of plants for years or decades. At Police Point there is no indication that rates of erosion and suspended sediment production have begun to decrease even after 28 years. Revegetation has been minimal, and plants which did manage to colonization the more stable parts of the landslide in dry years have been largely uprooted by sliding and headward gully erosion during the past three wet summers (1993-1995). Therefore landslide scarps and deposits are extremely significant sources of sediment input to the fluvial system, strongly contrasting the minimal input from the adjacent, dominantly well vegetated slopes.

The available chronological data demonstrate that most landslides in the western Cypress Hills have been active during the late Holocene. Despite clustering of events within this period (Goulden and Sauchyn, 1986), the data does not preclude that landsliding has been an essentially continuous process through the Holocene, following initial massive slope failures associated with deglaciation. Nonetheless, consideration needs to be given to factors beyond intrinsic slope properties that may influence the occurrence or reactivation of landslides. Given the geomorphic setting of Battle Creek, an underfit stream incised into its own floodplain, fluvial erosion is not considered a significant trigger mechanism. We suggest that climate, as a control of the regional groundwater table, represents one factor that influences landslide activity in this region. During the early and middle Holocene, climate was generally both warmer and drier than present and regional water tables were lowered markedly (Vance et al., 1995). A change to wetter and cooler climate after ca. 4 ka BP raised regional water tables (as reflected by lake level changes, Vance et al., 1995), providing conditions conducive to increased slope instability in response to short-term trigger events (e.g. heavy rainfall, rapid snowmelt). Extrapolation of our observations and interpretation of possible climatic controls to other valleys on the Interior Plains is constrained by the unique setting of the Cypress Hills. The geological setting, local relief exceeding 200 m, and mean annual precipitation 100 mm greater than the surrounding plains all promote deep-seated rotational landsliding (Goulden and Sauchyn, 1986). Although landsliding is common across the plains, it occurs under very different conditions than in the Cypress Hills. Much research remains to be conducted on the evolution of other valleys on the prairies and the comparison of hillslope activity in valleys occupied by underfit streams versus through-flowing rivers.

The recognition that landsliding is an important component in the geomorphic evolution of valley systems provides an invaluable context for the management of natural resources in parks and other protected areas, where structural (engineering) solutions to land and water management may not be feasible or desirable. The sediment shed from Police Point landslide limits fish productivity and reproduction in Battle Creek by inundating food supplies, eggs, and spawning beds (R. Jensen, pers. comm.), creating local ecological and economic impacts. Results and recommendations of studies evaluating fish habitat in the watershed (Clements and Radford, 1970; Clements et al., 1970; R.L. & L. Environmental Services Ltd., 1994) display an incomplete understanding of the geomorphic setting and processes. For example, grass seeding on the Police Point landslide soon after its occurrence was predictably futile since the landslide moves at depth and is subject to gully erosion and subsurface piping. Likewise attempts to stabilize stream banks have occurred without an appreciation of the hydraulic geometry of the creek. Management strategies should recognize that geological hazards are an integral part of natural ecosystems (in this case contrasting an introduced trout fishery) and that the impacts of the Police Point landslide in fact typify conditions that have characterized the valley for at least 4000 years.

## ACKNOWLEDGMENTS

## REFERENCES

**Christiansen, E.A. and Sauer, E.K.**
1988: Age of the Frenchman Valley and associated drift south of the Cypress Hills, Saskatchewan, Canada; Canadian Journal of Earth Sciences, v. 25, p. 1703-1708.
**Clements, S.H. and Radford, D.S.**
1970: Battle Creek Habitat Evaluation Project: physical features; Fish and Wildlife Division, Department of Lands and Forests, Lethbridge, Alberta.
**Clements, S.H., Lees, V.W., and Atwood, L.**
1970: Habitat Evaluation Project: a preliminary investigation of erosion control methods; Fish and Wildlife Division, Department of Lands and Forests, Lethbridge, Alberta.
**Collier, A.J. and Thom, W.T., Jr.**
1918: The Flaxville gravel and its relationship to other terrace gravels in the northern Great Plains; United States Geological Survey, Professional Paper 108J, p. 179-184.
**Cruden, D.M., Keegan, T.R., and Thomson, S.**
1993: The landslide dam on the Saddle River near Rycroft, Alberta; Canadian Geotechnical Journal, v. 30, p. 1003-1015.

**Furnival, G.M.**
1950: Cypress Lake map-area, Saskatchewan; Geological Survey of Canada, Memoir 242, 161 p.
**Goulden, M.R. and Sauchyn, D.J.**
1986: Age of rotational landsliding in the Cypress Hills, Alberta-Saskatchewan; Géographie physique et Quaternaire, v. 40, no. 3, p. 239-248.
**Janz, B. and Treffry, E.L.**
1968: Southern Alberta's paralyzing snowstorms in April, 1967; Weatherwise, April, p. 70-75, 94.
**Kehew, A.E. and Lord, M.L.**
1986: Origin and large-scale erosional features of glacial-lake spillways in the northern Great Plains; Geological Society of America, Bulletin 97, p. 162-177.
**Klassen, R.W.**
1994: Late Wisconsinan and Holocene history of southwestern Saskatchewan; Canadian Journal of Earth Sciences, v. 31, p. 1822-1837.
**Last, W.M. and Sauchyn, D.J.**
1993: Mineralogy and lithostratigraphy of Harris Lake, southwestern Saskatchewan, Canada; Journal of Paleolimnology v. 9, p. 23-39.
**Leckie, D.A. and Cheel, R.J.**
1989: The Cypress Hills Formation (Upper Eocene to Miocene): a semi-arid braidplain deposit resulting from intrusive uplift; Canadian Journal of Earth Sciences, v. 26, p. 1918-1931.
**Lemmen, D.S., Dyke, L.D., and Edlund, S.A.**
1993: The Geological Survey of Canada's Integrated Research and Monitoring Area (IRMA) Projects: a contribution to Canadian Global Change Research; Journal of Paleolimnology, v. 9, p. 77-83.
**R.L. & L. Environmental Services Ltd.**
1994: Preliminary Fisheries Investigation of Battle Creek and Graburn Creek, 1991-92; report prepared for Trout Unlimited Canada and Alberta Fish and Wildlife, Report No. 306F, 32 p.
**Sauchyn, D.J.**
1990: A reconstruction of Holocene geomorphology and climate, western Cypress Hills, Alberta and Saskatchewan; Canadian Journal of Earth Sciences, v. 27, p. 1504-1510.
1993: Quaternary and Late Tertiary landscape evolution in the western cypress hills; in Quaternary and Late Tertiary Landscapes of Southwestern Saskatchewan and Adjacent Area, (ed.) D.J. Sauchyn; Canadian Plains Research Center, Regina.
**Sauchyn, M.A. and Sauchyn, D.J.**
1991: A continuous record of Holocene pollen from Harris Lake, southwestern Saskatchewan, Canada; Palaeogeography, Palaeoclimatology, Palaeoecology v. 88, p. 13-23.
**Spence, C.D.**
1993: An evaluation of groundwater discharge and its role in valley development, upper Battle Creek basin, Alberta-Saskatchewan; MSc. thesis, University of Regina, Regina, Saskatchewan.
**Thomson, S. and Morgenstern, N.R.**
1977: Factors affecting the distribution of landslides along rivers in southern Alberta; Canadian Geotechnical Journal, v. 14, p. 508-523.
1978: Landslides in argillaceous rock, Prairie Provinces, Canada; in Rockslides and Avalanches 2, (ed.) B. Voight, Developments in Geotechnical Engineering, 14B, New York, Elsevier Scientific Publishing, p. 515-540.
**Vance, R.E. and Last, W.M.**
1994: Paleolimnology and global change on the southern Canadian prairies; in Current Research 1994-B; Geological Survey of Canada, p. 49-58.
**Vance, R.E., Beaudoin, A.B., and Luckman, B.H.**
1995: The paleoecological record of 6 ka climate in the Canadian prairie provinces; Géographie physique et Quaternaire, v. 49, p. 81-98.
**Vreeken, W.J.**
1990: Cypress Hills near Elkwater, Alberta; Canadian Geographer, v. 34, p. 89-92.
**Wolfe, S.A., Huntley, D.J., and Ollerhead, J.**
1995: Recent and late Holocene sand dune activity in southwestern Saskatchewan; in Current Research 1995-B; Geological Survey of Canada, 131-140.

# Organic facies in black shale of Devonian-Mississippian Bakken Formation, southeastern Saskatchewan

L.D. Stasiuk
GSC Calgary, Calgary

**Abstract:** Alginite, acritarch and sporinite macerals in the epicontinental black shale of the Devonian-Mississippian Bakken Formation in southeastern Saskatchewan have been studied with fluorescence incident light microscopy to evaluate the petrographic organic facies. Three organic facies have been defined for the upper and lower shale members of the Bakken Formation: (i) organic facies A is characterized by abundant, relatively large Prasinophyte alginites; (ii) organic facies B is characterized by small acanthomorphic acritarchs and small Prasinophyte alginite, sporinite may be present; and (iii) organic facies C contains macerals similar to organic facies B, sporinites and floral inertinite. Based on the distribution of macerals across a typical Devonian to Mississippian shelf, organic facies in the Bakken shale are interpreted to reflect the degee of water column agitation increasing from the organic facies A setting to the organic facies B and C settings. The lower shale member is dominated by organic facies A except for isolated pockets of organic facies B suggesting a more agitated water colum. The organic facies distribution in the upper shale is markedly different consisting of organic facies A in the west and organic facies B in the east.

**Résumé :** Les macéraux (alginite, acritarches et sporinite) des shales noirs épicontinentaux de la Formation de Bakken du Dévonien-Mississippien, dans le sud-est de la Saskatchewan, ont été analysés au moyen d'un microscope à lumière incidente (fluorescence) dans le but d'y identifier les divers faciès organiques (OF). Les trois faciès définis dans les shales supérieurs et inférieurs de la Formation de Bakken sont les suivants : i) Le faciès organique A (OF A) se caractérise par d'abondantes alginites (Prasinophyte) de plus ou moins grande taille. ii) Le faciès organique B (OF B) se distingue par la présence de petits acritarches acanthomorphiques et de petites alginites (Prasinophyte); des sporinites peuvent être observées. iii) Le faciès organique C (OF C) contient des macéraux semblables à ceux du faciès B, mais aussi des sporinites et une inertinite florale. En se basant sur la répartition des macéraux dans un milieu de plate-forme continentale typique du Dévonien au Mississippien, on déduit que les faciès organiques des shales de Bakken reflètent le degré d'agitation de la colonne d'eau, qui s'accroît quand on passe du milieu correspondant au faciès A à ceux associés aux faciès B et C. Dans les shales inférieurs, on observe principalement le faciès A, mais aussi des îlots du faciès B, laissant supposer une colonne d'eau plus agitée. La répartition des faciès organiques dans les shales supérieurs est nettement différente, avec le faciès A dans l'ouest et le faciès B dans l'est.

## INTRODUCTION

The paleodepositional environment of epicontinental black shale and the mechanisms which fostered enrichment of organic matter (generally a Type II kerogen) is a topic of controversy in sedimentology (e.g. Wignall, 1991) and in hydrocarbon source rock studies (e.g. Tyson, 1987). Upper Devonian and Lower Mississippian epicontinental black shale with excellent hydrocarbon source potential is widespread throughout North America including the Bakken Formation of the Williston Basin (Osadetz et al., 1992), the Exshaw Formation of the Alberta Basin (Creaney et al., 1994), the Cleveland Member of the Ohio Shale in the Black Warrior Basin, and the New Albany Shale in the Illinois Basin (e.g. Barrows et al., 1978; Parrish, 1982; Lineback et al., 1987). Subsidence occurred between Middle Devonian and early Mississippian time in most margin and interior basins of North America (Kominz and Bond, 1991), setting the stage for a major transgression and black shale formation. In an earlier model-based analysis, Parrish (1982) attributed the preservation of organic matter in the Upper Devonian-Mississippian black shale of North America to upwelling of deep, nutrient-rich waters which promoted high organic productivity and created an oxygen minimum zone.

The Bakken Formation black shale of the northern Williston Basin in Canada (Fig. 1, 2) has excellent potential for hydrocarbon source rocks (Type II-I kerogen; Table 1) (Osadetz et al., 1992). Throughout much of the Williston Basin, the Bakken Formation (Fig. 2b) consists of three informal members: (i) a lower black shale; (ii) a middle calcareous, fine grained sandstone to siltstone member; and (iii) an upper black shale (Christopher, 1961; Meissner, 1978; Kent, 1987; LeFever et al., 1991). In southeastern Saskatchewan, the study area for this investigation (Fig. 1),

the thickness of the lower and upper shale varies between 0 and 4 m. The thickness of the coarser grained middle member ranges from 2 to 30 m. Based mainly on the shallow water sedimentological characteristics of the middle sandstone member, Kent (1987) proposed a shallow water depositional environment for the Bakken shale in Saskatchewan, although a variety of environments ranging from a stagnant, marginal marine lagoon to a deep basin setting have been proposed for the Bakken in the United States portion of the Williston Basin (see summary in Webster, 1984 and LeFever et al., 1991). What is clear, as stated by Meissner et al. (1984), is that the Bakken shale accumulated following a low energy transgression over a broad and flat, mature topographic surface. This is corroborated by the numerous soil horizons which occur at the contact between the underlying Torquay Formation and the lower Bakken black shale (e.g. Christopher, 1961). Abundant fossils, including remnants of fish, cephlapods, ostracods, conodonts (remains of free-swimming eel-like organism), and inarticulate brachiopods, probably indicate that the water column was stratified during black shale accumulation (Christopher, 1961; Webster, 1984; Uyeno, 1989; LeFever et al., 1991). The Bakken, according to the paleoatmospheric model of Parrish (1982), was not influenced to the same degree of upwelling as other coeval North American black shale, adding to the enigma as to the origin of the kerogen in this epicontinental setting.

In this study, changes in the petrographic organic facies, as defined by dispersed organic components (macerals), are assessed laterally within and between the upper and lower Bakken shale members in an attempt to interpret relative water depths and the paleoenvironment. The type and abundance of well preserved alginite, acritarch, and sporinite macerals within a petrographic organic facies can essentially provide a snapshot of phytoplankton which lived in the water

*Figure 1.*

*Study area in southeastern Saskatchewan.*
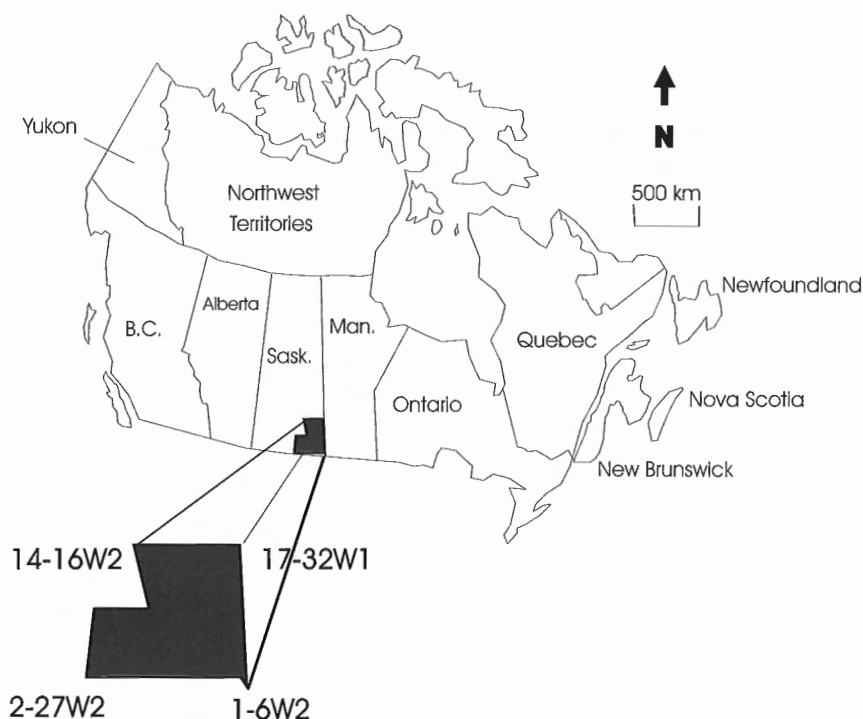
column and the relative degree of terrestrial input. In turn, this can provide the basis for assessing the relationship, if any, between water depth and degree of water column agitation, and distance from a terrigenous source during black shale formation (e.g. Dorning, 1987; Tyson, 1993; Chow et al., 1995).

## METHOD

Composite samples, collected over an interval of approximately 0.2 to 3.0 m, were selected from near the middle of the lower and upper black shale members. The samples were crushed (2-5 mm), homogenized and placed in teflon molds and filled with a resin-hardener mixture. Perpendicular, parallel, and random orientations of shale particles (with respect to bedding) were ensured during preparation. Grinding (carborundum grit) and polishing (alcohol plus alumina slurry) of the hardened pellets was conducted using a modified version of the procedure used for polishing coal blocks as described by Mackowsky (1982). The polished samples were studied using a Zeiss MPM II Universal incident light microscope equipped with Koehler Illuminator, and white (halogen 12V, 100W) and ultraviolet (HBO 100) light sources. Macerals were characterized using Epiplan-neofluor water and oil immersion objectives (total magnification x190 to x1024; Cargille Type FF and Type A immersion oil, n = 1.4810 and n = 1.518 at "e" line). Zeiss 400-440 nm (460 nm beam
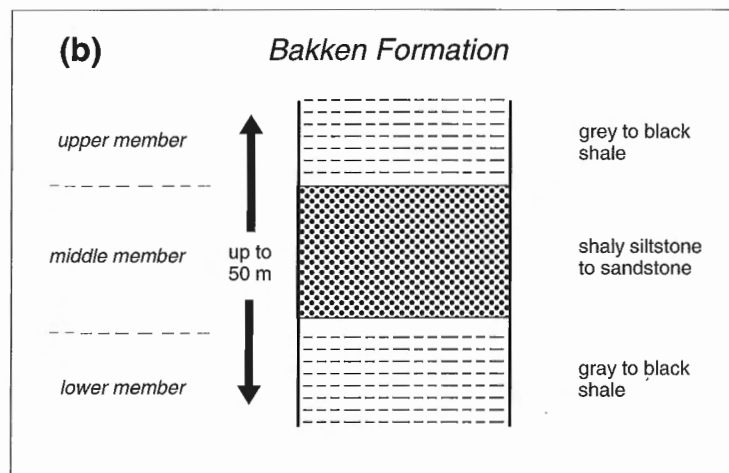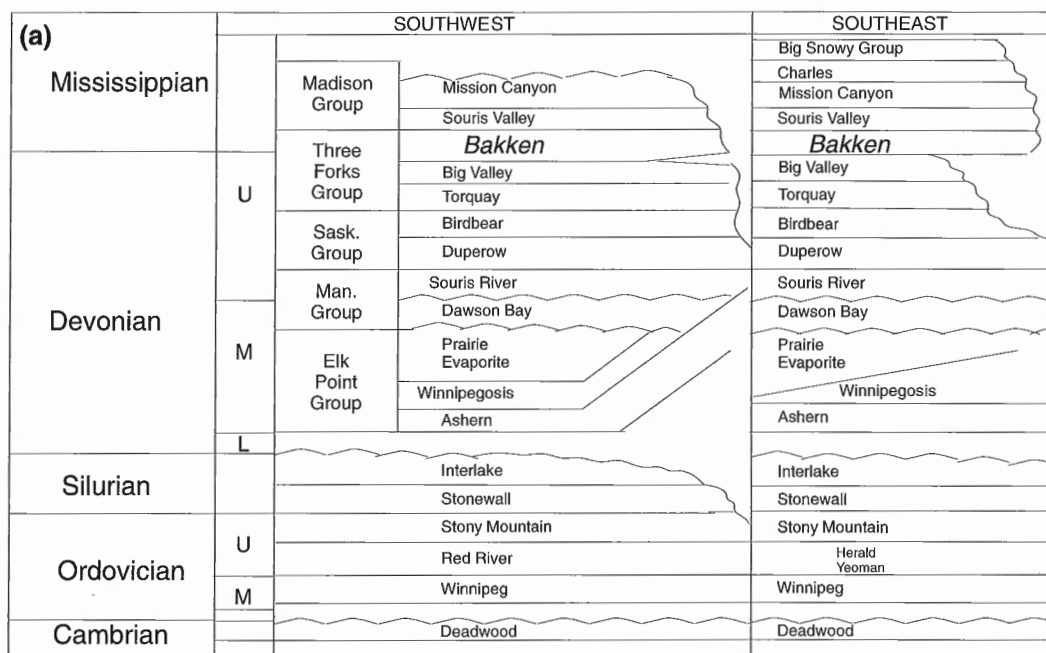


*Figure 2. a) Stratigraphic chart for Paleozoic of Saskatchewan. b) The Bakken Formation is divisible into 3 informal members. The lower shale is Late Fammenian in age whereas the upper shale is no younger than middle Kinderhookian (Uyeno, 1989).*

splitter; 470 nm barrier filter) and 510-560 nm (580 nm beam splitter; 590 nm barrier filter) excitation filters were used for fluorescence microscopic characterization of the macerals.

Alginite macerals are classified following the systematics of Peniquel et al. (1989) and maceral nomenclature of Stasiuk (1994). The morphology and types of acritarchs are classified following Downie et al. (1965) and information in Traverse (1988). Visual estimates of relative maceral abundance for each sample were made from between 70 and 90 fields of view, each with a radius of 270 μm. Most of the samples were reground and repolished several times to achieve a better evaluation of the maceral assemblage. Additional petrographic information such as the nature of amorphous kerogen, microfossils (e.g. scolecodonts), and assessory mineral components was also noted.

## RESULTS AND DISCUSSION

### Bakken Formation organic facies

Kerogen in the Bakken Formation shale can be broadly subdivided into two main maceral components: (i) a continuous, unstructured, amorphous kerogen component (hereinafter referred to as bituminite); and (ii) a unicellular alginite and/or acritarch component (structured macerals). Most of the bituminite is granular and low reflecting (%Ro 0.40) with occasional, low-intensity, brown fluorescence (Fig. 3a).

Based on specific varieties of alginite and acritarch macerals, and the extent of sporinite inclusions in the bituminite, three distinct petrographic organic facies are defined for the upper and lower black shale members. Organic facies A is characterized by abundant, relatively large (commonly up to and rarely exceeding 350 μm), thick-walled phycoma of unicellular *Tasmanites* and *Leiosphaeridia* alginite (Fig. 3b, c). Organic facies B consists of bituminite with maceral inclusions dominated by relatively small acanthomorphic acritarchs (including *Veryachium*-like and *Michrystridium*-like acritarchs < 20 μm in diameter) (Fig. 3d, e, g, j) and *Leiosphaeridia* and *Tasmanites* alginites that are much smaller than those in organic facies A (mainly < 20 μm but up to 100 μm diameter) (Fig. 3f, i); sporinites may or may not be present in organic facies B (Fig. 3k). Organic facies C is similar to organic facies B but contains a more diffuse bituminite and a persistent contribution of terrestrial-derived sporinite and floral inertinite (Fig. 3l). Trace, but persistent amounts of rounded to subrounded algal akinete (Fig. 3m) and filamentous alginite macerals (Fig. 3n) (see also Stasiuk, 1993) are common to all three organic facies in both the upper and lower black shale members.

The geographic distribution of organic facies A, B and C in the lower and upper Bakken shale is shown in Figure 4. Specific locations and depths are listed in Table 1. The lower shale is dominated by organic facies A throughout most of the study area (Fig. 4a; Table 1). Exceptions to this dominance include three locations with organic facies B shale along longitude 104°W and an isolated occurrence of an organic facies C shale (17-32W1) in the extreme northeast corner of the study area. The distribution of organic facies in the upper

shale does not reflect the distribution of organic facies in the lower shale (compare Fig. 4a and 4b). There is a change from the regional dominance of organic facies A in the lower Bakken shale to a dominance of both organic facies A and B in the upper shale (Fig. 4; Table 1). The distribution of organic facies for the upper shale marks a distinct partitioning into a zone dominated by organic facies A in the west, and a zone dominated by organic facies B in the eastern half of the study area (Fig. 4b). The lower shale and the most northeastward sample locations of the upper shale are characterized by organic facies C.

**Table 1.** Location, depth and dominant organic facies for lower (l), middle (m) and upper (u) members of Bakken Formation. Total organic carbon (% TOC), hydrogen index (HI = mg hydrocarbons/g TOC x 100), and oxygen index (OI = mg CO2/gm TOC x 100) from Rock Eval pyrolysis are also listed (from Osadetz and Snowdon, 1995).

| Location | Depth (m) | OF | % TOC | "HI, OI" | member |
|---|---|---|---|---|---|
| 12-27-1-6W2 | 2066.0 | B | 20.5 | 606/6 | u |
| 12-27-1-6W2 | 2082-84 | A | 18.8 | 549/6 | l |
| 2-14-1-16W2 | 2324.0 | B | 13.3 | 663/18 | u |
| 2-14-1-16W2 | 2341.0 | B | 11.2 | 531/13 | l |
| 3-34-2-27W2 | 2127.2 | A | 15.1 | 562/20 | l |
| 3-34-2-27W2 | 2128.7 | A | - | - | l |
| 16-10-3-25W2 | 2071.7 | A | 15.5 | 572/17 | u |
| 16-10-3-25W2 | 2087.9 | A | 15.9 | 541/17 | l |
| 15-31-3-11W2 | 1970.2 | B | 23.5 | 658/5 | u |
| 15-31-3-11W2 | 1988.2 | A | 13.0 | 547/11 | l |
| 8-20-4-14W2 | 1953.8 | B | 31.9 | 566/7 | u |
| 8-20-4-14W2 | 1971.1 | B | 29.8 | 553/10 | l |
| 9-13-5-13W2 | 1828.0 | B | 31.2 | 574/6 | u |
| 9-13-5-13W2 | 1845.3 | A | 13.8 | 566/10 | l |
| 6-7-5-18W2 | 2019.3 | B | 24.4 | 551/10 | u |
| 6-7-5-18W2 | 2022.7 | B | 0.5 | 55/81 | m |
| 2-5-5-27W2 | 2053.1 | A | 18.0 | 478/21 | u |
| 2-5-5-27W2 | 2066.7 | A | 15.6 | 504/19 | l |
| 5-4-6-24W2 | 1819.8 | A | 19.6 | 469/18 | l |
| 5-4-6-24W2 | 1821.2 | A | 21.6 | 121/22 | l |
| 1-2-6-25W2 | 1811.7 | A | 27.7 | 617/10 | u |
| 1-2-6-25W2 | 1827.4 | A | 20.3 | 620/16 | l |
| 16-23-7-3W2 | 1406.5 | B | 24.5 | 539/18 | u |
| 16-23-7-3W2 | 1414.4 | Ind | 1.9 | 46/31 | l |
| 16-10-7-15W2 | 1727.0 | A | 13.3 | 480/22 | l |
| 16-10-7-15W2 | 1728.5 | A | 9.6 | 629/27 | l |
| 13-30-7-23W2 | 1833.1 | A | 23.6 | 625/14 | u |
| 13-30-7-23W2 | 1846.2 | A | 15.4 | 525/21 | l |
| 14-27-8-26W2 | 1787.8 | A | 9.1 | 827/42 | l |
| 6-26-10-2W2 | 1257.6 | C | 29.7 | 436/18 | u |
| 6-26-10-2W2 | 1266.0 | A | 2.0 | 40/22 | l |
| 11-36-13-11W2 | 1259.3 | B | 25.8 | 488/15 | u |
| 11-36-13-11W2 | 1270.3 | A | 3.3 | 81/29 | l |
| 6-33-14-1W2 | 904.0 | Ind | - | - | l |
| 14-11-14-16W2 | 1226.2 | B | 4.4 | 99/41 | l |
| 4-20-17-32W1 | 679.7 | C | 1.9 | 224/79 | u |
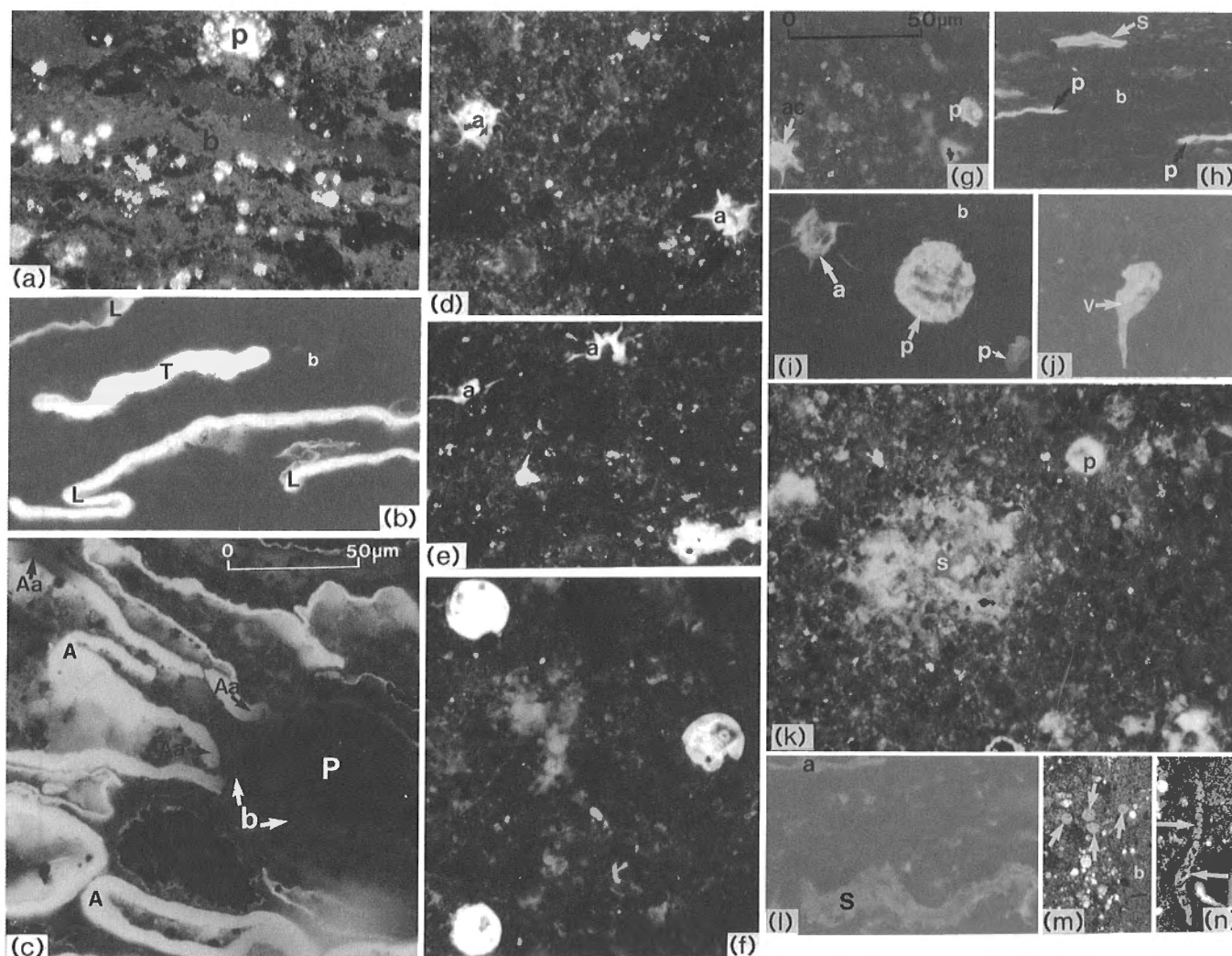
(a) Amorphous bituminite (b) associated with framboidal pyrite (p).

(b) Organic facies A with relatively abundant and large unicellular Tasmanites (T) and Leiosphaeridia (L) Prasinophyte alginite within a matrix of bituminite (b).

(c) Large Prasinophyte alginite associated with phosphatic nodules (P). Radioactivity from the nodules has resulted in a red shift in the fluorescence of the alginite (A-unaltered and Aa-altered alginite; b-bitumen) proximal to the phosphate particles.

(d), (e) Organic facies B dominated by spiny acanthomorphic acritarchs (a) within bituminite.

(f) Relatively small Prasinophyte alginites in organic facies B.

(g) Spiny acanthomorphic acritarchs (ac) and small Prasinophyte alginite (p).

(h) Small Prasinophytes (p) and terrestrial microsporinite (s) in organic facies B (b-bituminite).

(i) Acanthomorphic acritarchs (a) and Prasinophytes (p) in organic facies B (b-bituminite).

(j) Veryachium-like acritarch (V) in bituminite in organic facies B.

(k) Degraded sporinite with remnant radiating morphology similar to Grandiospora (s) and small Prasinophyte alginite (p) in organic facies B.

(l) Organic facies C with sporinite (s) and relatively small Prasinophyte alginite (a).

(m) Algal akinete "bloom" cells (arrows) probably derived from filamentous algae in bituminite (b).

(n) Filamentous alginite (arrows).

**Figure 3.** Photomicrographs of macerals in organic facies of Bakken Formation shale; oil immersion objectives, incident light; scale = 50 μm; (a), (m), (n), plane polarized white light; (b) to (i), fluorescent light.

**Figure 4.**

*Sketch map illustrating the distribution of organic facies in the lower **a**) and upper **b**) shale members of the Bakken Formation, southeast Saskatchewan. Organic facies A is characterized by large Prasinophyte alginites, organic facies B by acanthomorphic acritarchs, smaller Prasinophyte alginites, and an input from "near-shore" terrestrial sporinite. Organic facies A is characterized by macerals similar to organic facies B but with persistent sporinite and floral inertinite. A = organic facies A; B = organic facies B; C, organic facies C; $A^p$ = phosphate-rich particles in the lower shale member.*
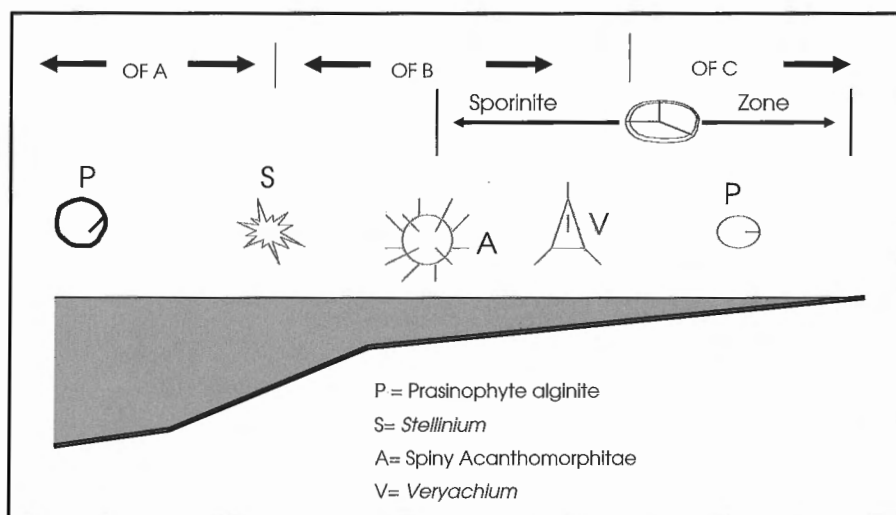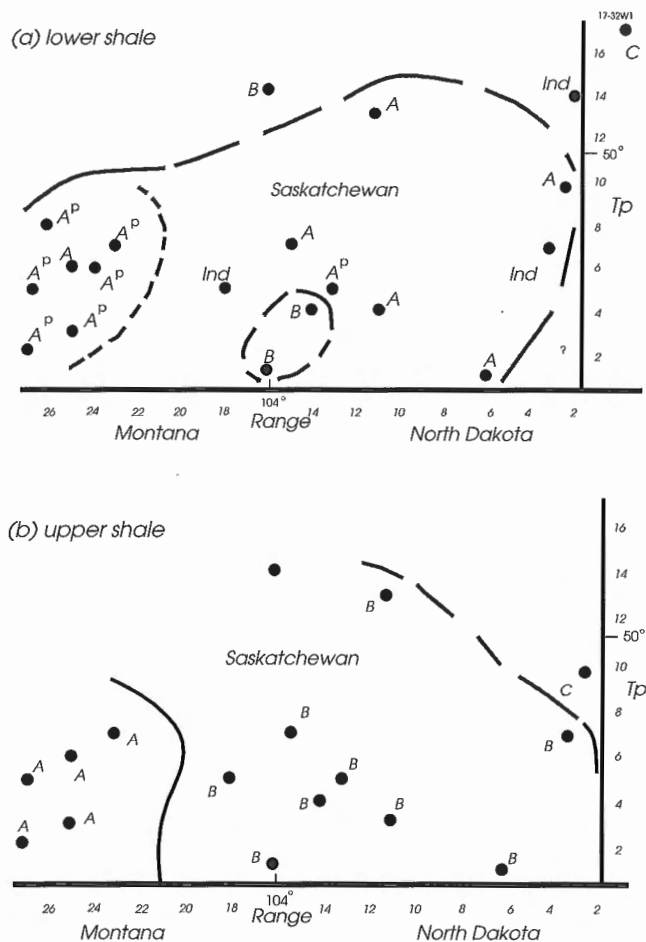


**Figure 5.**

*Model of alginite, acritarch and sporinite distribution across a typical Tournasian shelf (modified from Dorning, 1987) in relation to organic facies (OF) of the Bakken Formation shale.*

## General model

An idealized distribution of acritarch and alginite maceral varieties, and terrestrial plant-derived macerals (sporinite and inertinite), provides a basis for interpreting organic facies distribution in the upper and lower Bakken black shale members. Following from Dorning's (1987; Fig. 5) model, which describes the distribution of acritarch, alginite and sporinite types across a Tournasian (Kinderhookian) shelf, and from bank to basin: (i) organic facies A in the Bakken represents deposition in association with the least agitated water column and perhaps deepest water most basinal setting; and (ii) organic facies B and C represent deposition in association with a more agitated water column and perhaps shallower, shelf to nearshore settings (Fig. 5). A similar model has recently proven to yield an excellent correlation between lithofacies and petrographic organic facies in the Upper Devonian Duvernay Formation, Redwater reef complex, Alberta (Chow et al., 1995). Based on these models, most of the lower Bakken black shale samples examined in this study were probably deposited in relatively unagitated, perhaps deep water, basinal environment (compare Fig. 4a and 5). Petrographic facies in the upper black shale on the other hand demarcate two distinct zones, organic facies A in the western part of the study area and organic facies B in the eastern half of the study area (compare Fig. 4b and 5). The change from an organic facies A-dominated lower shale to an organic facies B-dominated upper shale in the eastern half of the study area may reflect a difference in the relative degree of upper water column agitation between "upper Bakken time" and "lower Bakken time".

The lateral distribution of organic facies in the upper and lower Bakken shale members needs further investigation. Future work will characterize, in detail, the vertical distribution of the organic facies in the upper and lower shale members at particular locations. These observations will then be assessed within a detailed stratigraphic and sedimentological framework of the black shale members and the middle sandstone member.

## CONCLUSIONS

Three petrographic organic facies occur within the upper and lower black shale members of the Bakken Formation: (i) organic facies A is characterized by large Prasinophyte alginites; (ii) organic facies B is characterized by small acanthomorphic acritarchs, smaller Prasinophyte alginite than in organic facies A and occasional terrestrial sporinite; and (iii) organic facies C contains macerals similar to organic facies B but contains persistent sporinites and floral inertinite. Based on the distribution of acritarch, alginite, and sporinites from bank to basin and across a typical Kinderhookian shelf, organic facies in the Bakken shale may represent deposition associated with a poorly agitated water colum, perhaps within a deep water basinal setting (organic facies A), and a more agitated, perhaps shallower shelf to nearshore setting (organic facies B to C). The lower shale member is dominated by organic facies A throughout the study area except for isolated pockets of organic facies B. The upper shale consists of two distinct zones of organic facies A and B. Future investigations will assess, in detail, the lateral and vertical distribution of organic facies in these shales within the context of a detailed stratigraphic and sedimentological framework.

## REFERENCES

**Barrows, M.H. , Cluff, R.M., and Harvey, R.D.**
1978: Petrology and maturation of dispersed organic matter in the New Albany Group of the Illinois Basin; in Proceedings of the Third Eastern Oil Shales Symposium, (ed.) H. Barlow; METC/SP-79/6, p. 85-114.

**Chow, N., Wendte, J.C., and Stasiuk, L.D**
1995: Productivity versus preservation controls on two organic-rich carbonate facies in the Devonian of the Western Canada Sedimentary basin; Bulletin of Canadian Petroleum Geology, v. 43.

**Christopher, J.E.**
1961: Transitional Devonian-Mississippian formations of southern Saskatchewan; Saskatchewan Department of Mineral Resources, Report No. 66, 103 p.

**Creaney, S., Allen, J., Cole, K.S., Fowler, M.G., Brooks, P.W.,**
**Osadetz, K.G., MacQueen, R.W., Snowdon, L.R., and Riedeger, C.L.**
1994: Petroleum generation and migration in the Western Canada Sedimentary basin; in Geological Atlas of the Western Canada Sedimentary basin, (comp.) G. Mossop and I. Shetson; Canadian Society of Petroleum Geologists and the Alberta Research Council, p. 455-468.

**Dorning, K.J.**
1987: The organic palaeontology of Paleozoic carbonate environments; in Micropalaeontology of carbonate environments, (ed.) M.B. Hart; Ellis Horwood, Chichester, p. 256-265.

**Downie, C., Eviit, W.R., and Sargeant, W.A.S.**
1965: Dinoflagellates, hystrichospheres and the classification of acritarchs; Stanford University Publication, Geological Sciences, v. 7, p. 1-16.

**Kent, D. M.**
1987: Paleotectonic controls on sedimentation in the northern Williston Basin, Saskatchewan; in Anatomy of a cratonic oil province, (ed.) M.W. Longman; Rocky Mountain Association of Geologists, Denver, p. 45-56.

**Kominz, M.A. and Bond, G.C.**
1991: Unusually large subsidence and sea-level events during middle Paleozoic time: new evidence supporting mantle convection models for supercontinent assembly; Geology, v. 19, p. 56-60.

**LeFever, J.A., Matiniuk, C.D., Dancsok, E.F.R., and Mahnic, P.A.**
1991: Petroleum potential of the middle member, Bakken Formation, Williston Basin; in Sixth International Williston Basin Symosium, (ed.) J.E. Christopher and F. Haidl; Saskatchewan Geological Society, Special Publication 6, p. 74-94.

**Lineback, J.A., Roth, M., and Davidson, M.L.**
1987: Sediment starvation in the Williston and Illinois Basins during the Devonian and Mississippian; in Anatomy of a cratonic oil province, (ed.) M.W. Longman; Rocky Mountain Association of Geologists, Denver, p. 147-155.

**Mackowsky, M.-Th.**
1982: Methods and tools of examination; in Stachs textbook of coal petrology, Third Edition, (ed.) E. Stach, M.-Th. Mackowsky, M. Teichmüller, G.H. Taylor, D. Chandra, and R. Teichmüller; Gebruder Borntraeger, Berlin, p. 295-299.

**Meissner, F.F.**
1978: Petroleum geology of the Bakken Formation, Williston Basin, North Dakota and Montana; in The Williston Basin Symposium, The Economic Geology of the Williston Basin; Montana Geological Society 24th Annual Conference, p. 207-227.

**Meissner, F.F., Woodward, J., and Clayton, J.L.**
1984: Stratigraphic relationships and distribution of source rocks in the greater Rocky Mountain region; in Hydrocarbon source rocks in the greater Rocky Mountain region, (ed.) J. Woodward, F.F. Meissner and J.L. Clayton; Rocky Mountain Association of Geologists, Denver, p. 1-34.

**Osadetz, K.G., Snowdon, L.R., and Brooks, P.W.**
1992: Oil families and their sources in Canadian Williston basin, (southeastern Saskatchewan and southwestern Manitoba); Bulletin of Canadian Petroleum Geology, v. 40, p. 254-273.

**Osadetz, K.G. and Snowdon, L.R.**
1995: Significant Paleozoic petroleum source rocks in the Canadian Williston Basin: their distribution, richness and thermal maturity (southeastern Saskatchewan and southwestern Manitoba); Geological Survey of Canada, Bulletin 487, 60 p.

**Parrish, J.T.**
1982: Upwelling and petroleum source beds, with reference to Paleozoic; American Association of Petroleum Geologists Bulletin, v. 66, p. 750-774

**Peniguel, G., Couderc, R., and Seyve, C.**
1989: Les microalgues actuelles et fossiles-intérêts stratigraphique et pétrolier; Bulletin Centres Recherche Exploration-Production, Elf-Acquitaine, v. 13, p. 455-481.

**Stasiuk, L.D.**
1993: Algal bloom episodes and the formation of bituminite and micrinite in hydrocarbon source rocks: evidence from the Devonian and Mississippian, northern Williston Basin, Canada; International Journal of Coal Geology, v. 24, p. 195-210.

1994: Oil-prone alginite macerals from organic-rich Mesozoic and Paleozoic strata, Saskatchewan, Canada; Marine and Petroleum Geology, v. 11, p. 208-218.

**Traverse, A.**
1988: Paleopalynology; Unwin Hyman, Boston, 600 p.

**Tyson, R.V.**
1987: The genesis and palynofacies characteristics of marine petroleum source rocks; in Marine Petroleum Source Rocks, (ed.) J. Brooks and A.J. Fleet; Geological Society Special Publication No. 26, Blackwell Scientific Publications, Oxford, p. 47-68.

1993: Palynofacies analysis; in Applied Micropaleontology, (ed.) D.G. Jenkins; Kluwer Academics, Netherlands, p. 153-191.

**Uyeno, T.T.**
1989: Report on 13 conodont samples from the lower and upper shale members of the Bakken Formation from 11 wells in southern Saskatchewan; Geological Survey of Canada, Internal Palentological Report 08-TTU-89, 6 p.

**Webster, R.L.**
1984: Petroleum source rocks and stratigraphy of the Bakken Formation in North Dakota; in Hydrocarbon source rocks of the greater Rocky Mountain region, (ed.) J. Woodward, F.F. Meissner, and J.L. Clayton; Rocky Mountain Association of Geologists, Denver, p. 57-81.

**Wignall, P. B.**
1991: Model for transgressive black shales?; Geology, v. 19, p. 167-170.

# Carnian and Norian (Triassic) strata in the British Mountains, northern Yukon Territory

J. Dixon, M.J. Orchard[1], and E.H. Davies[2]
GSC Calgary, Calgary

**Abstract:** The majority of the Triassic strata identified in northern Yukon has been dated as Norian, with a few isolated exposures of Ladinian strata, and some generally dated Triassic exposures. In the northern British Mountains, close to Fish Creek, there is a well-exposed Triassic succession previously mapped as part of the Permian to Lower Triassic Sadlerochit Group. This succession consists of a lower shaley interval gradationally overlain by sandstone, in turn succeeded by an interval dominated by limestone and sandy limestone. Conodonts and palynomorphs date these beds as Carnian and early Norian (Late Triassic). These Carnian and Norian beds are age-equivalent to part of the Shublik Formation of northeastern Alaska, although the facies are very different.

**Résumé :** La majorité des couches triasiques identifiées dans le nord du Yukon remontent au Norien, mais on compte quelques affleurements isolés de couches ladiniennes et quelques autres du Trias en général. Dans le nord des monts British, près du ruisseau Fish, il y a des affleurements d'une succession triasique, antérieurement assignée au Groupe de Sadlerochit du Permien au Trias inférieur. Cette succession se compose d'un intervalle inférieur argileux, graduellement recouvert de grès auquel succède un intervalle où dominent les calcaires (purs et sableux). Les conodontes et les palynomorphes permettent d'associer ces couches au Carnien et au Norien précoce (Trias tardif), un âge équivalent à celui d'une partie de la Formation de Shublik dans le nord-est de l'Alaska; les faciès y sont cependant très différents.

[1] GSC Victoria, Vancouver
[2] Branta Biostratigraphy Ltd., 4, 4640 Manhatten Road S.E., Calgary, Alberta T2G 4B5

## INTRODUCTION

In the British Mountains of northernmost Yukon, the only dated Triassic (Norian) strata were mapped as Shublik Formation by (Norris, 1981a, b). These strata are best known in Loney Syncline (Norris, 1981a) but also are present along Babbage River and its western tributaries (Norris, 1981b). Later, Norris (1985) tentatively identified the Permian to Lower Triassic Sadlerochit Group along a ridge north of Fish Creek, where previously he had mapped only Carboniferous strata (Norris, 1981a). Norris' (1985) identification of Sadlerochit strata at Fish Creek was based on lithological comparison with the type area in northeastern Alaska, without the benefit of paleontological data. Subsequent re-examination of the strata at Fish Creek and identification of conodonts and palynomorphs collected from the section places the strata within the Carnian and lower Norian (Upper Triassic), much younger than the Sadlerochit Group.

## FISH CREEK SECTION

An approximately 220 m thick section was measured near the ridge-top of a south-facing slope along the Fish Creek valley (Fig. 1), at latitude 69°27'17"N, longitude 140°19'50"W (located with a Global Positioning Satellite receiver in a helicopter; UTM grid 526100E, 7704800N) . Strata dip about 78°north-northeast and are well exposed. The section was measured in 1992 and revisited in 1994 for additional collections and to finish the measurements (Dixon's field section DFA92-20). A few kilometres to the west, along the same ridge system, there are additional exposures of the lowermost beds (Dixon's field section DFA92-19).

The Triassic strata rest disconformably on light-grey weathering limestone of the Carboniferous Lisburne Group (Fig. 2). The lower 104 m consist of light- to medium-grey weathering, fissile shale with thin interbeds of very fine to fine grained sandstone. Sandstone beds tend to be more frequent in the basal few metres and also become more common in the upper part of the shale interval, reflecting the overall coarsening-upward character. At section DFA92-19, the basal 2 to 3 m contains a thin conglomerate, grading upward into a silica-cemented, fine grained sandstone. Although sandstone interbeds within the shale succession are fine grained, a few granulestone and pebbly beds are present. The sandstone interbeds typically have no visible sedimentary structures although a few contain wave-ripple laminae.

Above the shale dominated interval there is a gradational change upward into a sandstone-rich succession that is approximately 43 m thick. Very fine to fine grained, silica-cemented sandstone dominates the interval, although a few beds of granulestone and conglomerate are present. Overlying the sandstones are two limestone units separated by a 15 m thick sandstone unit (Fig. 2). The lower limestone is dark grey to black and ranges from platy to thick bedded, commonly in beds 20 to 50 cm thick. The median sandstone is very fine



**Figure 1.**

*Location map of the Carnian and Norian strata at Fish Creek and Norian strata in Loney Syncline.*
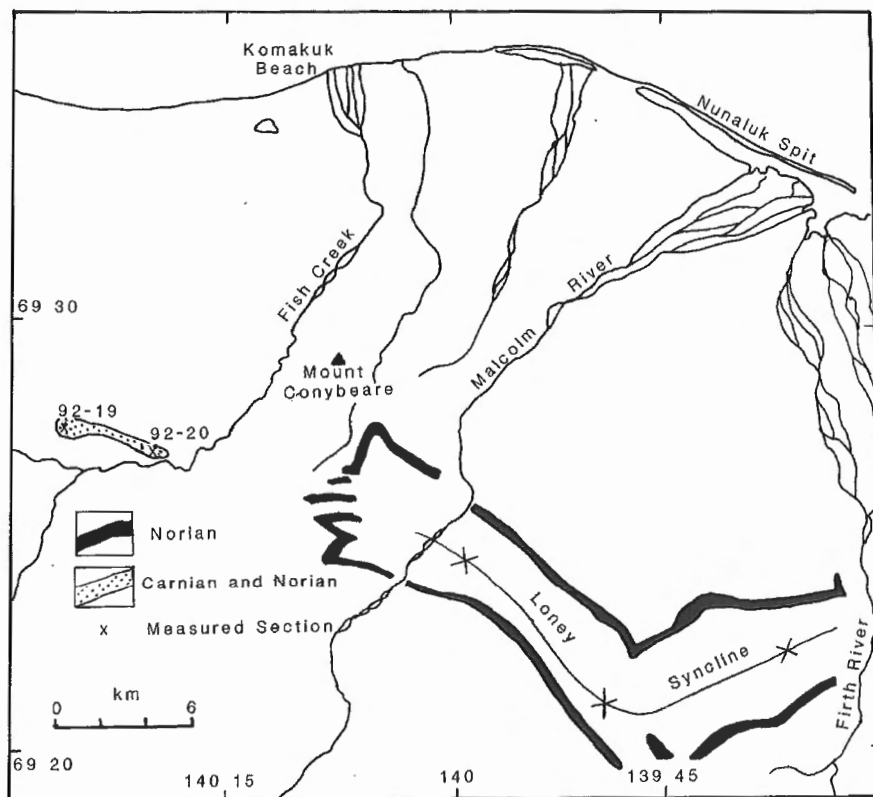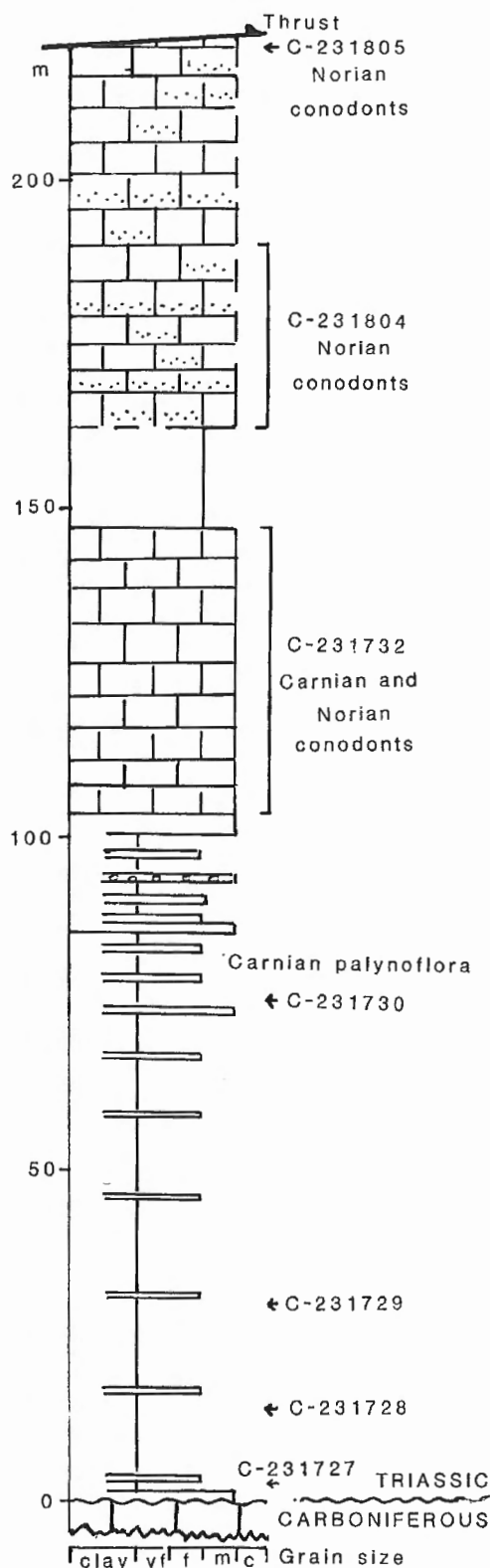
**Figure 2.** *Lithology log of section DFA92-20, Fish Creek, northern British Mountains. C-numbers are samples curated at GSC's office in Calgary.*

grained, siliceous, and highly fractured. The upper limestone weathers a light- to medium-grey colour, locally with a yellowish hue. Most of the exposures of the upper limestone are badly frost shattered. Much of the upper limestone interval consists of very calcareous sandstone to sandy limestone. A thrust fault separates the upper limestone from a recessive weathering interval of interbedded shale and sandstone of the Carboniferous Kayak Formation which, in turn, is overlain by limestone of the Lisburne Group.

Thin sections of samples from the lower limestone indicate a silty, bioclastic limestone composition. Abundant thin-walled shell debris and some scattered peloidal clasts "float" in a fine to medium crystalline calcite matrix. Thin sections from some beds in the upper limestone interval consist of very fine grained, silty, calcite-cemented sandstone, bioclastic, very fine to fine grained sandstone, and sandy, bioclastic limestone. Most of the bioclasts are shell fragments.

## BIOSTRATIGRAPHY

Four samples were collected from the shale interval (Fig. 2) and examined for palynomorphs. Although severely affected by thermal alteration (TAI of 3+ to 4) three of the samples yielded the following identifiable pollen and spores:

*Accintisporites* sp.

*Circulina meyeriana* Klaus 1960

*Discisporites niger* Leschik 1955

*Duplecisporites granulatus* Leschik 1955

*D. mancus* (Leschik 1955) Klaus 1960

*Eucommidites* sp.

*Paracingulina maljawkinae* Klaus 1960

*Pityosporites* sp.

*Podosporites amicus* Scheuring 1970

*Praecirculina granifer* (Leschik 1955) Klaus 1960

*Protohaploxypinus* sp.

*Retisulcites* sp.

*Anapiculatisporites* sp.

*Punctatisporites* sp.

The age of this assemblage is Carnian, equivalent to Zone VII of Fisher (1979).

Three composite samples of carbonate were collected from the lower (C-231732) and upper (C-231804, C-231805) limestone intervals for conodont analysis. Recovered faunas were small, and in the case of the upper limestone, highly fragmented. All have been thermally altered and have a CAI of 4 to 4.5.

The conodont faunas from the lower limestone comprise 12 elements of *Metapolygnathus* ex gr. *polygnathiformis* (Budurov and Stefanov 1965), 2 elements of *Neogondolella* sp. indet., and a nondiagnostic ramiform element. The first

and dominant species is a typical Carnian form which appears at the base of the Carnian and remains common through the lower Upper Carnian (Orchard, 1991a). Although similar forms might also be expected through the basal Norian, the younger faunas are dominated by other species of *Metapolygnathus* that do not occur in the present sample. The presence of *Neogondolella* sp. indet. suggests either an Early Carnian age, or an Early Norian age, depending on the species, which in this case is not identifiable. Because of the composite nature of the sample, it is also possible that two ages, Carnian and Early Norian, are represented by this collection.

The upper limestone has yielded two essentially identical collections consisting of a total of about 8 juvenile specimens of *Neogondolella navicula* (Huckriede 1958) associated with a few ramiform pieces. The fragmented nature of the conodont elements and the lack of large specimens implies breakage and possible hydrodynamic sorting under high energy conditions, but perhaps also reflects an original inhospitable environment. *N. navicula* appears at the base of the Norian and ranges through the Lower Norian (Orchard, 1991b).

## SEDIMENTOLOGY

In its simplest form, the overall succession can be interpreted to be a transgressive-regressive (T-R) cycle of sedimentation. However, the abrupt change to a carbonate succession midway through the succession, and the presence of a prominent sandstone within the upper carbonate, could be interpreted to suggest additional breaks in sedimentation. These features of the Fish Creek succession could be interpreted to indicate the presence of three T-R cycles. On a more regional scale, the eastward overlap of Carnian and early Norian beds by middle or late Norian strata suggests that the middle to late Norian succession represents another T-R cycle.

Transgression is recorded in the basal few metres of thinly interbedded sandstone and shale, which is overlain by regressive, marine shale deposited below "normal" storm wavebase on a shelf environment. Large storms created conditions necessary to mobilize coarse clastic sediment at, or near, the shoreline and transport them onto the shelf in sediment-gravity flows, depositing them as thin sandstone and/or granulestone beds (tempestites in the terminology of some writers).

As progradation proceeded, the nearshore and shoreline sediments migrated over the shelf shale, depositing fine grained sands. These latter beds are succeeded by bioclastic-rich beds of limestone and calcareous sandstone. The occurrence of limestone suggests a reduction in siliciclastic sediment into the Fish Creek area, especially during deposition of the lower limestone interval. However, above the lower limestone interval siliciclastics became more common and resulted in the deposition of sands and sand-rich carbonates in the upper part of the succession.

Although extensively recrystallized, the two limestone intervals contain mostly thin-walled, highly comminuted, shell clasts and some peloids. This suggests a moderate- to high-energy environment with a low-diversity fauna. The limestone-rich interval may in fact contain possibly two regional transgressive events, beginning some time at the end of the Carnian, and beginning of the Norian. However, insufficient details of the succession are known to locate the possible transgressive event in the lower limestone interval. The sandstone between the two limestone intervals could be interpreted to be a transgressive bed.

## REGIONAL COMPARISONS

The Fish Creek Triassic succession is the only firmly dated Carnian in this part of northernmost Yukon. Most other dated occurrences of Triassic strata in the British and Barn mountains are Norian (Fig. 3). About 12 to 15 km to the east-southeast of Fish Creek, middle or late Norian beds are exposed in Loney Syncline (Norris, 1981a; unpublished data by Orchard and Dixon). In the syncline, the Norian beds rest unconformably on Carboniferous limestone in the southwest and deformed lower Paleozoic phyllite along the rest of the synclinal flanks (Norris, 1981a). The absence of older Triassic beds in Loney Syncline indicates that Carnian strata have been eroded from this area.

Elsewhere in the northern Yukon, most of the dated Triassic occurrences also are Norian (Norris, 1981b, 1982), with at least one known Ladinian occurrence in the Fishing Branch area of the northern Ogilvie Mountains (Norris, 1982). On the east flank of the Richardson Mountains, at Salter Hill, small outliers of Triassic strata (Norris, 1981c) contain conodonts of either Ladinian or Carnian age (unpublished data by Orchard and Dixon).

In northeastern Alaska, both Lower and Upper Triassic strata are present (Detterman et al., 1975), with possibly some Lower Triassic (Ivishak Formation) extending as far east as Joe Creek, close to the international border (Fig. 3). Norris (in press) has suggested that Ivishak beds may be present along the southern British Mountains (section A29, Norris, 1981b), in the headwaters of Babbage River. The section is very poorly exposed and undated, and occurs between known Norian and Kungurian (Permian) beds, consequently the age of these beds remains speculative.

The Carnian and Norian strata of the British Mountains are age-equivalent to parts of the Shublik Formation of northeastern Alaska (Fig. 3; Detterman et al., 1975). Norris (1981a, b) mapped the Triassic as Shublik, even though it is only equivalent to the Clay-shale member of Alaska, a very different facies from the Norian limestone, sandstone, and siltstone successions in northern Yukon. The Carnian part of the Shublik Formation in Alaska is the Limestone and dolostone member, a facies which is also different from the Carnian in northern Yukon. These considerable facies

| TRIASSIC | | | NORTHEAST ALASKA (Detterman et al., 1975) | | BRITISH MOUNTAINS | | |
|---|---|---|---|---|---|---|---|
| | | | | | Joe Creek | Fish Creek | Loney Syncline |
| POST-TRIASSIC | | | KINGAK FM (Jurassic) | | | | KINGAK FM (Jurassic) |
| | UPPER | RHAETIAN | KAREN CREEK SANDSTONE | | | | Limestone - sandstone |
| | | NORIAN | SHUBLIK FORMATION | Clay shale member | | Limestone Sandstone Shale | |
| | | CARNIAN | | Limestone and dolostone member | | | |
| | MIDDLE | LADINIAN | | Siltstone member | | | |
| | | ANISIAN | | | | | |
| | LOWER | SPATHIAN | SADLEROCHIT GROUP — IVISHAK FM | Fire Creek Siltstone member | ? | | |
| | | SMITHIAN | | Ledge Sandstone member | IVISHAK FM | | |
| | | DIENERIAN | | | ? | | |
| | | GRIESBACHIAN | | Kavik member | | | |
| PRE-TRIASSIC | | | ECHOOKA FM (Permian) | | ECHOOKA FM (Permian) | LISBURNE GP (Carb.) | Lower Paleozoic |

*Figure 3.*

*Correlation table of Triassic strata in the British Mountains and northeastern Alaska.*

differences from the type Shublik Formation and the stratigraphic and physical separation of Carnian and lower Norian from middle or upper Norian strata in the northern Yukon raise some doubts as to the usefulness of continuing to name the Yukon strata the Shublik Formation. However, until a more thorough regional analysis of the Triassic in the northern Yukon is undertaken, the use of Shublik Formation will be retained.

## ACKNOWLEDGMENTS

## REFERENCES

**Detterman, R.J., Reiser, H.N., Brosge, N.P., and Dutro, J.T., Jr.**
1975: Post-Carboniferous stratigraphy, northeastern Alaska; United States Geological Survey, Professional Paper 886, 46 p.

**Fisher, M.J.**
1979: The Triassic palynofloral succession in the Canadian Arctic Archipelago; American Association of Stratigraphic Palynologists, Contribution Series, v. 5B, p. 83-100.

**Norris, D.K.**
1981a: Geology, Herschel Island-Demarcation Point; Geological Survey of Canada, Map 1514A, 1:250 000 scale.
1981b: Geology, Blow River-Davidson Mountains; Geological Survey of Canada, Map 1516A, 1:250 000 scale.
1981c: Geology, Trail River; Geological Survey of Canada, Map 1524A, 1:250 000 scale.
1982: Geology, Ogilvie River; Geological Survey of Canada, Map 1526A, 1:250 000 scale.
1985: Geology of the northern Yukon and northwestern District of Mackenzie; Geological Survey of Canada, Map 1581A, 1:500 000 scale.

**Norris, D.K.** (cont.)

in press:   Triassic, Chapter 9; in The Geology, Mineral and Hydrocarbon Potential of the Northern Yukon and Northwestern District of Mackenzie, (ed.) D.K. Norris;   Geological Survey of Canada, Bulletin.

**Orchard, M.J.**

1991a:   Late Triassic conodont biochronology and biostratigraphy of the Kunga Group, Queen Charlotte Islands, British Columbia; in Evolution and Hydrocarbon Potential of the Queen Charlotte Basin, British Columbia, (ed.) G.J. Woodsworth; Geological Survey of Canada, Paper 90-10, p. 173-193.

**Orchard, M.J.** (cont.)

1991b:   Upper Triassic conodont biochronology and new index species from the Canadian Cordillera; in Ordovician to Triassic conodont paleontology of the Canadian Cordillera, (ed.) M.J. Orchard and A.D. McCracken; Geological Survey of Canada, Bulletin 417, p. 299-335.

# Detrital zircon ages from two wells in the Northwest Territories: implications for the correlation and provenance of Proterozoic subsurface strata

R.H. Rainbird[1], M.E. Villeneuve[2], D.G. Cook, and B.C. MacLean
GSC Calgary, Calgary

**Abstract:** Detrital zircons, extracted from industry well cores of Precambrian sandstones from the Colville Hills and Mackenzie Plains regions, indicate a marked contrast in the age of source material for two sampled intervals. A sample from Mobil E-15 (Colville Hills) contains zircons older than $1914 \pm 4$ Ma but younger than $2677 \pm 2$ Ma. Ten analyses suggest that most of the detritus was derived from the Taltson/Thelon magmatic zone or perhaps from the Hottah Terrain and its cryptic basement. A $2677 \pm 2$ Ma grain may have been derived from granite of the Slave Province. The E-15 sample likely represents strata intermediate in age between the Coronation Supergroup and the Mackenzie Mountains/Shaler supergroups, such as the Hornby Bay or Dismal Lakes groups.

A sample from PCI Sammons H-55 (Mackenzie Plains) contains zircons older than $1070 \pm 4$ Ma but younger than $1641 \pm 12$ Ma. The high percentage of concordant "Grenvillian" age zircons (6 of 9) indicates that the rock likely belongs to the Katherine Group of the Mackenzie Mountains Supergroup and supports a model for the existence of an ancient pan-continental river system draining the foreland of Grenville orogen.

**Résumé :** Des zircons détritiques, extraits de carottes prélevées par l'industrie dans les grès précambriens des collines Colville et des plaines du Mackenzie, indiquent un contraste marqué dans l'âge du matériau d'origine de deux intervalles échantillonnés. Une roche provenant du puits Mobil E-15 (collines Colville) contient des zircons plus anciens que $1\,914 \pm 4$ Ma mais plus récents que $2\,677 \pm 2$ Ma. Selon dix analyses, la plupart des débris proviennent de la zone magmatique de Taltson-Thelon ou peut-être du terrane de Hottah et de son socle cryptique. Un grain de $2\,677 \pm 2$ Ma pourrait provenir d'un granite de la Province des Esclaves. L'échantillon E-15 représente probablement des couches intermédiaires en âge, soit entre le Supergroupe de Coronation et les supergroupes de Mackenzie Mountains et de Shaler, comme les groupes de Hornby Bay ou de Dismal Lakes.

Un échantillon du puits PCI Sammons H-55 (plaines du Mackenzie) contient des zircons plus anciens que $1\,070 \pm 4$ Ma mais plus récents que $1\,641 \pm 12$ Ma. Le pourcentage élevé de zircons dont l'âge correspond au Grenvillien (6 sur 9) indique que la roche fait probablement partie du Groupe de Katherine (Supergroupe de Mackenzie Mountains); ces données corroborent un modèle selon lequel il aurait existé un ancien réseau fluvial pancontinetal drainant l'avant-pays de l'orogène de Grenville.

---

[1] 1725 Grasmere Crescent, Ottawa, Ontario K1V 7V1
[2] Continental Geoscience Division, Ottawa

# INTRODUCTION

Correlation of Mackenzie Mountains Supergroup strata in the northern Canadian Cordillera with Shaler Supergroup strata in the Amundsen Basin (Fig. 1) is relatively well established and accepted (e.g. Young et al., 1979; Aitken, 1982; Jefferson and Young, 1989; Hofmann and Rainbird, 1995; Rainbird et al., in press). A corroborating factor in making those correlations is the presence of concentrations of Grenville Province age (~1400-1000 Ma) detrital zircons in a well defined quartz arenite marker horizon at a number of locations both in the Cordillera and Amundsen Basin (Rainbird et al., 1992; Rainbird et al., 1994; Rainbird and McNicoll, unpub. data, 1994). The age and correlation of Proterozoic strata in the intervening subsurface of the Colville Hills region is much less certain. There, strata immediately underlying the sub-Cambrian unconformity were initially correlated with the Mackenzie Mountains Supergroup (e.g., Aitken and Pugh, 1984; Cook, 1988; Cook and Mayers, 1990). Others (e.g., Young, 1977; Jefferson and Young, 1989; Rainbird et al., in press) interpreted Mackenzie Mountains and Shaler super-groups to flank a broad continental upland (Fig. 1) and therefore to be absent under the Colville Hills, where Proterozoic strata were unspecified but clearly older than Mackenzie Mountains Supergroup. Cook and MacLean (in press) subdivided the Proterozoic underlying Colville Hills into three unconformity bounded sequences, which they correlated with the Hornby Bay, Dismal Lakes, and Coppermine River groups of Coppermine Homocline. Those correlations were made on the basis of a variety of structural and stratigraphic comparisons with the homocline sequence, but nonetheless were interpretive due to the absence of chronostratigraphic control.

One method of gaining age control for the seismic-based interpretations is to indirectly date the clastic intervals using U-Pb zircon geochronology. Detrital zircon analysis simply provides a maximum age (sediments must postdate the youngest zircon), but by comparing zircon analyses of different units it is possible to infer relative ages based on the age distribution of the analyzed zircons. This report deals with detrital zircons obtained from drill core from two petroleum exploration wells, PCI Sammons H-55, from the Mackenzie Plain near the Mackenzie Mountains front, and Mobil Colville E-15, from the Colville Hills region (Fig. 1).

# DESCRIPTION OF SAMPLES

Samples were selected for detrital zircon analysis on the basis of coarsest grain size to obtain the largest possible zircon grains, and highest quartz content (highest maturity) for greatest possible yield. Only very small samples were permitted owing to the destructive nature of the analytical process and to the lack of available core.

In the Colville E-15 well (Fig. 1, 2, 3), 300 m (1529-1829 m) of sedimentary strata were cored beneath the sub-Cambrian unconformity. The core consists mainly of a fine grained siliciclastic sequence with an approximately 70 m thick stromatolitic carbonate in the lower third of the section (Fig. 3). The sample collected for detrital zircon geochronology included several small pieces of material from coarser grained intervals between 1637 and 1697 m. The core is essentially homogenous over this part of the section and is characterized by wavy- to lenticular-bedded very fine- to fine-grained grey sandstone and black siltstone and mudstone. Grading is common in the sandstone layers and some of the thicker beds show low-angle crossbedding. The sample collected for analysis is a very fine grained sublitharenite to quartz arenite. Mean grain size is about 0.07 mm and grains are subangular to subrounded and well sorted. A small hand specimen exhibits thick parallel-laminated grey sand with thin darker grey silt interlaminations.
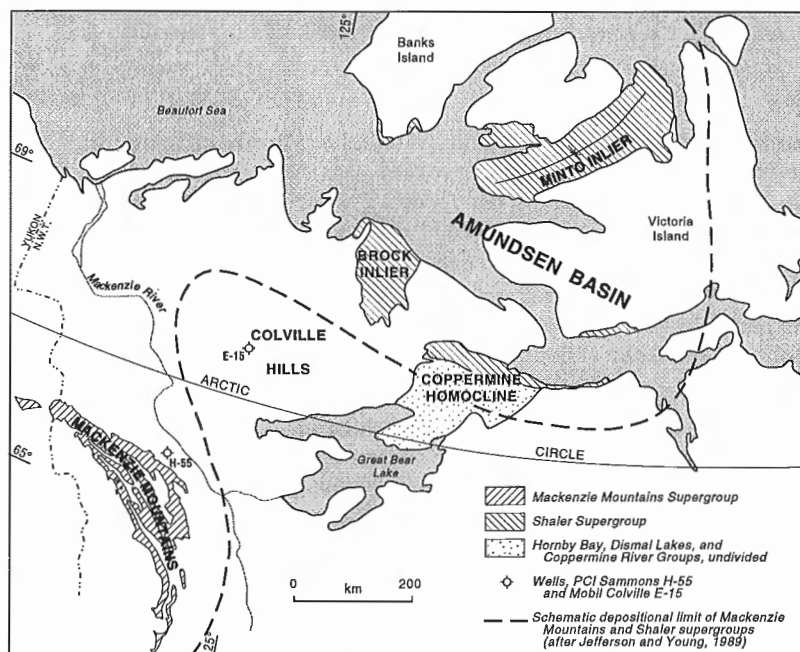


***Figure 1.***

*Location map showing the location of wells E-15 and H-55, and Mackenzie Mountains/ Shaler supergroups limit (after Jefferson and Young, 1989).*

In the Sammons H-55 well (Fig. 1, 4), only two short segments of Proterozoic strata were cored. The lowermost (1687.8-1695.2 m) is green, parallel-laminated siltstone with interbeds of buff, very fine- to fine-grained quartz arenite, increasing in thickness and abundance upsection. The lowermost part of the section is composed of about 2 m of thinly laminated mudstone overlain by thick-laminated green siltstone. Load structures are common at the bases of the sandstone beds. This latter feature suggests rapid deposition on an unstable slope and, together with the coarsening upward aspect, a prograding depositional environment such as a river-dominated delta is envisaged.

The upper segment (1449.0-1452.1 m), from which the detrital zircon sample was collected, is a fine- to coarse-grained, feldspathic sublitharenite. It is massive to faintly parallel-stratified and cross-stratified and is buff to pink with ubiquitous red hematite spotting. Mean grain size is about 0.5 mm (medium-coarse sand) and grains are subangular to well rounded. The rock is well indurated by pervasive syntaxial quartz cement; red colouration is attributable to earlier diagenetic hematite cementation. Framework components include a high percentage of strained quartz (~50%) and sedimentary rock fragments, mostly chert (15%). Heavy minerals are rare except for a few well-rounded grains of zircon.
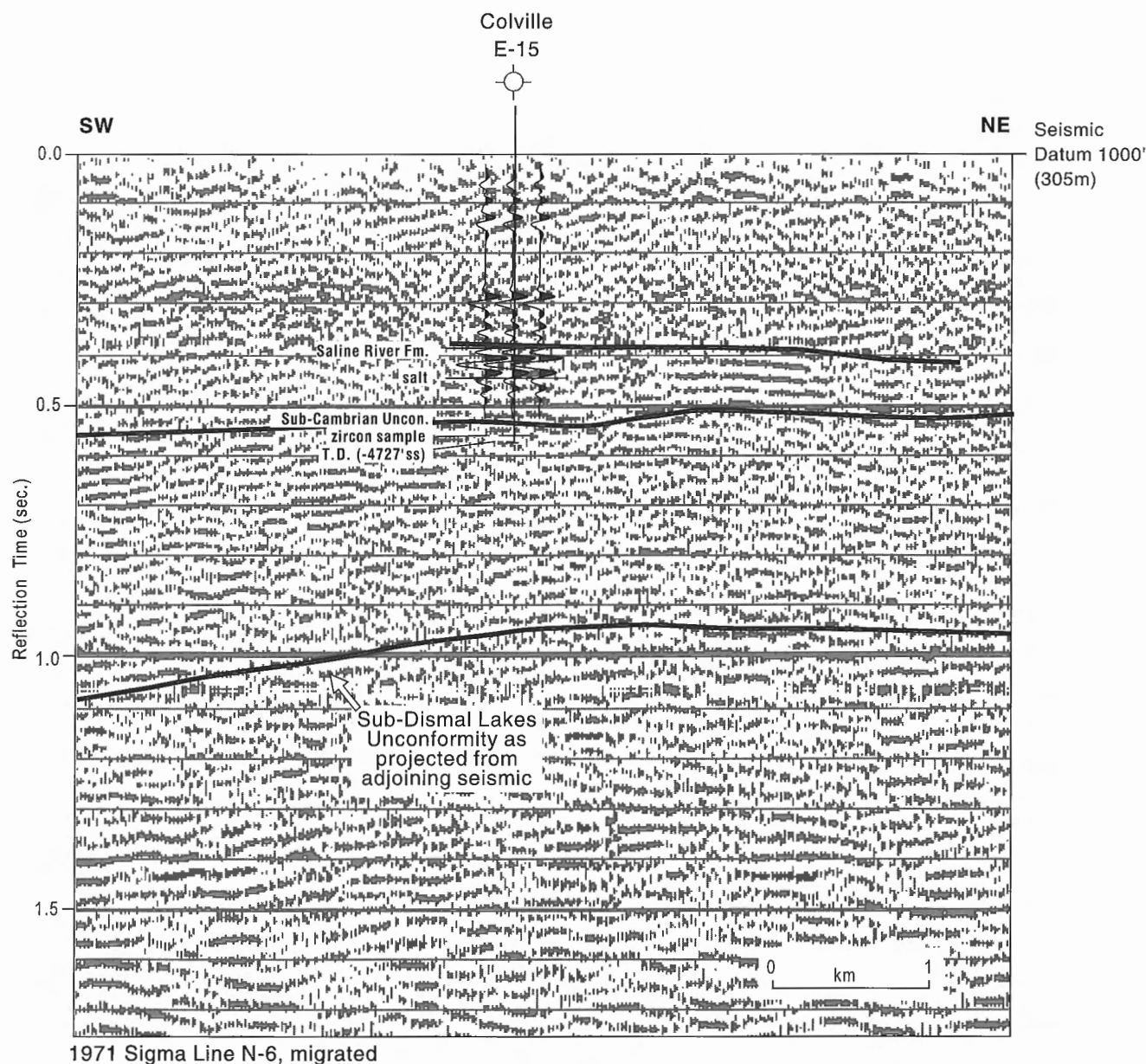


*Figure 2. Synthetic seismogram and seismic section for Colville E-15 well.*

31

# Colville E-15

Cambrian (Mt. Clark Fm.)
Proterozoic

red/green variegated above this point

1600m

sample Z3893

basalt flow?

1700m

dolostone

### SYMBOLS

| | |
|---|---|
| ~ | wavy bedding |
| ⌒ | starved ripple |
| ⫶⫶⫶ | ripple crosslamination |
| ⫴⫴ | crossbedding |
| ● | chert alteration |
| V V | desiccation cracks |
| ∿ | soft-sediment folding |
| ⌣ | load structure |
| ⌁ | intraformational breccia |
| ≋ | crinkly microbial lamination |
| G | glauconite |

G

G

G

G

G

1800m

V V

coarse intraformational breccia

silt
very fine sand
medium sand
conglomerate

*Figure 3. Graphic representation of cored segment of Colville E-15 examined in this study and location of sampled interval.*

# GEOCHRONOLOGY

## Methodology

Samples were processed using standard techniques described in Parrish et al. (1987). Each fraction analyzed consisted of a single grain, 0.074 to 1.00 mm in diameter, abraded to remove the outer portions, which are most susceptible to Pb-loss (Krogh, 1982) and thereby increase concordance. Data have been reduced and errors propagated using numerical methods of Roddick (1987). Data are presented in Table 1, and errors on $^{207}Pb/^{206}Pb$ ages are given at the 95% confidence level. The degree of discordance is calculated as the per cent discordance from concordia, calculated on a line passing through the analysis point and the origin. Only clear, coreless and

inclusion-free grains were selected to reduce the risk of discordance. Zircons from both samples show a high degree of rounding by natural abrasion, and in general are colourless anhedral crystals with a length:width ratio ranging from 1:1 to 3:1. All grains have rounded edges and terminations, with some frosting of the grain surface. Analytical results are plotted on Figure 5; errors for individual analyses are given in Table 1.

## U-Pb results

The data indicate that inheritance and Pb-loss are negligible in most analyses (<2.5% discordance) and therefore the $^{207}Pb/^{206}Pb$ age determinations represent the primary crystallization ages of the source rocks. The data also illustrate
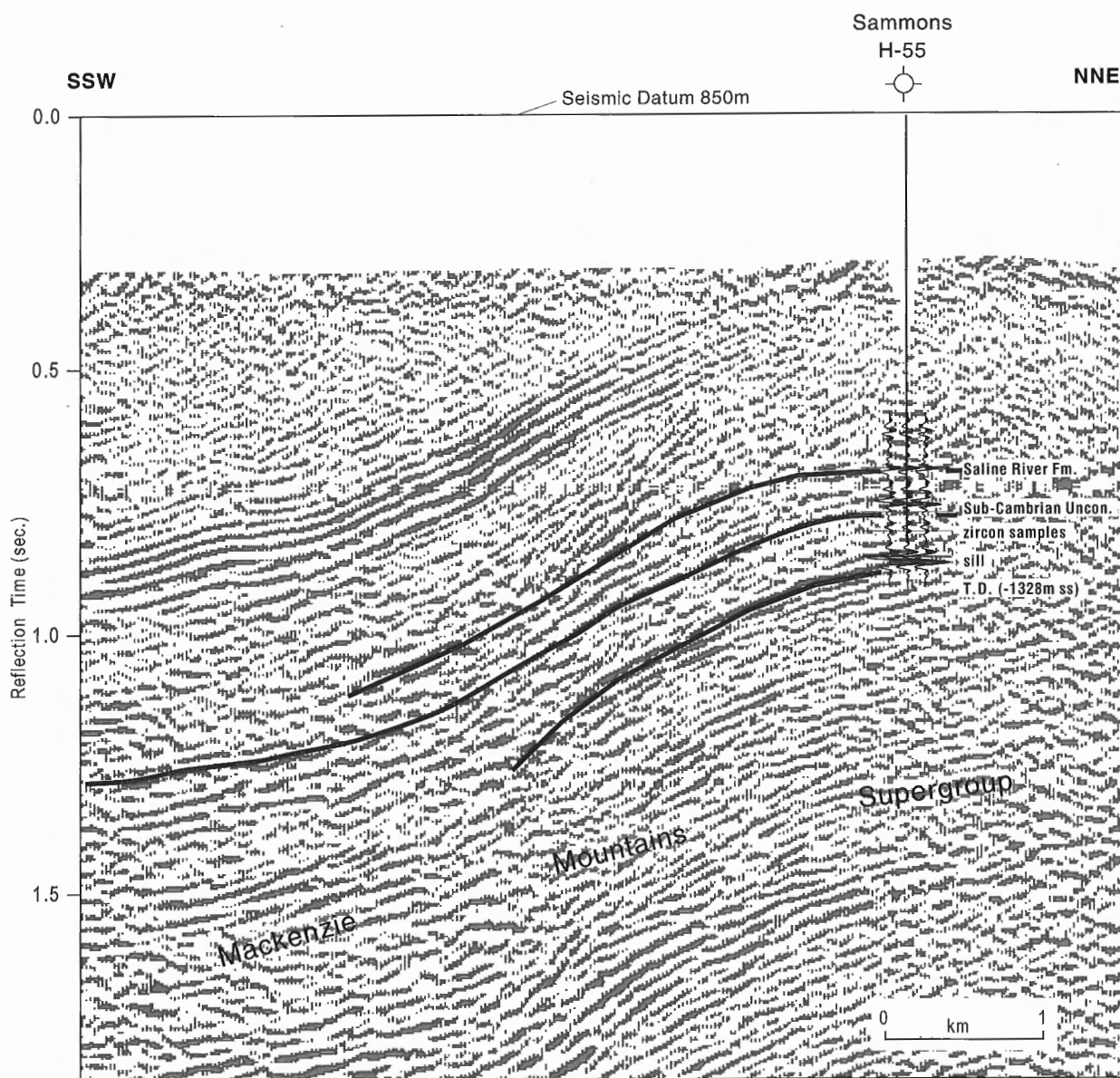


**Figure 4.** *Synthetic seismogram and seismic section for PCI Sammons H-55 well.*

**Table 1.** U-Pb data.

| Fraction[a] | Wt.[b] μg | U ppm | Pb[c] ppm | $\frac{206Pb[d]}{204Pb}$ | Pb[e] pg | $\frac{208Pb[f]}{206Pb}$ | Radiogenic ratios (±1σ, %)[f] $\frac{207Pb}{235U}$ | $\frac{207Pb}{206Pb}$ | $\frac{207Pb}{206Pb}$ | $\frac{207Pb}{206Pb}$ Age (Ma)[g] | Discord.[h] % |
|---|---|---|---|---|---|---|---|---|---|---|---|
| E-15 MOBIL COLVILLE SANDSTONE (Z3893; 67.2384°N 126.3071°E) | | | | | | | | | | | |
| A (Z) | 3 | 32 | 16 | 453 | 5 | 0.220 | 8.721±0.38 | 0.4177±0.43 | 0.15141±0.30 | 2362±10 | 5.60 |
| B (Z) | 5 | 188 | 73 | 896 | 22 | 0.200 | 5.553±0.17 | 0.3437±0.11 | 0.11719±0.11 | 1914±4 | 0.57 |
| C (Z) | 2 | 165 | 67 | 1170 | 1 | 0.260 | 5.530±0.17 | 0.3418±0.15 | 0.11732±0.10 | 1916±4 | 1.23 |
| D (Z) | 4 | 123 | 47 | 1655 | 5 | 0.270 | 5.034±0.15 | 0.3198±0.15 | 0.11415±0.10 | 1867±4 | 4.77 |
| E (Z) | 4 | 89 | 41 | 1854 | 5 | 0.110 | 8.485±0.16 | 0.4193±0.14 | 0.14676±0.09 | 2309±3 | 2.64 |
| F (Z) | 5 | 365 | 133 | 3857 | 9 | 0.130 | 5.529±0.11 | 0.3399±0.09 | 0.11799±0.04 | 1926±2 | 2.40 |
| G (Z) | 3 | 53 | 28 | 192 | 25 | 0.180 | 9.951±0.52 | 0.4549±0.28 | 0.15867±0.40 | 2442±13 | 1.22 |
| H (Z) | 4 | 54 | 30 | 1127 | 6 | 0.100 | 12.706±0.21 | 0.5047±0.21 | 0.18260±0.06 | 2677±2 | 1.94 |
| I (Z) | 2 | 233 | 108 | 806 | 17 | 0.090 | 9.348±0.16 | 0.4282±0.12 | 0.15832±0.10 | 2438±3 | 6.83 |
| J (Z) | 3 | 116 | 45 | 1792 | 2 | 0.200 | 5.463±0.20 | 0.3380±0.19 | 0.11723±0.13 | 1914±5 | 2.25 |
| H-55 SAMMONS SANDSTONE (Z3894; 65.4077°N 128.4126°E) | | | | | | | | | | | |
| A (Z) | 5 | 102 | 26 | 639 | 11 | 0.200 | 2.795±0.31 | 0.2341±0.22 | 0.08658±0.26 | 1351±10 | -0.41 |
| B (Z) | 3 | 156 | 40 | 545 | 12 | 0.120 | 3.044±0.31 | 0.2446±0.19 | 0.09026±0.24 | 1431±9 | 1.60 |
| C (Z) | 5 | 123 | 26 | 1710 | 4 | 0.140 | 2.210±0.21 | 0.2017±0.20 | 0.07945±0.16 | 1183±6 | -0.10 |
| D (Z) | 3 | 295 | 54 | 1342 | 8 | 0.090 | 1.872±0.17 | 0.1809±0.13 | 0.07507±0.10 | 1070±4 | -0.15 |
| E (Z) | 5 | 40 | 9 | 450 | 6 | 0.170 | 2.372±0.56 | 0.2124±0.45 | 0.08099±0.27 | 1221±11 | -1.84 |
| F (Z) | 3 | 131 | 32 | 1145 | 3 | 0.110 | 2.907±0.30 | 0.2379±0.25 | 0.08864±0.18 | 1396±7 | 1.65 |
| H (Z) | 3 | 91 | 28 | 390 | 13 | 0.140 | 4.033±0.50 | 0.2899±0.37 | 0.10089±0.34 | 1641±12 | -0.03 |

[a] All zircon fractions are abraded; (Z)=zircon, T=titanite
[b] Error on weight =±0.001 mg
[c] Radiogenic Pb
[d] Measured ratio corrected for spike and Pb fractionation of 0.09±0.03%/AMU
[e] Total common Pb on analysis corrected for fractionation and spike, of blank model Pb composition
[f] Corrected for blank and spike Pb and U and common Pb (Stacey-Kramers model Pb composition equivalent to the $^{207}$Pb/$^{206}$Pb age)
[g] Age error is ±2SE in Ma
[h] Discordance along a discordia to origin.
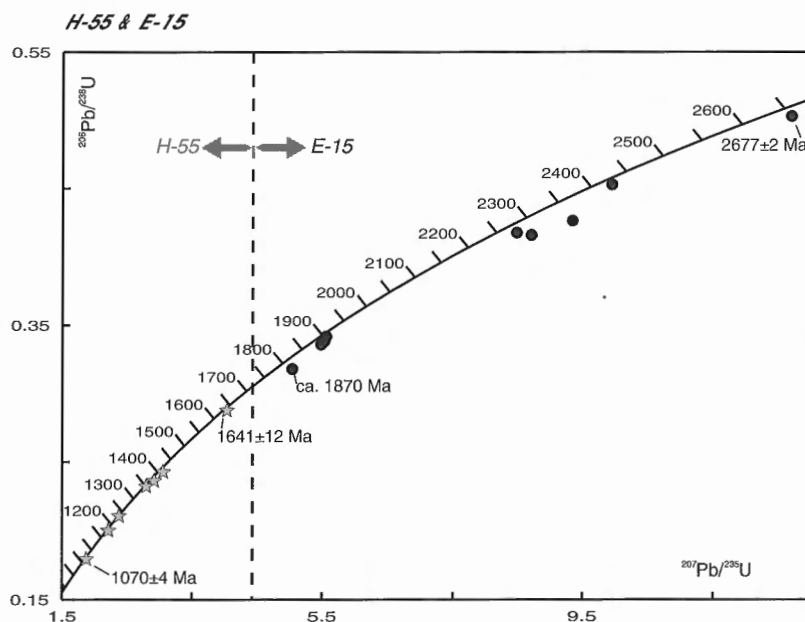


*Figure 5.* *Analytical results.*

the marked contrast in the age of source material between the two sampled intervals.

Samples of Proterozoic quartzite from Sammons H-55 (Fig. 4) yielded zircons with ages ranging from 1070 Ma to 1641 Ma. The samples are from an interval assigned by Wissner (1986) to the Tsezotene Formation of the Mackenzie Mountains Supergroup. The ages of five of six concordant zircons fall in the range 1000 Ma to 1450 Ma and thus provide further documentation of a Grenville-age source area for Mackenzie Mountains Supergroup strata and further support for the correlation of Mackenzie Mountains and Shaler supergroups.

Samples from Colville E-15 (Fig. 3), from strata which Cook and MacLean (in press) considered equivalent to the Dismal Lakes Group (younger than 1663 Ma and older than 1267 Ma), yielded zircons with ages ranging from 1914 Ma to 2677 Ma. The strata are thus younger than 1914 Ma, and are compatible with either a Dismal Lakes Group or a Hornby Bay Group assignment. The E-15 material is of three distinct ages: 1914 Ma, 2300 to 2450 Ma, and ca. 2680 Ma. The significance of the analysis with the youngest age of 1867 ± 4 Ma is difficult to ascertain because the sample is close to 5% discordant and assumptions about Pb-loss or inheritance cannot be adequately constrained.

## PROVENANCE

Paleocurrent data for the Hornby Bay and Dismal Lakes groups (Kerans et al., 1981) show variable transport from southwest to northwest, compatible with a broad potential source region to the east. Two possible source terranes for the Colville E-15 sample occur in the western Canadian Shield. The detrital zircons could have come from the Talston/Thelon magmatic zone (van Breemen et al., 1992a), with batholithic rocks providing the 1914 Ma material, and the basement of the Taltson/Thelon magmatic zone providing the 2300 to 2450 Ma material (Bostock and van Breemen, 1994). Such a source may be from due east in the exposed part of the belt, or from the southeast in a part of the belt covered by Phanerozoic strata, with the 2.0 to 2.4 Ga Buffalo Head domain (Ross et al., 1991; Villeneuve et al., 1993) as an alternative source. Another potential source of 1914 Ma material could be the Hottah Terrane, a 1.94 to 1.90 Ga volcanic arc that occupies the western exposed edge of Wopmay orogen (Hildebrand et al., 1987). The 2300 to 2450 Ma zircons therefore might represent the cryptic basement to the Hottah Terrane, interpreted to be juvenile crust of 2.0 to 2.4 Ga age on the basis of tracer isotope studies (Bowring and Podosek, 1989). The more discordant analyses, among the 2300 to 2450 Ma material (Table 1), could be zircon grains with cryptic cores derived from younger or older sources. The 2677 ± 2 grain represents a typical age for magmatism accompanying cratonization of the Slave Province (cf. van Breeman et al., 1992b).

The feldspathic sublitharenite sample from Sammons H-55 yielded a suite of mainly concordant age determinations that are comparable to suites of detrital zircons from Mackenzie Mountains and Shaler supergroups. Although it is presently impossible to pinpoint exact sources for these zircons, it is possible to make some generalizations concerning their provenance. All of the concordant analyses in this sample can be matched to potential source regions in the Laurentian segment of Grenville orogen. As indicated elsewhere (Rainbird et al., 1992), this is compatible with regionally consistent northwest paleocurrents from correlative rocks in the Mackenzie Mountains and Amundsen Basin. It also is consistent with other criteria, which would permit long distance fluvial transport of detritus shed from the rising Grenville Orogen (op. cit.). Zircons with U-Pb ages between 1070 and 1350 Ma were likely formed during synorogenic plutonic activity accompanying the mainly collisional phases of the Grenvillian orogeny. Older ages can be matched to anorogenic plutonism which predated the principal orogenic phases but which are now preserved within the broad northeast-trending belt known as the Grenville Province (see Fig. 5 of Davidson, 1995 for a summary of Grenville geochronology).

## DISCUSSION

### Colville E-15

Detrital zircon geochronology of the Colville E-15 sample indicates that it is younger than 1914 ± 4 Ma. This is not particularly definitive, but some deductive eliminations can be made. The rock is unlikely to be as old as Coronation Supergroup. Most of it, and its equivalents, are older than 1914 Ma (Bowring and Grotzinger, 1992) and the rocks show no evidence of the penetrative deformation that characterizes Coronation Supergroup strata in the nearest exposures of Wopmay orogen to the east (Hoffman et al., 1988). The suite of age determinations for the sample (Fig. 5) includes no "Grenvillian" or Mesoproterozoic ages, such as those that uniquely distinguish detrital zircon analyses of the Shaler and Mackenzie Mountains supergroups and equivalent sandstones from this region (e.g., Sammons H-55 sample; Rainbird et al., 1992; Rainbird et al., 1994; and Rainbird and McNicoll, unpub. data, 1994). The rock, therefore, is likely intermediate in age between the Coronation Supergroup and the Mackenzie Mountains Supergroup (i.e., 1914-1000 Ma). Two successions exposed on Coppermine Homocline are possible candidates: the Hornby Bay Group (1840-1663 Ma; Bowring and Ross, 1985; Bowring and Grotzinger, 1992) and Dismal Lakes Group (1663-1270 Ma; Bowring and Ross, 1985; LeCheminant and Heaman, 1989). Although seismic data in the vicinity of E-15 are of poor quality (Fig. 2), we consider the E-15 beds to be equivalent to some part of the Dismal Lakes Group on the basis of regional seismic interpretation (Cook and MacLean, in press). The detrital-zircon ages are compatible with that interpretation, but do not preclude correlation with the Hornby Bay Group.

Direct unit-by-unit lithological correlations are hazardous because the Colville Hills are nearly 300 km west of the most westward exposures of Hornby Bay and Dismal Lakes groups (Fig. 1). Paleogeographic information indicates that the position of Colville E-15 would have been basinward of the present day exposures in Coppermine Homocline so similar

lithofacies might not be expected. Moreover, the 300 m section in E-15 is but a fraction of the greater than 8 km (about 2.5 seconds) of Proterozoic rock in the vicinity of the well.

The sandstone and siltstone-mudstone in E-15 resemble rocks from the basal Dismal Lakes and upper Hornby Bay successions described by Kerans et al. (1981). It is possible that the underlying carbonate unit is equivalent to the East River Formation carbonates in the upper part of the Hornby Bay Group (Ross and Kerans, 1989) which contains numerous intraformational breccias and similar shallow water depositional features to those described in Colville E-15. Overlying siliciclastic strata could be equivalents of the Kaertok, LeRoux, or Fort Confidence formations (Ross and Kerans, 1989) which are dominated by features, such as wavy and lenticular bedding, small-scale crossbedding, desiccation features, and variegated beds (see descriptions of units 10, 11, and 12 in Kerans et al., 1981).

Alternatively, the carbonate beds in the lower part of E-15 could be equivalent to one of a number of stromatolitic units with intraformational breccias in the Dease Lake, Sulky, or Greenhorn Lakes formations at the top of the Dismal Lakes Group. However, in that rationale, the fine grained siliciclastic strata in E-15 would have no lithological counterpart on the homocline.

### Sammons H-55

The ages of dated detrital zircons from the Sammons H-55 quartz arenite are distinctly different from the Colville E-15 sample and imply a much younger stratigraphic level. The interval we examined appears to be of Proterozoic age, owing to the absence of body and trace fossils. The youngest zircon age (Fig. 5) implies that the rock must be younger than 1074 Ma and therefore belongs to either the Neoproterozoic Mackenzie Mountains Supergroup (~1000-750 Ma) or to the Windermere Supergroup (~750-550 Ma). Correlation with the Windermere Supergroup is unlikely because the Windermere is typified by cycles of coarse, immature to fine, basinal clastics overlain by shallower water carbonates (Aitken, 1989; Narbonne and Aitken, 1995). Wissner (1986) assigned the Proterozoic section in H-55 to the Tsezotene Formation of the Mackenzie Mountains Supergroup, although no criteria were cited. Finer grained, variegated rhythmites from the lower cored segment, 240 m stratigraphically below the sampled segment, might represent delta slope deposits of the lower Katherine Group or red member of the Tsezotene Formation (Long, 1991). The well cuttings log for H-55, prepared by Canadian Stratigraphic Services Ltd. (1988), and synthetic seismic data (Fig. 4) indicate a mafic sill in the uncored segment between the two sections of core. Sills are noticeably absent from outcrops of Katherine Formation, but are widespread in the Tsezotene, thus lending strong support to the idea that the lower part of the H-55 section is the Tsezotene Formation. Although the upper cored quartz arenite section from Sammons H-55 is only 3 m thick, its textural and compositional maturity point to siliciclastic

deposition in a shallow water marine or terrestrial environment more alike the delta-top quartz arenites of the Katherine Group (Mackenzie Mountains Supergroup; Aitken and McMechan, 1991; D. Long, pers. comm., 1994). Moreover, Katherine Group quartzites outcrop in the Mackenzie Mountains, only about 25 km away.

The most definitive case for assigning the upper cored (sampled) segment of Sammons H-55 to the Katherine Group can be made by comparing the distribution of concordant U-Pb zircon age determinations (Fig. 5) with similar determinations from an outcrop sample of the Katherine Group from the nearby Mackenzie Mountains, along with several quartz arenite samples from correlative units in the northern Cordillera and Amundsen Basin (see Rainbird et al., 1992; Rainbird et al., 1994; Rainbird and McNicoll, unpub. data, 1994). All samples contain a representative scattering of "Grenvillian" (1400-1000 Ma) ages and very little else (see Provenance), suggesting that they are correlative and part of the same huge braided fluvial system that originated from the foreland of Grenville orogen.

## CONCLUSIONS

Detrital zircons from Colville E-15 establish the containing strata to be younger than 1914 Ma. Detritus was apparently derived from the east, either from the Taltson/Thelon Magmatic Zone or perhaps from the Hottah Terrain and its cryptic basement. An older grain (2677 Ma) likely represents granite from the Slave Province. Because the suite of age determinations includes no "Grenvillian" ages, characteristic of detrital zircons from the Shaler and Mackenzie Mountains supergroups, the E-15 strata likely belong to a succession of intermediate age between the Coronation Supergroup and the Mackenzie Mountains/Shaler supergroups (i.e., 1914-1000 Ma). The Hornby Bay and Dismal Lakes groups exposed on Coppermine Homocline are candidates. Cook and MacLean (in press) considered the section to be equivalent to Dismal Lakes Group, whereas lithologically the section is perhaps more readily compared to the upper part of the Hornby Bay Group. Identification of Hornby Bay strata at the sub-Cambrian unconformity would imply a Proterozoic uplift at this locale. Seismic data in the vicinity of E-15 are of too poor quality to confidently resolve this question.

Detrital zircons from Sammons H-55 establish the containing strata to be younger than 1070 Ma. The high percentage of concordant "Grenvillian" age detrital zircons in the upper cored segment of the drill hole is significant because it establishes, with a high degree of certainty, that the rock belongs to the Katherine Group of the Mackenzie Mountains Supergroup. Also, in concert with parallel detrital zircon studies, it establishes that Grenville Province detritus was shed over a wide area of northwestern Canada, lending further support for the existence of an ancient pan-continental river system draining the foreland of Grenville orogen.

# REFERENCES

**Aitken, J.D.**
1982: Precambrian of the Mackenzie Fold-Belt – a stratigraphic and tectonic overview; in Precambrian Sulfide Deposits, H.S. Robinson Memorial Volume, (ed.) R.W. Hutchinson, C.D. Spence, and J.M. Franklin; Geological Association of Canada, Special Paper 25, p. 149-161.
1989: Uppermost Proterozoic formations in central Mackenzie Mountains, Northwest Territories; Geological Survey of Canada, Bulletin 368, 26 p.

**Aitken, J.D. and Pugh, D.C.**
1984: The Fort Norman and Leith Ridge structures: Major, buried, pre-Cambrian features underlying Franklin Mountains and Great Bear and Mackenzie Plains; Bulletin of Canadian Petroleum Geology, v. 32, p. 139-146.

**Aitken, J.D. and McMechan, M.E.**
1991: Middle Proterozoic assemblages, Chapter 5 in Geology of the Cordilleran Orogen in Canada, (ed.) H. Gabrielse, and C.J. Yorath; Geological Survey of Canada, p. 97-102 (also Geological Society of America, The Geology of North America, v. G-2).

**Bostock, H.H. and van Breemen, O.**
1994: Ages of detrital and metamorphic zircons and monazites from a pre-Taltson magmatic zone basin at the western margin of Rae Province; Canadian Journal of Earth Sciences, v. 31, p. 1353-1364.

**Bowring, S.A. and Grotzinger, J.P.**
1992: Implications of new chronostratigraphy for tectonic evolution of Wopmay Orogen, northwest Canadian Shield; American Journal of Science, v. 292, p. 1-20.

**Bowring, S.A. and Ross, G.M.**
1985: Geochronology of the Narakay volcanic complex: implications for the age of the Coppermine homocline and Mackenzie igneous events; Canadian Journal of Earth Sciences, v. 22, p. 774-781.

**Bowring, S.A. and Podosek, F.A.**
1989: Nd isotopic evidence from Wopmay Orogen for 2.0-2.4 Ga crust in western North America; Earth and Planetary Science Letters, v. 94, p. 217-230.

**Canadian Stratigraphic Services Ltd.**
1988: PCI Sammons H-55, N 65°24'28" W 128°24'45", Northwest Territories - Canada, Log No. NWT-711.

**Cook, D.G. and MacLean, B.C.**
in press: The intra-cratonic Paleoproterozoic Forward Orogeny, and implications for regional correlations, Northwest Territories, Canada; Canadian Journal of Earth Sciences.

**Cook, D.G. and Mayers, I.R.**
1990: Precambrian structure and stratigraphy based on seismic interpretation, Colville Hills region, Northwest Territories; in Current Research, Part C; Geological Survey of Canada, Paper 90-1C, p. 339-348.

**Cook, F.A.**
1988: Proterozoic thin-skinned thrust and fold belt beneath the Interior Platform in northwest Canada; Geological Society of America Bulletin, v. 100, p. 877-890.

**Davidson, A.**
1995: A review of the Grenville orogen in its North American type area; AGSO Journal of Australian Geology and Geophysics, v. 16, p. 3-24.

**Hildebrand, R.S., Hoffman, P.F., and Bowring, S.A.**
1987: Tectono-Magmatic evolution of the 1.9 Ga Great Bear Magmatic Zone, Wopmay Orogen, northwestern Canada; Journal of Volcanology and Geothermal Research, v. 32, p. 99-118.

**Hoffman, P.F., Tirrul, R., King, J.E., St. Onge, M.R., and Lucas, S.B.**
1988: Axial projections and modes of crustal thickening, eastern Wopmay Orogen, northwest Canadian Shield; in Processes in continental lithospheric deformation, (ed.) S.B. Clark Jr., B.C. Burchfiel, and J. Suppe; Geological Society of America, Special Paper 218, p. 1-19.

**Hofmann, H.J. and Rainbird, R.H.**
1995: Carbonaceous megafossils from Neoproterozoic Shaler Supergroup, Victoria Island, Arctic Canada; Paleontology, v. 37, p. 721-731.

**Jefferson, C.W. and Young, G.M.**
1989: Late Proterozoic orange-weathering stromatolite biostrome, Mackenzie Mountains and western Arctic Canada; in Reefs, Canada and Adjacent Area, (ed.) H.H.J. Geldsetzer, N.P. James, and G.E. Tebbutt; Canadian Society of Petroleum Geologists, Memoir 13, p. 72-80.

**Kerans, C., Ross, G.M., Donaldson, J.A., and Geldsetzer, H.J.**
1981: Tectonism and depositional history of the Helikian Hornby Bay and Dismal Lakes Groups, District of Mackenzie; in Proterozoic Basins of Canada, (ed.) F.H.A. Campbell; Geological Survey of Canada, Paper 81-10, p. 157-182.

**Krogh, T.E.**
1982: Improved accuracy of U-Pb zircon ages by the creation of more concordant systems using an air abrasion technique; Geochimica et Cosmochimica Acta, v. 46, p. 637-649.

**LeCheminant, A.N. and Heaman, L.M.**
1989: Mackenzie igneous events, Canada: Middle Proterozoic hotspot magmatism associated with ocean opening; Earth and Planetary Science Letters, v. 96, p. 38-48.

**Long, D.G.F.**
1991: The Tzesotene Formation: a prograding muddy shelf deposit in the Mackenzie Mountains, N.W.T.; Geological Association of Canada and Mineralogical Association of Canada, Program with Abstracts, v. 16, p. A75.

**Narbonne, G.M. and Aitken, J.D.**
1995: Neoproterozoic of the Mackenzie Mountains, northwestern Canada; Precambrian Research, v. 73, p. 101-121.

**Parrish, R.R., Roddick, J.C., Loveridge, W.D., and Sullivan, R.W.**
1987: Uranium-lead analytical techniques at the geochronology laboratory, Geological Survey of Canada; in Radiogenic age and isotope studies: Report 1; Geological Survey of Canada, Paper 88-2, p. 3-7.

**Rainbird, R.H., Heaman, L.M., and Young, G.M.**
1992: Sampling Laurentia: detrital zircon geochronology offers evidence for an extensive Neoproterozoic river system originating from the Grenville orogen; Geology, v. 20, p. 351-354.

**Rainbird, R.H., Jefferson, C.W., and Young, G.M.**
in press: The early Neoproterozoic Succession B of northwestern Laurentia: correlations and paleogeographic significance; Geological Society of America Bulletin.

**Rainbird, R.H., McNicoll, V.J., and Heaman, L.M.**
1994: Detrital zircon studies of Neoproterozoic quartzarenites from northwestern Canada: additional support for an extensive river system originating from Grenville orogen; in Eighth International Conference on Geochronology, Cosmochronology and Isotope Geology, p. 258.

**Roddick, J.C.**
1987: Generalized numerical error analysis with applications to geochronology and thermodynamics; Geochimica and Cosmochimica Acta, v. 51, p. 2129-2135.

**Ross, G.M. and Kerans, C.**
1989: Geology, Hornby Bay and Dismal Lakes groups, Coppermine Homocline, District of Mackenzie, Northwest Territories; Geological Survey of Canada, Map 1663A, scale 1:250 000.

**Ross, G.M., Parrish, R.R., Villeneuve, M.E., and Bowring, S.A.**
1991: Geophysics and geochronology of the crystalline basement of the Alberta Basin, western Canada; Canadian Journal of Earth Sciences, v. 28, p. 512-522.

**van Breemen, O., Bostock, H.H., and Loveridge, W.D.**
1992a: Geochronology of granites along the margin of the northern Taltson Magmatic zone and western Rae Province, Northwest Territories; in Radiogenic Age and Isotopic Studies: Report 5; Geological Survey of Canada, Paper 91-2, p. 17-24.

**van Breemen, O., Davis, W.J., and King, J.E.**
1992b: Temporal distribution of granitoid plutonic rocks in the Archean Slave Province, northwest Canadian Shield; Canadian Journal of Earth Sciences, v. 29, p. 2186-2199.

**Villeneuve, M.E., Ross, G.M., Theriault, R.J., Miles, W., Parrish, R.R., and Broome, J.**
1993:   Tectonic subdivision and U-Pb geochronology of the crystalline basement of the Alberta Basin, western Canada; Geological Survey of Canada, Bulletin 447, 86 p.

**Wissner, U.**
1986:   A new look at the Imperial Anticlinorium, Mackenzie Plain Northwest Territories; Program and Abstracts, Canadian Society of Petroleum Geologists, 1986 Convention, p. 97.

**Young, G.M.**
1977:   Stratigraphic correlation of Upper Proterozoic rocks of northwestern Canada; Canadian Journal of Earth Sciences, v. 14, p. 1771-1787.

**Young, G.M., Jefferson, C.W., Delaney, G.D., and Yeo, G.M.**
1979:   Middle and Upper Proterozoic evolution of the northern Canadian Cordillera and Shield; Geology, v. 7, p. 125-128.

# Carboniferous-Permian strata in the Unak L-28 and adjacent wells, Mackenzie Delta, Northwest Territories

J. Dixon, B.L. Mamet[1], and J.H. Wall
GSC Calgary, Calgary

**Abstract:** Although the presence of Carboniferous strata in the subsurface of Mackenzie Delta has been reported in some wells, paleontological data to support this claim has not yet been published. In Unak L-28, Carboniferous and Permian strata are identified between log depths 2470 and 3190 m based on paleontological data and regional comparisons. Microfossils indicate that between about 2969 and 3175 m, the predominantly limestone succession is Serpukhovian to Bashkirian (Carboniferous) in age. Strata between 2745 and 2969 m, consisting of interbedded calcareous sandstone, sandy limestone, and shale, contain a very different fossil assemblage, believed to be Permian in age. Between 2470 and 2745 m, the shale and siltstone succession contains a predominantly arenaceous foraminiferal assemblage that, although it contains no age-specific fossils, is comparable to assemblages in the Permian in the nearby northern Richardson Mountains. Correlative Carboniferous strata have been penetrated only in Kugpik O-13 and Napoiak F-31, and Permian beds are known from Aklavik A-37 and F-38, Beaverhouse Creek H-13, Ulu A-35, Unak B-11, Tullugak K-31, and Kugpik L-24, as well as in Kugpik O-13 and Napoiak F-31.

**Résumé :** Même si la présence de couches carbonifères a été signalée dans certains puits forés dans le sous-sol du delta du Mackenzie, les données paléontologiques appuyant ce fait n'ont pas encore été publiées. Dans le puits Unak L-28, des couches carbonifères et permiennes ont été recoupées entre 2 470 m et 3 190 m de profondeur, leur identification reposant sur des données paléontologiques et des comparaisons régionales. Les microfossiles indiquent que, entre environ 2 969 m et 3 175 m, la succession principalement calcaire date du Serpukhovien au Bashkirien (Carbonifère). Les couches situées entre 2 745 m et 2 969 m, composées d'interstratifications de grès calcareux, de calcaire sableux et de shale, contiennent une association de fossiles très différente considérée d'âge permien. Entre 2 470 m et 2 745 m, la succession de shale et de siltstone est caractérisée par une association de foraminifères surtout arénacés qui, même si elle ne recèle aucun fossile d'âge spécifique, est comparable aux associations présentes dans le Permien de la partie nord des monts Richardson adjacents. Des couches carbonifères corrélatives n'ont été recoupées que par les puits Kugpik O-13 et Napoiak F-31; quant aux couches permiennes, elles l'ont été par les puits Aklavik A-37, Aklavik F-38, Beaverhouse Creek H-13, Ulu A-35, Unak B-11, Tullugak K-31, Kugpik L-24, Kugpik O-13 et Napoiak F-31.

---

[1] Department of Geology, University of Montreal, C.P. 6128, succursale Centre-ville, Montréal, Quebec H3C 3J7

## INTRODUCTION

Although a number of wells on the southern and central parts of Mackenzie Delta are known to contain Permian siliciclastic successions (Fig. 1), there was no report of Carboniferous strata in the subsurface until the Shell et al. Unak L-28 (Fig. 1) well was drilled in 1986. The operator identified Mississippian strata between 2969 and 3190 m in an unpublished, but commercially available, well history report. The operator also identified strata between 2745 and 2969 m as possibly Triassic. Paleontological data to confirm the Triassic and Mississippian ages were not released by the operator; consequently some doubt as to the proposed ages remained.

This report confirms the Carboniferous age of some of the strata in Unak L-28 but suggests that Permian rather than Triassic strata are present. The regional context will be discussed by comparing and correlating the Unak L-28 succession with that in nearby wells and outcrop.

### Lithostratigraphy

Figure 2 illustrates the general lithological succession and the gamma-ray log response of the Carboniferous and Permian succession in Unak L-28. Between about 3190 m and the total well depth at 3259 m, the shale succession is identified as the Jurassic to Lower Cretaceous Husky Formation (Fig. 2). This is confirmed by the presence of Jurassic foraminifers in the core from depths of 3250 to 3259 m (D.H. McNeil,

unpublished GSC paleontological report 1-DHM-1987). A thrust fault at about 3190 m separates the Husky Formation from the overlying Carboniferous succession.

The Carboniferous succession begins with a thin sequence of interbedded calcareous shale and siltstone, with a few thin sandstone beds, between 3190 and 3166 m. Red, brown, and green units are common. Overlying the siliciclastics is a thick interval (2969-3166 m) dominated by limestone but also containing minor amounts of interbedded shale, chert, and calcareous sandstone. Thin-sections of cutting samples indicate the presence of bioclastic and pellet packstone, grainstone, silicified limestone, spiculite, sandy limestone, and minor amounts of sandstone.

A significant facies change occurs at 2969 m, above which sandstone becomes more prominent. This succession of coarse grained siliciclastics continues up to 2745 m. Interbeds of conglomerate, limestone, and shale are also present. Many of the limestone beds are bioclastic grainstones. Shale beds are commonly brown, green, or red. Characteristic fresh, green glauconite grains are a common component of the sandy facies. The top of this succession, between 2745 and 2749 m, is capped by a very prominent limestone bed. A Permian age is suggested for the 2745 to 2969 m succession, based on calcareous foraminifers and associated microfossils (see later discussion).

A shale-dominant succession (between 2470 and 2745 m) with some interbedded sandstone and siltstone abruptly overlies the interval of interbedded sandstone and limestone. The well operator considered this succession to be correlative with the Jurassic Husky
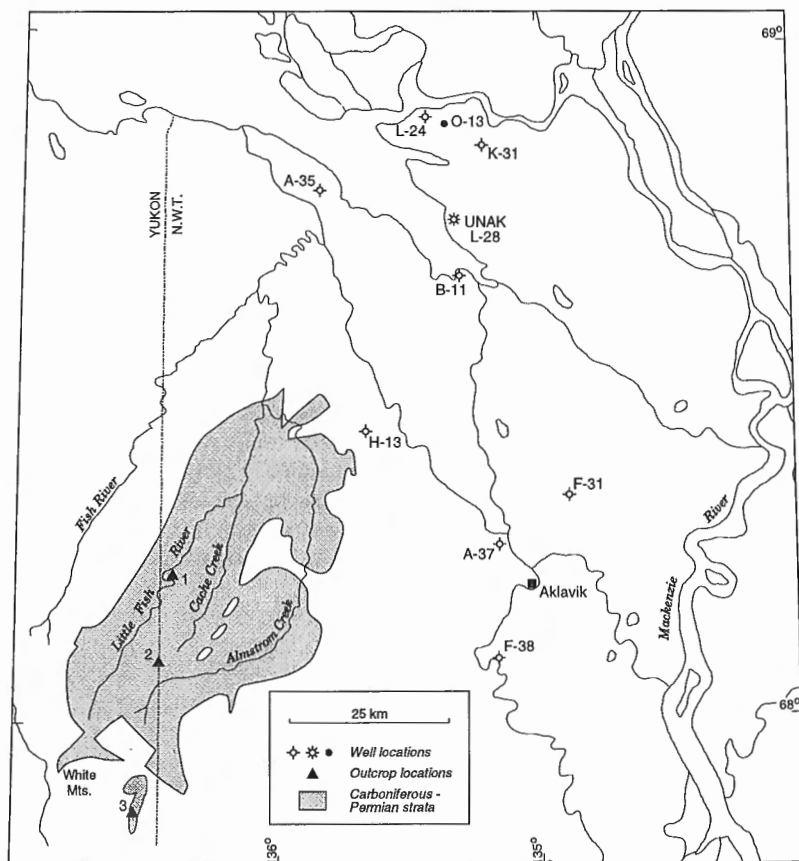


**Figure 1 .**

*Location of wells and outcrops cited in the text. 1. Little Fish Creek; 2. headwaters of Cache Creek and Almstrom Creek; 3. southeast margin of White Mountain Uplift.*

and Bug Creek formations. However, arenaceous foraminifers with a known age range of Permian to Triassic have been recovered from sidewall cores. Thus, based on regional and local considerations, it seems more likely that this interval is Permian in age (see later discussion). This interval can be subdivided into (Fig. 2): 1) a basal zone of thinly interbedded shale and siltstone, with very thin beds of sandstone, 2725 to 2745 m; 2) a shale-rich succession that contains several prominent, thick sandstone beds, 2540 to 2725 m; and 3) a succession of thinly interbedded siltstone, shale, and sandstone, 2470 to 2540 m. Each succession has a distinct log signature. The uppermost unit is abruptly overlain by Mesozoic shale.

## Biostratigraphy

Sidewall cores from depths 2484 to 2739 m were examined for foraminifers and associated faunas. Composite samples of the cuttings were collected in 50 m intervals between 2750



*Figure 2. Lithology, gamma-ray signature, and Carboniferous-Permian stratigraphy of the Unak L-28 well.*

and 3175 m, and thin-sections were made for calcareous foraminifers and associated microfossils (benthic algae and microfossils of uncertain affinity). The results are as follows:

**Interval 2484-2739 m**
(principally foraminifers)

| 2484 m | *Ammodiscus* sp. |
| | *Bathysiphon* sp. |
| | *Reophax* sp. |
| 2524 m | *Ammodiscus* sp. |
| | *Reophax* sp. |
| | *Saccammina*(?) sp. |
| | *Textularia* sp. |
| | *Trochammina* sp. |
| 2541 m | *Ammobaculites* sp. |
| | *Ammodiscus* sp. |
| | *Bathysiphon* sp. |
| 2555.5 m | *Ammobaculites* sp. |
| | *Haplophragmoides* spp. (common) |
| | *Saccammina* sp. |
| 2570.5, 2585.5, and 2600.5 m | |
| | *Ammodiscus* sp. cf. *A. nitidus* Parr |
| | *Bathysiphon* sp. |
| | *Haplophragmoides* sp. |
| | *Hippocrepina* sp. |
| | *Textularia* spp. |
| | *Saccammina* spp. |
| 2631.5 m | *Ammodiscus* sp. cf. *A. nitidus* Parr |
| | *Hippocrepina* sp. |
| | *Reophax*(?) sp. |
| | *Saccammina* sp. |
| 2646.5 m | *Ammobaculites*(?) sp. |
| | *Ammodiscus* sp. ex gr. *A. septentrionalis* Gerke |
| | *A. nitidus* Parr |
| | *Bathysiphon* spp. (common) |
| | *Hyperammina* sp. |
| | *Saccammina* sp. |
| | *Textularia* sp. |
| | *Trochammina* sp. |
| 2661.5 m | *Ammobaculites* ? |
| | *Ammodiscus* sp. (as above) |
| | *Bathysiphon* sp. |
| | *Glomospira* sp. |
| | *Hippocrepina* sp. |
| | *Saccammina* sp. |
| 2674.5 m | *Ammodiscus* sp. (as above) |
| | *Bathysiphon* sp. |
| | *Glomospira* sp. |
| | *Haplophragmoides* sp. |
| | *Saccammina* sp. |
| | *Textularia* sp. |
| | *Trochammina* sp. |
| 2693.5 m | *Ammodiscus* sp. |
| | *Bathysiphon* sp. |

*Glomospira* sp.
*Haplophragmoides* sp.
*Saccammina* sp.
*Textularia* sp.
*Trochammina* sp.

2708.5 m    (Calcareous foraminifers become more
             prominent below 2708.5 m)
             *Ammodiscus* sp. cf. *A. nitidus* Parr
             *Haplophragmoides* sp.
             *Nodosaria tereta* Crespin
             Ostracoda: *Healdia*(?) sp.
             brachiopod shell fragments and spines

2723.5 m    *Ammodiscus* sp. ex gr. *A. septentrionalis* Gerak
             *A. nitidus* Parr
             *Haplophragmoides* sp.
             *Nodosaria tereta* Crespin
             *Textularia* sp.
             Ostracoda: *Healdia*(?) sp.
             brachiopod spines

2739 m      *Haplophragmoides* sp.
             *Hemigordius harltoni* Cushman and Waters
             *Nodosaria tereta* Crespin
             Ostracoda: *Healdia*(?) sp.
             gastropod
             brachiopod shell fragments and spines

The above faunal assemblage is very different from the overlying Mesozoic assemblage, but the fossils are not age specific, known to range from the Permian to the Triassic, with some extending into younger strata. However, the assemblage is very similar to foraminiferal assemblages collected from dated Permian strata in the northern Richardson Mountains (unpublished field data of Dixon). Of special note is the assemblage between 2708.5 and 2739 m which is very similar to an assemblage described from the basal part of the Permian shale succession at Little Fish Creek (locality 1, Fig. 1) by Seo (1977). These comparisons strongly indicate a Permian age for the foraminiferal assemblage.

## Interval 2750-2950 m

2750-2800 m: *Apterinellids*
             *Calcisphaera* sp.
             *Calcitornella* sp.
             *Climacammina* sp.
             *Endothyra* sp.
             *Globivalvulina* sp.
             *Nodosinelloides* sp.
             *Protonodosaria* sp. (abundant)
             Stacheiinae
             *Stacheoides* sp.
             *Syzrania* sp.
             staffelids
             *Tuberitina* sp.
             *Ungdarella* sp.

2850-2900 m: apterinellids
             *Protonodosaria*
             *Stacheoides* sp.

2900-2950 m: *Orthovertella* sp.
             *Pseudoendothyra*? sp.

The age of these microfossils is believed to be Early Permian, based on a comparable assemblage in Early Permian beds in the basal Jungle Creek Formation of west-central Yukon (Bamber and Waterhouse, 1971).

## Interval 2950-3175 m

2950-3000 m: *Cuneiphycus* sp.
             *Stacheoides* sp. (possibly caved material)

This composite sample spans the presumed Permian-Carboniferous boundary at 2969 m and it is suspected that most of the fossil-bearing material came from below this depth.

3000-3050 m: *Ammovertella* sp.

3050-3100 m: *Ammovertella* sp.
             *Asteroarchaediscus* (abundant)
             *Biseriella* sp.
             *Calcisphaera* sp.
             *Globivalvulina* sp. (primitive forms)
             *Neoarchaediscus* sp.
             *Planospirodiscus* sp.
             *Profusulinella* sp.
             *Volvotextularia* sp.

3100-3150 m: *Calcisphaera* sp.
             *Neoarchaediscus* sp. (abundant)
             *Priscella* sp.

3150-3175 m: *Calcisphaera* sp.
             *Neoarchaediscus* sp.
             *Planospirodiscus* sp.

The age of these microfossils spans the Serpukhovian to Bashkirian, with strata of the latter age possibly beginning at about 3000 m.

The paleontological data from L-28 suggests that the Permian sits on a truncated Carboniferous succession because there is no evidence for the presence of post-Bashkirian (Carboniferous) strata. This unconformable relationship is typical of the Carboniferous-Permian contact throughout northern Yukon and northeastern Alaska (Bamber and Waterhouse, 1971).

### *Local and regional comparisons*

Only Unak L-28 and Napoiak F-31 contain paleontologically dated Carboniferous strata in the Mackenzie Delta area (this report; microfossils in core 4, 4970-5005 ft. in Napoiak F-31, identified by B.L. Mamet), and Permian ages have been determined for some cored intervals (Napoiak F-31, Unak B-11, Ulu A-35, and Beaverhouse Creek H-13 - J. Utting, unpublished GSC paleontological report 6-JU-89). Carboniferous and/or Permian strata have been identified (by lithological correlation and/or paleontological data) in the following wells: Kugpik L-24 and O-13, Tullugak K-31, Unak B-11, Ulu A-35, Beaverhouse Creek H-13, Napoiak F-31, Aklavik A-37 and F-38 (Fig. 1). Most of these wells do

not penetrate beyond Permian strata but, as will be reasoned below, it seems that the Kugpik O-13 well penetrated Carboniferous strata.

The closest wells to Unak L-28 are Kugpik O-13 and L-24, and Tullugak K-31. Of these, the O-13 well contains the most comparable succession, starting with a lowermost interval of interbedded shale, sandstone, and conglomerate (11 570-12 101 ft.), overlain by carbonate-rich beds (11 355-11 570 ft.), followed by sandstone-dominant strata (10 630-11 355 ft.), in turn overlain by interbedded shale and sandstone (9695-10 630 ft.). Based on the similar lithological succession to L-28, the shale, sandstone, and carbonate interval in the bottom of the O-13 well is believed to be Carboniferous. The L-24 and K-31 wells did not penetrate the entire Permian succession, but their geographic proximity and comparable Permian stratigraphic succession to that in L-28 and O-13 would suggest that Carboniferous strata are likely to be present below the drilled section.

At Napoiak F-31, between 3900 ft. and the total well depth, there is a succession of interbedded sandstone, shale, and limestone, with the succession below 4030 ft. very rich in limestone. Cored material from 4061 to 4132 ft. contain Permian palynomorphs (J. Utting, unpublished GSC paleontological report 6-JU-89), and a limestone bed in the core from 4970-5005 ft., within the limestone-rich succession, contains Carboniferous, possibly Moscovian, microfossils (identified by B.L. Mamet: *Climacammina* sp., *Cuneiphycus* sp., *Endothyra* sp., *Fourstonella* sp., *Fusulinella*? sp., *Komia* sp.,

*Microdium* sp., *Planoendothyra* sp., *Profusulinella* sp., *Schubertella* sp., *Stacheoides* sp., *Staffella* sp., *Tetrataxis* sp., *Ungdarella* sp.).

The overall succession of the Carboniferous and Permian strata in the Unak L-28 well is comparable to that exposed in the northern Richardson Mountains, in the core of the Cache Creek Uplift (Norris, 1981a). A succession originally described by Bamber and Waterhouse (1971, fig. 10, section 117A-8), and more thoroughly by Nassichuk and Bamber (1978), and also examined by one of us (Dixon), from the middle reaches of Little Fish River (Fig. 1, locality 1; Fig. 3) is similar to that at Unak L-28. The exposed section consists of a basal unit of mixed carbonates and siliciclastics in which Carboniferous and Permian macro- and microfossils have been found (Nassichuk and Bamber, 1978; Mamet et al., 1987), abruptly overlain by a thick, shale-dominant interval, in turn gradationally succeeded by an interval of interbedded shale, siltstone, and sandstone, commonly arranged in a series of coarsening-upward cycles.

The thickness of the basal unit is not accurately known because the basal contact is faulted. There are at least 100 to 200 m of exposed strata, although both Bamber and Waterhouse (1971) and Nassichuk and Bamber (1978) estimated a considerably thicker succession. Within these lower beds is the Carboniferous-Permian contact. Nassichuk and Bamber (1978, Fig. 44, 45) indicated the contact was faulted, whereas subsequent re-examination by Dixon in 1993 failed to find evidence of a fault. There is an abrupt facies change at the presumed boundary. The Carboniferous succession is dominated by bioclastic limestone, whereas the Permian is more
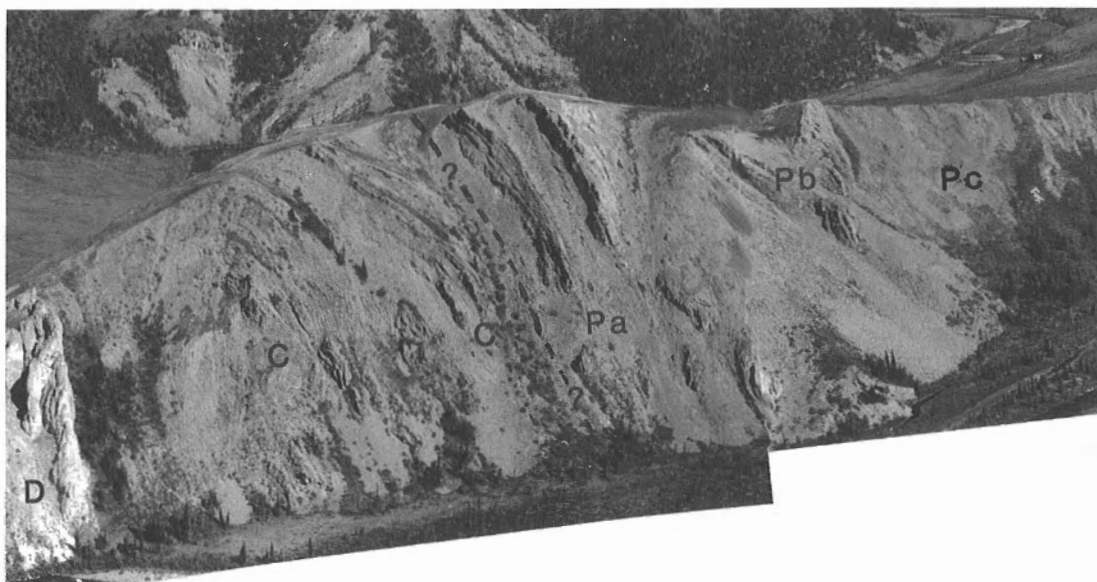


*Figure 3. Carboniferous to Permian strata on Little Fish River (locality 1, Fig. 1). These strata are lithologically and biostratigraphically comparable to strata in Unak L-28. D – Devonian; C – Carboniferous; Pa – Permian sandstone with some limestone; Pb – Palaeoaplysina-bearing Permian limestone; Pc – interbedded Permian shale, siltstone, and thin beds of sandstone. Carboniferous beds are faulted against Devonian carbonates. Note the presence of medium-scale folds in the Carboniferous and basal Permian beds. Unit Pb is repeated due to a tight fold and associated fault. ISPG photos 4150-1 and 4150-2*

siliciclastic-rich, along with some interbedded sandy limestone. This facies change at the presumed Carboniferous-Permian boundary is comparable to that seen in the subsurface section at Unak L-28. Also similar is the presence of a prominent limestone bed at the top of the lower unit. In outcrop, this limestone bed is a *Palaeoaplysina*-bearing biostrome (Davies, 1971; Nassichuk and Bamber, 1978; Mamet et al., 1987) and is present in the same stratigraphic position in a number of areas throughout the Cache Creek Uplift. The nature of the limestone bed in the subsurface remains unknown.

Although the general lithology and age range of the Carboniferous in the northern Richardson Mountains is similar to that of the subsurface, the surface section also contains some post-Bashkirian beds. Nassichuk and Bamber (1978) identified Moscovian fossils in the Little Fish River outcrop. Also, Pinard and Rui (unpublished GSC paleontological report SP-3-93) identified foraminifers that range in age from the Kasimovian to Early Permian from strata above the Moscovian beds. Thus, the Little Fish River outcrop contains the youngest known Carboniferous strata in the northern Yukon (Mamet and Mason, 1970). The surface and subsurface successions are age-equivalent to the Lisburne Group of the British Mountains and adjacent northeast Alaska (Mamet and Mason, 1970; Armstrong and Mamet, 1975).

About 15 km south of the Little Fish River locality there is another well exposed Carboniferous-Permian section (locality 2, headwaters of Cache and Almstrom creeks, Fig. 1) but here the basal beds are dominated by siliciclastics in both the Carboniferous and Permian parts (unpublished field data by Dixon). The basal beds are capped by a *Palaeoaplysina*-bearing limestone bed, abruptly overlain by a thick, shale-dominant succession, in turn succeeded by interbedded shale, siltstone, and sandstone.

A third locality of known Carboniferous-Permian strata has been mapped on the southeast flank of the White Mountain Uplift (locality 3, Fig. 1; locality 7a of Norris, 1981b; locality 116P-7 of Bamber and Waterhouse, 1971, Fig. 2). Bamber (1972, p. 134) described an incomplete section consisting of 107.3 m of Carboniferous and Permian bioclastic limestone resting unconformably on Devonian beds, and a faulted upper contact. Late Bashkirian or Moscovian foraminifers were identified from the upper 61 m (Bamber and Waterhouse, 1971, p. 86).

Within the Richardson Mountains, the Permian shale and sandstone succession overlying the basal beds is considerably thicker than in Unak L-28, and the uppermost beds, consisting of coarsening-upward cycles of interbedded shale, siltstone, and sandstone, appear to be absent in the Unak L-28 well. In the latter location, the upper preserved beds are considered to be stratigraphically lower than the uppermost beds in the outcrops. This implies considerable erosion prior to Jurassic deposition, which is consistent with known regional trends.

On a more regional scale, the Carboniferous-Permian strata in the Unak L-28 well are age equivalent to the Ettrain, Blackie, and Jungle Creek formations of north-central Yukon (Bamber and Waterhouse, 1971), and part of the Kayak Formation, Lisburne Group, and Echooka Formation of the British Mountains (northern Yukon) and northeast Alaska (Mamet and Mason, 1970; Bamber and Waterhouse, 1971; Armstrong and Mamet, 1975).

## CONCLUSIONS

Although suggestions of the presence of Carboniferous strata in the subsurface of Mackenzie Delta have been indicated in well history reports, the documentation of Carboniferous microfossils from the Unak L-28 and Napoiak F-31 wells is the first confirmed report. Correlations between Unak L-28 and Kugpik O-13 also indicate the presence of Carboniferous strata in the latter well.

## ACKNOWLEDGMENTS

## REFERENCES

**Armstrong, A.K. and Mamet, B.L.**
1975: Carboniferous biostratigraphy, northeastern Brooks Range, Arctic Alaska; United States Geological Survey, Professional Paper 884, 29 p.

**Bamber, E.W.**
1972: Descriptions of Carboniferous and Permian stratigraphic sections, northern Yukon Territory and northwestern District of Mackenzie (NTS 106M, 116C, F, G, H, H, J, P: 117A, B, C); Geological Survey of Canada, Paper 72-19, 161 p.

**Bamber, E.W. and Waterhouse, J.B.**
1971: Carboniferous and Permian stratigraphy and paleontology, northern Yukon Territory, Canada; Bulletin of Canadian Petroleum Geology, v. 19, p. 29-250.

**Davies, G.R.**
1971: A Permian hydrozoan mound, Yukon Territory; Canadian Journal of Earth Sciences, v. 8, p. 973-988.

**Mamet, B.L. and Mason, D.**
1970: Lisburne Group lithostratigraphy and foraminiferal zonation, British Mountains, northern Yukon Territory; Bulletin of Canadian Petroleum Geology, v. 18, p. 556-565.

**Mamet, B., Roux, A., and Nassichuk, W.W.**
1987: Algues carbonifieres et permiennes de l'Arctique Canadien; Geological Survey of Canada, Bulletin 342, 163 p.

**Nassichuk, W. and Bamber, E.W.**
1978: Site 8: Pennsylvannian and Permian stratigraphy at Little Fish Creek; in Geological and Geographical Guide to the Mackenzie Delta Area, (ed.) F.G. Young; Canadian Society of Petroleum Geologists, p. 85-89.

**Norris, D.K.**
1981a: Blow River and Davidson Mountains; Geological Survey of Canada, Map 1516A, scale 1:250 000.
1981b: Bell River; Geological Survey of Canada, Map 1519A, scale 1:250 000.

**Seo, Haeyoun**
1977: Permian non-Fusulinid Foraminifera from the northern Yukon Territory; MSc. thesis, University of Saskatchewan, Saskatoon, Saskatchewan, 199 p.

# Petrophysical characteristics of shale from the Beaufort-Mackenzie Basin, northern Canada: permeability, formation factor, and porosity versus pressure

T.J. Katsube, D.R. Issler[1], and K. Coyner[2]
Mineral Resources Division, Ottawa

**Abstract:** Permeability, formation factor, and porosity as a function of pressure have been measured on shale samples from different depths and from areas with different sedimentation rates in the Beaufort-Mackenzie Basin. Preliminary results indicate that permeabilities decrease by 1-2 orders of magnitude over effective pressures of 1-50 MPa. Vertical permeability, corrected to subsurface pressure conditions, is strongly correlated with porosity and decreases by a factor of 3 (from $1.5 \times 10^{-19}\,m^2$ to $1.9 \times 10^{-22}\,m^2$) as porosity decreases from 15% to 5%. Horizontal permeability exceeds vertical permeability by a factor of 2.5 for one of the samples. Effective porosity decreases with pressure (1-50 MPa) from 12.2 to 9.5% and 6.9 to 6.6% for uncemented and cemented shale samples, respectively, a trend consistent with previous studies. Apparent formation factor (100-200) and true formation factor (80-90) values are low for these shale samples, probably due to their poorly cemented characteristics.

**Résumé :** La perméabilité, le facteur de formation et la porosité en fonction de la pression ont été mesurées sur une série d'échantillons de shale prélevés à diverses profondeurs dans des zones caractérisées par des vitesses de sédimentation différentes dans le bassin de Beaufort-Mackenzie. Les résultats préliminaires indiquent que la perméabilité diminue de dix à cent fois à mesure que la pression efficace passe de 1 MPa à 50 MPa. Dans le cas de carottes échantillonnées dans le sens vertical, il y a une bonne correspondance entre la perméabilité (corrigée par rapport à la surface) et la porosité, la première diminuant mille fois (de $1,5 \times 10^{-19}\,m^2$ à $1,9 \times 10^{-22}\,m^2$) pendant que la seconde passe de 15 % à 5 %. La perméabilité mesurée dans le cas d'une carotte échantillonnée dans le sens horizontal est $10^{2,5}$ fois plus importante que dans celui d'une carotte échantillonnée dans le sens vertical. La porosité efficace diminue aussi à mesure que la pression augmente de 1 MPa à 50 MPa, ce qui correspdond aux résultats des études antérieures. Dans le cas des échantillons de shale non cimenté, elle passe de 12,2 % à 9,5 % et dans celui des échantillons de shale cimenté, de 6,9 % à 6,6 %. Les valeurs du facteur de formation (apparent, 100-200; vrai, 80-90) sont faibles, ce qui est probablement dû au fait que les roches sont peu cimentées.

[1] GSC Calgary, Calgary
[2] Verde GeoScience, R.R.#1 Box 117 Tunbridge, Vermont 05077 U.S.A.

# INTRODUCTION

Petrophysical characteristics of shale from different depths (0.9-4.5 km) in areas with different sedimentation rates in the Beaufort-Mackenzie Basin are being studied (e.g. Issler and Katsube, 1994; Katsube et al., 1995a) to obtain a better understanding of shale compaction and abnormal pressure (overpressure and underpressure) development. Data regarding porosity and pore-size distribution (e.g. Issler and Katsube, 1994; Katsube and Issler, 1993; Katsube and Best, 1992) are being used to develop physical compaction models of shale (Katsube and Williamson, 1994, 1995; Katsube et al., 1995a). However, these porosity data were not measured under in situ formation pressure conditions. Furthermore, there is little information on the bulk fluid transport properties of the shale matrix. In this paper, we present some preliminary results for measurements of permeability, formation factor and porosity as a function of pressure for shale samples from the Beaufort-Mackenzie Basin. These data are necessary for determining porosity and fluid transport properties of shale at representative formation pressures and are required inputs for models of abnormal pressure development.

# METHODS OF INVESTIGATION

## Samples and experimental approach

Pore-size distribution has been determined by mercury porosimetry for two sets of shale core samples from the Beaufort-Mackenzie Basin. One set consists of 10 samples from 6 wells (Katsube and Best, 1992) and the other set comprises 41 samples from 9 wells (Issler and Katsube, 1994; Katsube and Issler, 1993), with both sets including samples from 4 different compaction zones (Issler, 1992) of the Beaufort-Mackenzie Basin. The Pliocene-Pleistocene sedimentation rates in these zones range from approximately 0 to 660 m/Ma (Table 1). From these two suites of samples, six samples have been selected for permeability versus effective pressure measurements (k-$P_e$), two for effective porosity and apparent formation factor versus pressure measurements ($\phi_E F_a$-P), and two for true formation factor (F) measurements, as indicated in Table 1. One of these samples (B-ML-2) consists of two sub-samples, one vertically cored and the other horizontally cored. The remainder of the samples were cored in the vertical direction. Results of permeability measurements for two of these samples (B-5, B-9) have been published previously (Katsube and Coyner, 1994), but not within the appropriate regional context as shown in Table 1. Apparent formation factor values ($F_a$), determined from $\phi_E F_a$-P measurements, typically deviate from the true formation factor (F) values by 10-200% because of the difficulty in eliminating pore surface conduction effects. True formation factor determinations eliminate surface conduction effects and are estimated to be accurate to within ±20% (Katsube et al., 1995b). Information on the geological environment and on the compaction zones from which the samples have been taken can be found in Issler (1992) and Issler and Katsube (1994).

## Sample preparation

One inch (2.5 cm) plugs were taken from selected core samples of Beaufort-Mackenzie Basin shales. Several disc specimens, 0.5-1.5 cm in thickness, were cut from each of these plugs for the k-$P_e$, $\phi_E F_a$-P, and F measurements. The disc specimens used for the F measurements were placed between two porous disc-shaped graphite electrodes, of the same diameter, and the entire specimen-electrode assembly was jacketed by a heat shrunken tube to prevent disintegration of the specimen during the tests. As these samples were not expected to display high resistivities, the possibility of specimen surface leakage effects due to the jacketing was not considered.

## Permeability – effective pressure (k-$P_e$) Tests

Permeabilities were measured at multiple confining pressures ranging between 10 and 110 MPa, using the transient pulse decay techniques first introduced by Brace and Orange (1968). Unless stated otherwise, all permeabilities were measured in the vertical direction. Details of both the equipment and the standard procedures used for measuring these tight shale samples are described in Coyner et al. (1993), and to a lesser extent, in Katsube and Coyner (1994).

**Table 1.** List of samples and types of measurement performed.

| Sample Number | $v_{sd}$ (m/m.y.) | h (TVD, km) | k/$P_e$ | $\phi_E F_a$/P | F |
|---|---|---|---|---|---|
| (Zone-1)<br>B-5* | 380-660 | 3.76 | X | | |
| (Zone-2)<br>B-9<br>B-AR-5* | 190-380 | 2.44<br>4.38 | X<br>X | | |
| (Zone-3)<br>B-TA-1<br>B-TG-6 | 40-190 | 2.88<br>2.46 | X<br>X | X | |
| (Zone-4)<br>B-ML-2*<br>B-RE-11*<br>B-RE-12* | 0-40 | 3.18<br>2.92<br>3.15 | X | X | X<br>X |

| | |
|---|---|
| * | = overpressured, |
| $v_{sd}$ | = Pliocene-Pleistocene sedimentation rates (Issler, 1992), |
| h | = depth, |
| TVD | = true vertical depth, |
| k/$P_e$ | = permeability versus effective pressure measurements, |
| $\phi_E F_a$/P | = porosity and apparent formation factor versus pressure measurements, |
| F | = formation factor measurements, |
| X | = measurements made. |

## Porosity and formation factor versus pressure ($\phi_E F_a$-P) measurements

Bulk electrical resistivities, $\rho_b$, were measured at multiple confining pressures between 3.5 and 51.8 MPa (500 to 7500 psi), at a frequency of 1000 Hz, using a Hewlett Packard Model 4276A LCZ meter. The samples were tested in a two-electrode system using a stainless steel electrode and end piece assembly. As confining pressure was increased, the amount of brine squeezed out of the sample was measured volumetrically to determine the porosity value at each of the confining pressures (Loman et al., 1993). The apparent formation factor, $F_a$, is determined using the following equation (Archie, 1942):

$$F_a = \rho_b/\rho_w,$$

where $\rho_w$ is the pore fluid resistivity. Further details of the standard procedures used for the measurement of these shale samples are found in Loman et al. (1993).

## True formation factor measurements

True formation factor (F) values for these shale samples were determined from electrical resistivity measurements made using specimens saturated with brines composed of five different NaCl concentrations (0.02 N, 0.05 N, 0.1 N, 0.2 N, and 0.5 N). Variable brine compositions were used to eliminate pore surface conduction effects, and thereby obtain true F values. Further details of the standard procedure used for these shale samples are described in Katsube and Scromeda (1993) and Katsube et al. (1995b).

## EXPERIMENTAL RESULTS

The results of the permeability versus effective pressure (k-$P_e$) measurements for these shale samples are listed in Table 2 and shown in Figure 1. Also included in Figure 1 are previously published k-$P_e$ measurements for Beaufort-Mackenzie Basin shale samples (samples B-5 and B-9; Katsube and Coyner, 1994). The range of values for these Beaufort-Mackenzie Basin samples ($2 \times 10^{-22}$-$40 \times 10^{-19}$ m$^2$) are within the range ($10^{-22}$-$7.4 \times 10^{-19}$ m$^2$) determined for shale from the Venture Gas Field (offshore Nova Scotia) (Coyner et al., 1993; Katsube and Coyner, 1994), and well within the range ($10^{-23}$-$7.4 \times 10^{-18}$ m$^2$) reported for shale in general (Brace, 1980).

The results of the effective porosity and apparent formation factor versus pressure ($\phi_E F_a$-P) measurements are listed in Table 3. The range of $\phi_E$ values for these samples (6-12%) is generally larger than that reported (0.1-8%) for the Venture shale (Loman et al., 1993; Katsube and Williamson, 1994). However, the range and magnitude of $F_a$ values for the Beaufort-Mackenzie Basin samples (100-200) are significantly smaller than those (290-5600) reported for the Venture shale (Loman et al., 1993).

Results of the true formation factor (F) determinations are listed in Table 4. These values (80-90) are also smaller than those (120-1700) reported for the Venture shale (Katsube et al., 1995b). Both the apparent and true formation factor measurements provide valuable constraints on the interconnectivity of the pore network. When used in combination, both permeability and formation factor measurements provide information on the diameter of pore throats comprising the main flow paths (Katsube et al., 1991, 1992). These data will be analyzed in detail in future studies.

## DISCUSSION AND CONCLUSIONS

Table 5 shows estimated lithostatic, pore fluid, and effective pressures for the depths from which the shale samples were recovered. Lithostatic pressures were calculated using assumed matrix and pore fluid densities and porosity-depth

**Table 2.** Permeability (k) of shale samples from the Beaufort-Mackenzie Basin.

| Sample Number | Depth (km) | Pressures (MPa) | | | Permeability ($10^{-21}$ m$^2$) |
|---|---|---|---|---|---|
| | | Confining | Pore | Effective ($P_e$) | |
| (Zone-2) | | | | | |
| B-AR-5 | 4.38 | 15.0 | 10 | 5.0 | 4.7 ± 0.8 |
| | | 20.0 | 10 | 10 | 1.8 ± 0.0 |
| | | 25.0 | 10 | 15 | 1.2 ± 0.2 |
| | | 30.0 | 10 | 20 | 0.77± 0.05 |
| | | 35.0 | 10 | 25 | 0.85± 0.05 |
| | | 40.0 | 10 | 30 | 0.60± 0.10 |
| (Zone-3) | | | | | |
| B-TG-6 | 2.46 | 15.0 | 10 | 5.0 | 188. ± 8 |
| | | 20.0 | 10 | 10 | 65. ± 5 |
| | | 25.0 | 10 | 15 | 23. ± 4 |
| | | 30.0 | 10 | 20 | 8.7 ± 0.0 |
| | | 35.0 | 10 | 25 | 6.3 ± 0.3 |
| | | 40.0 | 10 | 30 | 4.7 ± 0.2 |
| | | 45.0 | 10 | 35 | 4.5 ± 0.5 |
| | | 50.0 | 10 | 40 | 3.2 ± 0.8 |
| | | 55.0 | 10 | 45 | 2.3 ± 0.1 |
| | | 60.0 | 10 | 50 | 1.7 ± 0.4 |
| B-TA-1 | 2.88 | 12.5 | 10 | 2.5 | 7.6 ± 1.2 |
| | | 15.0 | 10 | 5.0 | 2.9 ± 0.9 |
| | | 17.5 | 10 | 7.5 | 1.7 ± 0.2 |
| | | 20.0 | 10 | 10 | 0.96± 0.38 |
| | | 25.0 | 10 | 15 | 0.54± 0.04 |
| | | 30.0 | 10 | 20 | 0.39± 0.02 |
| | | 35.0 | 10 | 25 | 0.24± 0.04 |
| (Zone-4) | | | | | |
| B-ML-2(V) | 3.22 | 12.5 | 10 | 2.5 | 0.5 ± 0.12 |
| | | 15.0 | 10 | 5.0 | 0.32± 0.09 |
| | | 20.0 | 10 | 10 | 0.32± 0.05 |
| | | 25.0 | 10 | 15 | 0.22± 0.0 |
| | | 40.0 | 10 | 30 | 0.17± - |
| | | 12.5 | 10 | 2.5 | 2.9 ± 0.3 |
| B-ML-2(H) | | 15.0 | 10 | 5.0 | 1.8 ± 0.2 |
| | | 20.0 | 10 | 10 | 1.0 ± 0.1 |
| | | 30.0 | 10 | 20 | 0.6 ± 0.0 |
| | | 40.0 | 10 | 30 | 0.4 ± - |
| | | 60.0 | 10 | 50 | 0.3 ± - |

profiles determined from sonic logs (Issler, 1992) for individual well locations. The assumed average shale matrix density ($2720$ kg/m$^3$) was based on core measurements (Youn, 1974; Katsube and Issler, 1993) and the average pore fluid density was assumed to be $1075$ kg/m$^3$. Pore fluid pressures were interpolated using drillstem test (DST) and repeat formation tester (RFT) data. Effective pressure at in situ formation conditions was determined as the difference between lithostatic and pore fluid pressure. In situ effective pressures were used to estimate permeability and porosity under original subsurface conditions, using the permeability versus effective pressure (k-P$_e$) and effective porosity versus pressure ($\phi_E$-P) curves. These estimated values are represented by arrows in Figures 1 and 2.

In Figure 1, measured shale permeability decreases by 1 to 2 orders of magnitude over the effective pressure range of 1 to 50 MPa. Permeability does not show a simple correlation with sample depth because the samples were collected from areas with significantly different sedimentation rates and porosity-depth trends. For example, overpressured samples B-5 (3.76 km) and B-AR-5 (4.38 km) have permeabilities which are significantly higher than the shallower, normally pressured sample, B-TA-1 (2.88 km). Two-directional permeability was measured for sample B-ML-2. Measured



***Figure 1.*** *Permeability (k) as a function effective pressure (P$_e$) for seven Beaufort-Mackenzie Basin shale samples. All permeabilities were measured in the vertical direction unless otherwise noted. Arrows indicate permeability at estimated in situ effective pressure for corresponding sample depths.* * – *overpressured samples.*

| | | |
|---|---|---|
| *B-9:* | *zone-2* | *h=2.44km* |
| *B-5:* | *zone-1* | *h=3.76km* |
| *B-TG-6:* | *zone-3* | *h=2.46km* |
| *B-AR-5:* | *zone-2* | *h=4.38km* |
| *B-TA-1:* | *zone-3* | *h=2.88km* |
| *B-ML-2,H:* | *zone-4* | *h=3.18km* |
| *B-ML-2,V:* | *(h – depth; H – horizontal; V– vertical)* | |

**Table 3.** Effective porosity and formation-factor values as a function of confining pressure for shale samples from the Beaufort-Mackenzie Basin.

| Sample | h (km) | k$_a$ (µD) | P (MPa) | $\phi_E$ (%) | $\rho_w$ (Ω-m) | F$_a$ |
|---|---|---|---|---|---|---|
| (Zone-3) B-TG-6b | 2.46 | 147 | 3.5 | 12.2 | 0.0843 | 98.5 |
| | | | 6.9 | 12.2 | (22.4 °C) | 105.0 |
| | | | 13.8 | 11.1 | | 123.0 |
| | | | 27.6 | 10.3 | | 157.0 |
| | | | 34.5 | 10.0 | | 177.7 |
| | | | 51.8 | 9.5 | | 204.3 |
| (Zone-4) B-ML-2 | 3.22 | 27 | 3.5 | 6.9 | 0.0843 | 161.7 |
| | | | 6.9 | 6.9 | (22.4 °C) | 147.8 |
| | | | 13.8 | 6.8 | | 146.1 |
| | | | 27.6 | 6.7 | | 160.0 |
| | | | 34.5 | 6.7 | | 168.0 |
| | | | 51.8 | 6.6 | | 183.0 |

| | | |
|---|---|---|
| h | = | Depth. |
| k$_a$ | = | Gas permeability. |
| P | = | Confining pressure. |
| $\phi_E$ | = | Effective porosity. |
| $\rho_w$ | = | Pore fluid resistivity. |
| F$_a$ | = | Apparent formation factor. |

**Table 4.** Formation-factor, surface resistivity and bulk electrical resistivities for different NaCl solutions for water-saturated shale samples from the Beaufort-Mackenzie Basin.

| Sample | $\rho_{rn}$ (Ω-m) | | | | | F ±% | $\rho_c$±% |
|---|---|---|---|---|---|---|---|
| $\rho_w$ (Ω-m) | 0.28 ±0.001 | 0.31 ±0.001 | 0.42 ±0.001 | 0.62 ±0.002 | 1.14 ±0.003 | | (Ω-m) |
| NaCl (N) | 0.5 | 0.4 | 0.3 | 0.2 | 0.1 | | |
| B-RE-12 | 8.59 X | 11.0 X | 11.4 X | 14.7 X | 14.4 X 16.1 | 83.3 | 17.4 |
| B-RE-11 | 14.1 X | 13.0 X | 12.0 X | 18.1 X | 21.8 X 21.5 | 87.2 | 27.5 |

| | | |
|---|---|---|
| $\rho_w$ | = | pore fluid resistivity |
| $\rho_{rn}$ | = | bulk resistivity of the rock for solutions of different salinities |
| F | = | formation-factor |
| $\rho_c$ | = | surface resistivity |
| X | = | data points used for formation factor determination |

vertical permeability (sub-sample B-ML-2V) is lower than horizontal permeability (sub-sample B-ML-2H) by a factor of two to six (Fig. 1 and Table 2).

The arrows in Figure 1 indicate permeability at estimated subsurface effective pressure conditions (Table 5). Estimated in situ permeability values occur near significant shifts in the trend of the permeability-pressure data for samples B-9, B-5, and B-TG-6 but the other samples do not show any obvious correlation. Further work is necessary to determine whether this has any petrophysical significance. In situ permeability cannot be accurately determined for sample B-TA-1 because the permeability-pressure measurements terminate at 25 MPa, well below the estimated in situ effective pressure of 36 MPa (Table 5). Horizontal permeability is greater than vertical permeability by a factor of approximately 2.5 at the estimated in situ effective pressure for sample B-ML-2 (Fig. 1).

Effective porosity versus pressure ($\phi_E$-P) curves for two samples (B-TG-6, B-ML-2) are displayed in Figure 2. The higher porosity sample (B-TG-6) shows a much greater decrease in $\phi_E$ with increasing pressure then the lower porosity sample (B-ML-2) for which $\phi_E$ remains almost constant. Shale texture analysis reveals that the former sample lacks

cementation whereas the latter is well cemented (Bloch and Issler, in prep.). Because these samples are from different depths, differences in the degree of compaction might explain the disparity in observed $\phi_E$-P trends. However, the lack of $\phi_E$ variation with increased pressure (B-ML-2) is consistent with trends observed previously for well cemented shale (Katsube and Williamson, 1994). Also, the k-$P_e$ curve for B-ML-2 shows less variation than that of B-TG-6 (Fig. 1).

**Table 5.** Estimated in situ formation pressures for samples.

| Sample | Depth | (MPa) | | |
|---|---|---|---|---|
| Number | (km) | $P_L$ | $P_f$ | $P_e$ |
| B-5 | 3.76 | 83 | 65 | 18 |
| B-9 | 2.44 | 53 | 25 | 28 |
| B-AR-5 | 4.38 | 99 | 75 | 23 |
| B-TA-1 | 2.88 | 65 | 29 | 36 |
| B-TG-6 | 2.46 | 55 | 26 | 29 |
| B-ML-2 | 3.18 | 75 | 50 | 25 |
| B-RE-11 | 2.92 | 70 | 44 | 26 |
| B-RE-12 | 3.15 | 75 | 49 | 26 |

$P_L$ - estimated lithostatic pressure
$P_f$ - interpolated pore pressure from DST, RFT data
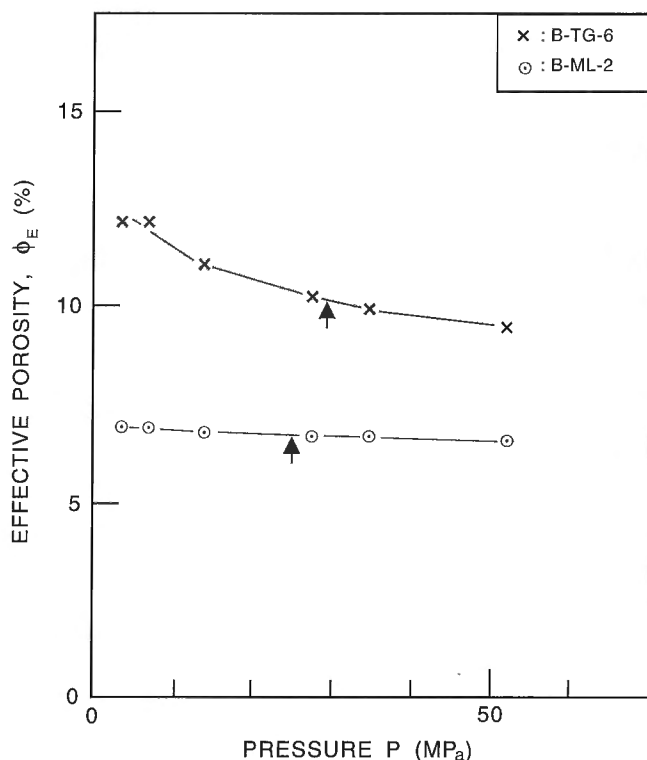$P_e$ - calculated effective pressure



**Figure 2.** Effective porosity ($\phi_E$) as a function confining pressure (P) for two Beaufort-Mackenzie Basin shale samples. Arrows indicate effective porosity at estimated in situ effective pressure for corresponding sample depths.

B-TG-6b:    zone-3    not cemented
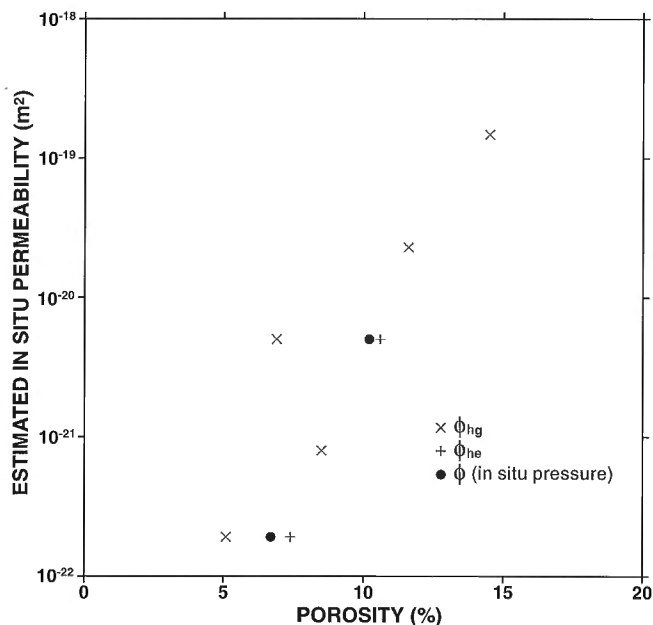B-ML-2:     zone-4    cemented



**Figure 3.** Vertical permeability versus porosity for five Beaufort-Mackenzie Basin shale samples. $\phi_{hg}$ – mercury porosity; $\phi_{he}$ – helium porosity; black dots are in situ corrected porosity values from Figure 2.

The two samples (B-RE-11, B-RE-12) that have true formation factor (F) determinations either lack cement or are poorly cemented (Issler and Bloch, in prep.). This may be the reason why the F values for these samples are smaller than those of the Venture shale samples, which are either well cemented or have experienced diagenetic cementation at some time (Katsube and Williamson, 1994).

Figure 3 shows a plot of estimated in situ vertical permeability versus porosity for five of the samples in Figure 1. Mercury porosity ($\phi_{hg}$) and helium porosity ($\phi_{he}$) values are from Katsube and Best (1992) and Issler and Katsube (1993) and were not corrected for in situ pressure. Also shown in Figure 3 are pressure corrected porosity values (Table 3, Fig. 2). There is a significant correlation between permeability and porosity for these shale samples with permeability decreasing by a factor of 3 ($1.5 \times 10^{-19}\,m^2$ to $1.9 \times 10^{-22}\,m^2$) from approximately 15% to 5% porosity. The good correlation between porosity and permeability may result from the overall compositional homogeneity of the shale samples (Bloch and Issler, in prep.).

## ACKNOWLEDGMENTS

## REFERENCES

**Archie, G.E.**
1942:   The electrical resistivity log as an aid in determining some reservoir characteristics; Transactions of the American Institute of Mining, Metallurgical and Petroleum Engineers, v. 146, p. 54-67.

**Brace, W.F.**
1980:   Permeability of crystalline and argillaceous rocks; International Journal of Rock Mechanics, Mining Sciences and Geomechanics Abstracts, v. 17, p. 241-251.

**Brace, W.F. and Orange, A.S.**
1968:   Further studies of the effects of pressure on electrical resistivity of rocks; Journal of Geophysical Research, v. 73, p. 5407-5420.

**Coyner, K., Katsube, T.J., Best, M.E., and Williamson, M.**
1993:   Gas and water permeability of tight shales from the Venture Gas Field offshore Nova Scotia; in Current Research, Part D; Geological Survey of Canada, Paper 93-1D, p. 129-136.

**Issler, D.R.**
1992:   A new approach to shale compaction and stratigraphic restoration, Beaufort-Mackenzie Basin and Mackenzie Corridor, Northern Canada; American Association of Petroleum Geologists Bulletin, v. 76, p. 1170-1189.

**Issler, D.R. and Katsube, T.J.**
1994:   Effective porosity of shale samples from the Beaufort-Mackenzie Basin; in Current Research 1994-B; Geological Survey of Canada, p. 19-26.

**Katsube, T.J. and Best, M.E.**
1992:   Pore structure of shales from the Beaufort-Mackenzie Basin, Northwest Territories; in Current Research, Part E; Geological Survey of Canada, Paper 92-1E, p. 157-162.

**Katsube, T.J. and Coyner, K.**
1994:   Determination of permeability(k)-compaction relationship from interpretation of k-stress data for shales from eastern and northern Canada; in Current Research 1994-D; Geological Survey of Canada, p. 169-177.

**Katsube, T.J. and Issler, D.R.**
1993:   Pore-size distribution of shales from the Beaufort-Mackenzie Basin, northern Canada; in Current Research, Part E; Geological Survey of Canada, Paper 93-1E, p. 123-132.

**Katsube, T.J. and Scromeda, N.**
1993:   Formation factor determination procedure for shale sample V-3 from the Scotian Shelf; in Current Research, Part E; Geological Survey of Canada, Paper 93-1E, p. 321-330.

**Katsube, T.J. and Williamson, M.A.**
1994:   Effects of diagenesis on shale nano-pore structure and implications for sealing capacity; Clay Minerals, v. 29, p. 451-461.
1995:   Critical depth of burial of subsiding shales and its effect on abnormal pressure development; in Proceedings of the Oil and Gas Forum' 95, "Energy from Sediments"; Geological Survey of Canada, Open File 3058, p. 283-286.

**Katsube, T.J., Best, M.E., and Mudford, B.S.**
1991:   Petrophysical characteristics of shales from the Scotian shelf; Geophysics, v. 56, p. 1681-1689.

**Katsube, T.J., Bloch, J., and Issler, D.R.**
1995a:  Shale pore structure evolution under variable sedimentation rates in the Beaufort-Mackenzie Basin; in Proceedings of the Oil and Gas Forum' 95, "Energy from Sediments"; Geological Survey of Canada, Open File 3058, p. 211-215.

**Katsube, T.J., Scromeda, N., and Williamson, M.A.**
1995b:  Improving measurement accuracy of formation resistivity factor measurements for tight shales from the Scotian Shelf; in Current Research 1995-D; Geological Survey of Canada, p. 65-71.

**Katsube, T.J., Williamson, M., and Best, M.E.**
1992:   Shale pore structure evolution and its effect on permeability; in Symposium Volume III of the Thirty-Third Annual Symposium of the Society of Professional Well Log Analysts (SPWLA), Oklahoma City, Oklahoma, June 15-17, 1992; The Society of Core Analysts Preprints, Paper SCA-9214, p. 1-22.

**Loman, J.M., Katsube, T.J., Correia, J.M., and Williamson, M.A.**
1993:   Effect of compaction on porosity and formation factor for tight shales from the Scotian Shelf, offshore Nova Scotia: in Current Research, Part E; Geological Survey of Canada, Paper 93-1E, p. 331-335.

**Youn, S.H.**
1974:   Comparison of porosity and density values of shale from cores and well logs; M.Sc. thesis, University of Tulsa, Tulsa, Oklahoma, 62 p.

# Early land plants from the Late Silurian-Early Devonian of Bathurst Island, Canadian Arctic Archipelago

J.F. Basinger[1], M.E. Kotyk[1], and P.G. Gensel[2]
GSC Calgary

**Abstract:** Silurian/Devonian (Ludlow to Pragian) rocks of Bathurst Island, Canadian Arctic Archipelago, have yielded an abundance of well preserved fossil plants, including some of the earliest known land plants. Pre-Emsian plants are rare globally, yet represent the critical early stages in the evolution of vascular land plants. The Bathurst Island fossils now represent the most diverse pre-Emsian flora known from North America. Of additional significance is the discovery of basal parts of plants with attached rooting structures, organs generally unknown for early land plants.

**Résumé :** Les roches siluro-dévoniennes (du Ludlow au Pragien) de l'île Bathurst, dans l'archipel arctique canadien, ont livré d'abondantes plantes fossiles bien conservées, notamment certaines des plus anciennes plantes terrestres connues. Les plantes antérieures à l'Emsien sont globalement rares, mais elles sont les vestiges des premiers stades critiques de l'évolution des plantes vasculaires terrestres. Les fossiles de l'île Bathurst sont, pour le moment, les représentants de la flore antérieure à l'Emsien la plus diversifiée qui soit connue en Amérique du Nord. Fait supplémentaire à noter, on a découvert les parties basales de plantes dotées de structures d'enracinement, desquelles les premières plantes terrestres étaient généralement dépourvues.

[1] Department of Geological Sciences, University of Saskatchewan, Saskatoon, Saskatchewan S7N 5E2
[2] Department of Biology, The University of North Carolina, Chapel Hill, NC 27599-3280 U.S.A.

## INTRODUCTION

Recent reinvestigation of Silurian/Devonian rocks of Bathurst Island by members of the Geological Survey of Canada revealed additional occurrences of macrofossil plants and presented the opportunity for continuation of work initiated by Hueber (1971). As originally described, the fossils reported by Hueber (1971) represented five genera, including the new genus *Bathurstia* Hueber, found in the uppermost beds of the Bathurst Island Formation and the lower beds of the Stuart Bay Formation, beds now interpreted to represent the Pragian (Siegenian). The Lower Devonian age of the fossils was significant, as macrofossils of this age are poorly represented in North America.

Current investigations of Bathurst Island and Stuart Bay beds have revealed an abundance of well preserved remains representing substantially more diversity than that previously reported. Furthermore, localities now known represent Ludlow to Pragian deposits, and include some of the earliest known land plants.

The fossil flora of the Buchanan Lake and Stewart Bay beds is forming the basis for a program of systematic research on early land plants, including MSc. research by M.E. Kotyk. Initial evaluation of the flora indicates that many of the taxa are new, and that the Bathurst collection represents a significant contribution to our understanding of early land plant diversification. In this report, some of the taxa recovered during recent fieldwork are shown with tentative identifications.

## GEOLOGY

Fossil plants were largely collected from four different areas on eastern Bathurst Island (Fig. 1). These include: the region north of Polar Bear Pass; the section studied by Hueber (1971) near Young Inlet; the Cheyne River valley; and a small tributary of the Cheyne River. Approximately 1300 specimens have been collected. Plants were found primarily in thin bedded, calcareous marine siltstones and fine grained
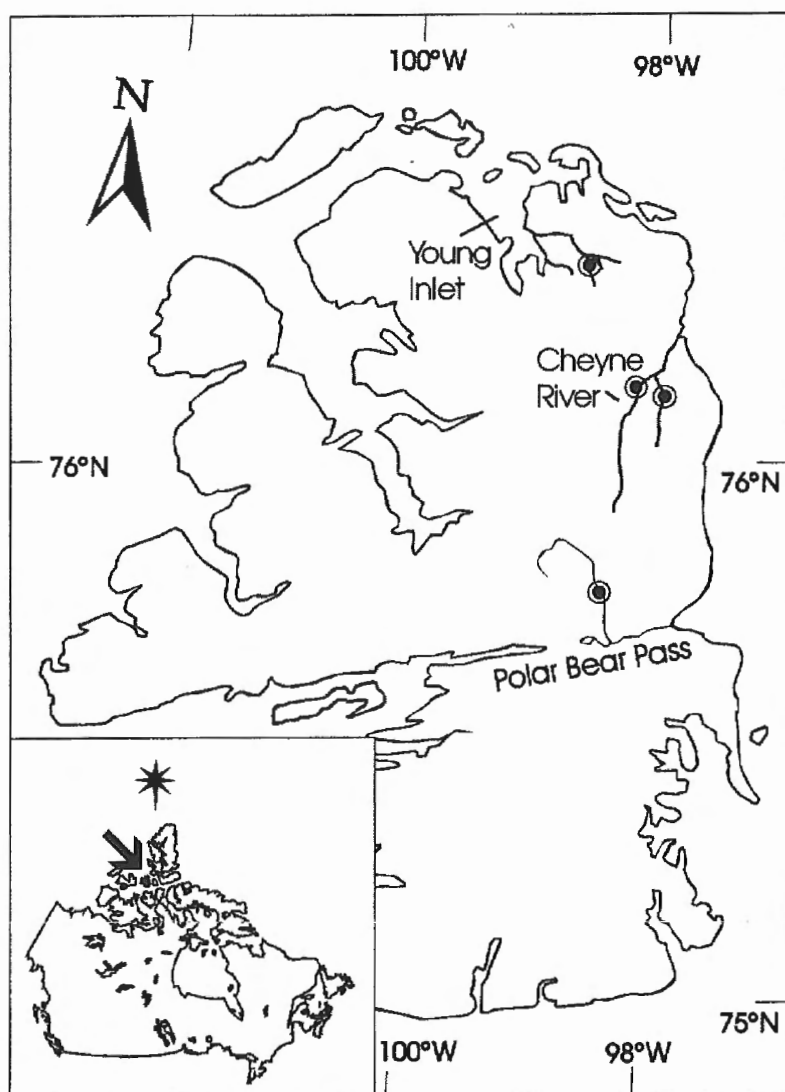


*Figure 1.*

*Geographic location of the principal study areas on Bathurst Island. The Polar Bear Pass area includes localities of Ludlow to Pragian age; Cheyne River and Cheyne River tributary, Lochkovian to Pragian; and Young Inlet, Pragian.*

**Table 1.** Stratigraphic column for eastern Bathurst Island, showing the stratigraphic level of principal sources of plant remains as well as the earliest occurrence of plants. Modified after de Freitas et al. (1993). Geological time scale based on Harland et al. (1990).

| Ma | Period | Epoch | Stage | | |
|---|---|---|---|---|---|
| 386.0 | Devonian | Early Devonian | Emsian | **Eids beds** | |
| 390.4 | | | | **Stuart** | upper member |
| | | | Pragian | **Bay** | middle member |
| 396.3 | | | | **beds** | lower member |
| | | | Lochkovian | **Bathurst** | |
| | | | | **Island** | upper member |
| | | | | **beds** | |
| 408.5 | Silurian | | Pridoli | | |
| 410.7 | | | | | lower member |
| | | | Ludlow | | |
| 415.1 | | | | | |

Source of majority of plant localities

Earliest plant locality
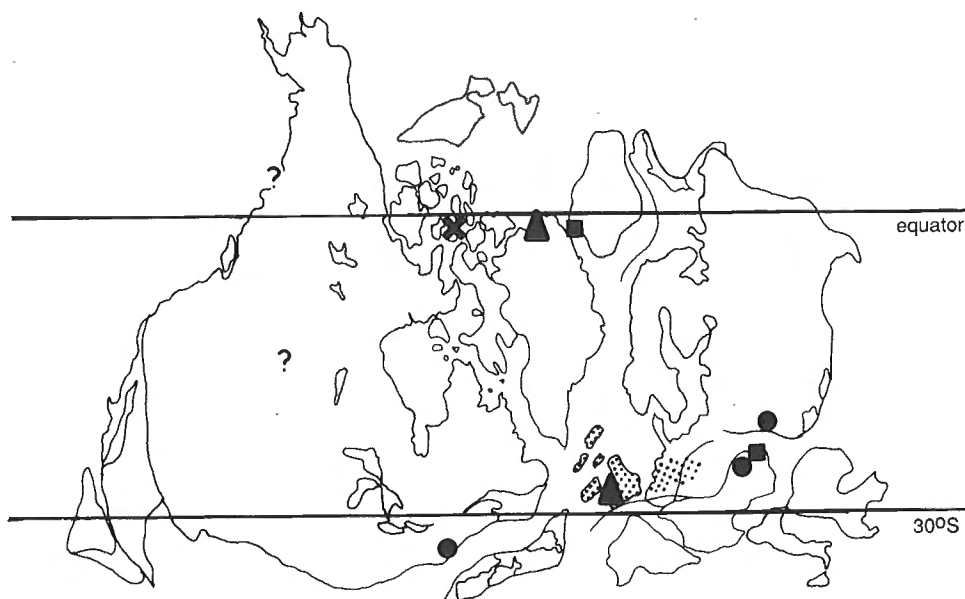
**Figure 2.** *Paleogeographic map of Laurussia showing the location of principal sources of Silurian to Pragian plant macrofossils, based on reconstructions of Scotese and McKerrow (1990). X, Bathurst Island; triangles, Ludlow; circles, Pridoli; squares, Lochkovian; ?, isolated Lower Devonian occurrences, epoch uncertain. Shaded area includes numerous occurrences in western Europe from Pridoli to Pragian (data from Dorf, 1934; Churkin et al., 1969; Edwards and Rogerson, 1979; Tanner, 1982; Edwards et al., 1983; Gensel and Andrews, 1984; Larsen et al., 1987; Edwards, 1990; Raymond, 1987; and papers therein).*

equator

30°S

sandstones referred to as the Stuart Bay beds (de Freitas et al., 1993). Plants were also recovered from the underlying, finer grained Bathurst Island beds. Formational status of these beds is abandoned in the present work in view of the current reinterpretation of Silurian and Devonian rocks of Bathurst Island by T. de Freitas, J.C. Harrison, and R. Thorsteinsson (de Freitas et al., 1993; Harrison et al., 1993).

The greatest concentrations of plant fossils, along with abundant remains of *Monograptus yukonensis*, were found in the lower member of the Stuart Bay beds, as defined by de Freitas et al. (1993), and were commonly associated with interbedded chert pebble conglomerates. Other fossils that were commonly found in beds with fossil plants include eurypterid cuticle, fish skeletal fragments, dendroid graptolites, bivalves, brachiopods, and tentaculitids.

Sediments of the Bathurst Island and Stuart Bay beds are generally accepted as deep water deposits (Smith, 1980; Mayr, 1980; Polan and Stearn, 1984; de Freitas et al., 1993), and the plant remains are believed to have been rafted out to sea. Turbidity currents are also thought to have been responsible for sweeping land plants as well as continental conglomerates basinward from the positive Boothia uplift, located to the east. The shoreline during this time is interpreted to have lain along the eastern margin of Bathurst Island, at a distance of roughly 10 to 20 km from the plant localities.

In the study area of eastern Bathurst Island, lower Stuart Bay beds are interpreted as being Pragian (Siegenian), in part on the basis of the ubiquitous presence of the graptoloid *Monograptus yukonensis* (de Freitas et al., 1993) (Table 1). Biostratigraphic correlation, particularly on the basis of graptolites and as interpreted by de Freitas et al. (1993), indicates that the Lochkovian/Pragian (Gedinnian/Siegenian) boundary lies within the uppermost Bathurst Island beds. The occurrence of *Monograptus uniformis* from several localities on northern Bathurst Island indicates that the Pridoli/Lochkovian (Silurian/Devonian) boundary lies within the lower beds of the upper member of the Bathurst Island beds. The occurrence of *Monograptus formosus* and fragmentary *Bohemograptus* sp. about 5 km north of Polar Bear Pass indicates that the Ludlow/Pridoli boundary lies within the lower member of the Bathurst Island beds (T. de Freitas, pers. comm., 1995). Plant remains are rare in the Bathurst Island beds, but have been found in Lochkovian and Ludlow rocks in the Polar Bear Pass area (Fig. 1; Table 1).

---

**Figure 3.** *A cooksonioid-type plant with large globose sporangia terminating short branches. This is the oldest plant recovered from Bathurst Island. Ludlow, Lower Bathurst Island beds. Polar Bear Pass, 75°50'22.3"N, 98°37'00.2"W. US383-2385. x2.*

**Figure 4.** cf. Barinophytales, *with a dense terminal strobilus. Pragian, Stewart Bay beds. Cheyne River, 76°11'23.7"N, 98°12'27.6"W. US665-6379. x2.*

**Figure 5.** *Possible pre-lycopsid, with leaf-like emergences and probable adventitious roots. Pragian, Stewart Bay beds. Polar Bear Pass, 75°48'59.8"N, 98°24'11.2"W. US604-6380. x1.*

**Figure 6.** cf. Bathurstia, *bifurcate axis with terminal strobili. Pragian, Stewart Bay beds. Cheyne River, 76°11'23.7"N, 98°12'27.6"W. US 665-6381. x1.*

## DISCUSSION

As presently known, the Emsian represents peak diversity of early land plants. Plants predating the Emsian are rare in North America (Fig. 2), and indeed globally (Edwards, 1990). Thus, the discovery of rich sources of plants of Silurian and earliest Devonian age (Ludlow–Pragian) on Bathurst Island is of great significance in providing much needed evidence of the inception and early evolution of some early land plant lineages. The Bathurst Island fossils, in fact, now represent the most diverse pre-Emsian flora known from North America. The Ludlow to Lochkovian remains are of special significance in this regard (Fig. 3).
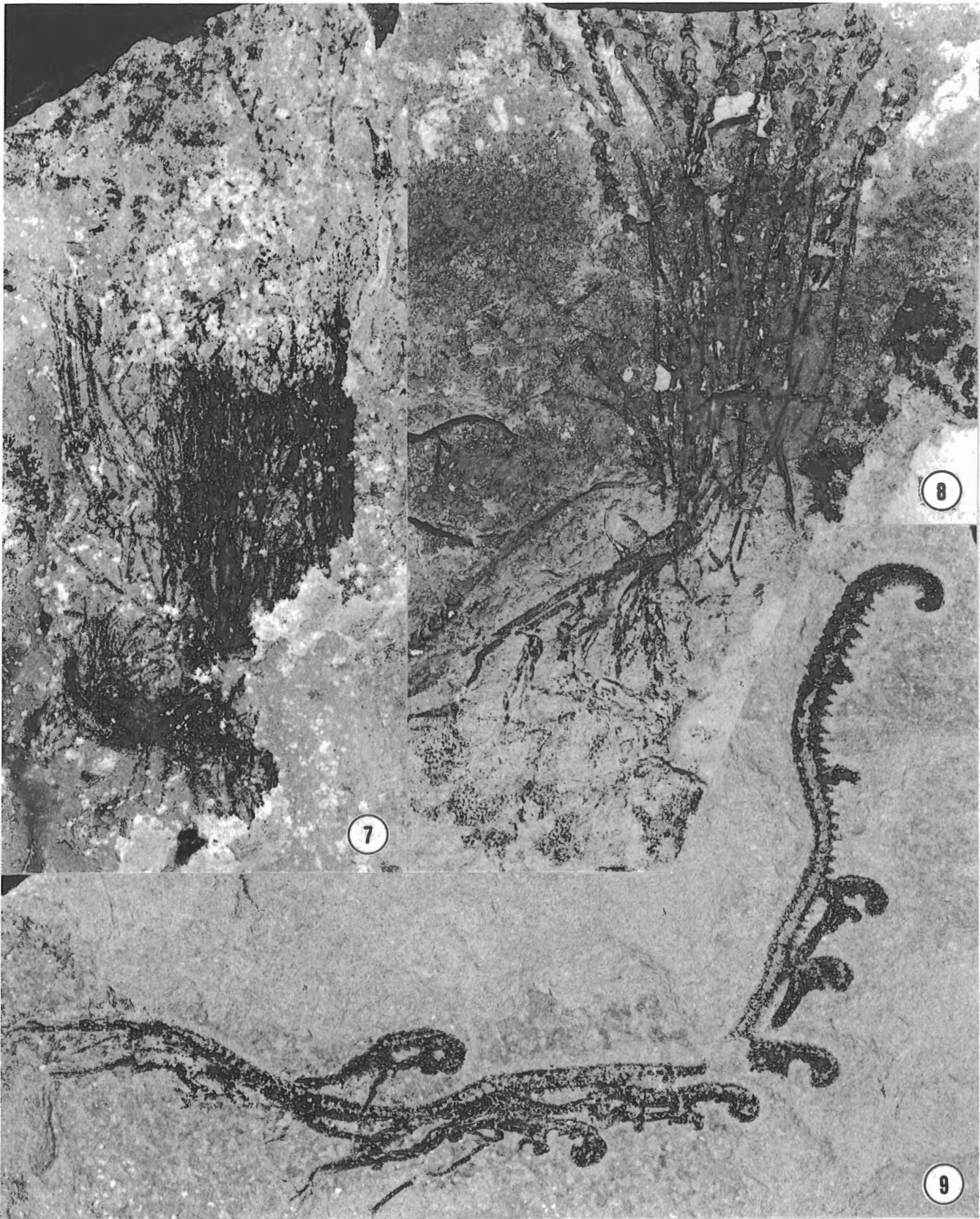
The Bathurst collections expand the number of taxa known from northern North America, revealing that, in addition to earlier records, several species of *Zosterophyllum* and *Zosterophyllum*-like plants (Fig. 7, 8, 10-14, 16) and one or more plants referable to the Barinophytales are present (Fig. 4). Some less readily identifiable forms appear to represent pre-lycopsids or possibly early lycopsids (Fig. 5, 6, 9, 15); more study is needed to determine their affinities.

The genus *Zosterophyllum* is globally distributed, and the zosterophylls as a whole reach a peak of diversity in the Pragian/Emsian. At this early stage of our investigation, some of the plants most closely resemble taxa known previously from the Pragian of Wales, China, and Siberia. The stobili resembling those of barinophytes such as *Krithodeophyton* or *Protobarinophyton* strengthen the similarity to the Siberian flora.

This similarity is particularly interesting, because current paleocontinental reconstructions, such as that of Scotese and McKerrow (1990) where Bathurst is equatorial, or those of others (e.g., Scotese, 1986) where the equator more nearly approximates Europe, would place Bathurst Island, Siberia, and indeed China well north of the rest of Siluro-Devonian North America and the European parts of Laurussia. Bathurst Island would, therefore, be predicted to lie within a climatic belt different from central Laurussia. Most accounts of paleobiogeography in recent years have hinted at some regional differences, particularly at higher latitudes, in early Devonian floras, although to date Lochkovian and even Pragian occurrences are too few to ascertain degree of cosmopolitanism. Further work on the Bathurst fossils may help with such determinations. As land plants are typically good paleoenvironmental indicators, this may have implications for interpretation of early Devonian paleoclimates.
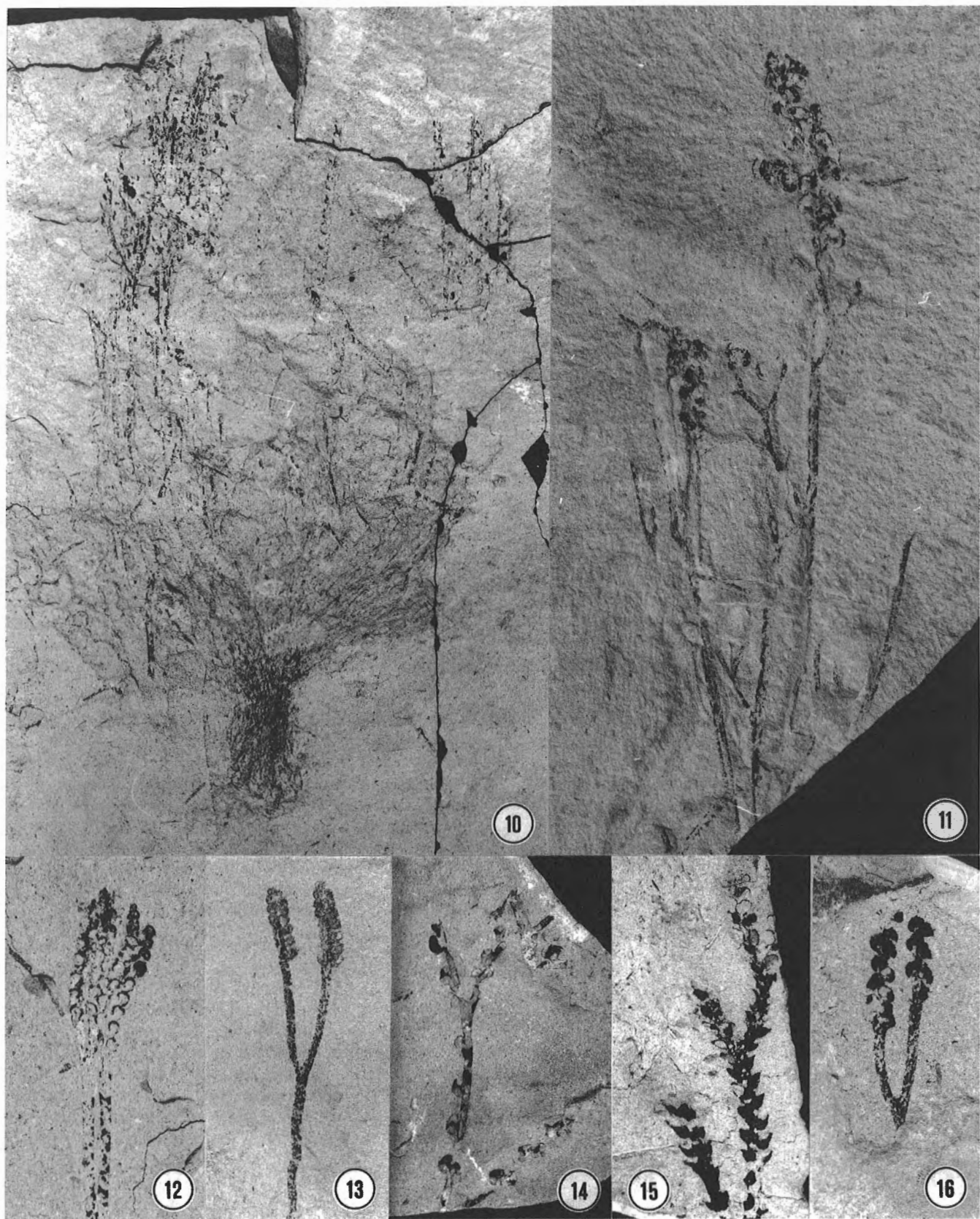
Some major early land plant lineages are missing from the flora as presently known, or at least are less conspicuous than expected, namely rhyniophytes and trimerophytes. Branched sterile axes resembling the latter are found, but no definitive identification can be made. The apparent rarity of these floral groups may be taphonomic and correlated with facies differences. In other words these groups may be rare in the habitats that supplied plant remains to these offshore deposits. On the other hand, it may be of some significance biogeographically, as discussed for other floras by Edwards (1990).

Another aspect of significance, independent of systematic or biogeographic considerations, is the discovery of plants with basal regions, including rooting structures, preserved. The early plant record lacks information about how soon root systems evolved. The initial impression based on these finds is that, in addition to adventitious roots (Fig. 5, 9), some other form of rooting organ (Fig. 7, 8, 10), that may prove to be true roots, a rhizoidal system, or perhaps even a mycorrhizal system, existed by the Pragian. Study of these remains will add considerable information about this crucial component of early plant structure and evolution.

*Figure 7.* Zosterophyllum *sp., with basal rooting structure. Terminal strobili faintly visible in upper part of plant, where rock is weathered. Pragian, Stewart Bay beds. Polar Bear Pass, 75°48′59.8″N, 98°24′11.2″W. US605-6377. x0.8.*

*Figure 8.* Zosterophyllum cf. Z. myretonianum, *with terminal strobili and basal rooting structures. Pragian, Stewart Bay beds. Polar Bear Pass, 75°48′59.8″N, 98°24′11.2″W. US609-6376. x1.*

*Figure 9.* Unknown plant, possibly a zosterophyll, with stout spiny emergences and croziers. Note apparent adventitious roots. Pragian, Stewart Bay beds. Cheyne River, 76°06′11.7″N, 98°23′15.5″W. US680-6375. x0.7.*

**Figure 10.** *cf.* Zosterophyllum *sp. Large, entire plant, with terminal strobili and basal rooting structure. Pragian, Stewart Bay beds. Cheyne River, 76°11′24.0″N, 98°12′45.3″W. US667-6374. x0.5.*

**Figure 11.** *cf.* Zosterophyllum *sp. with very large reniform sporangia borne in a lax strobilus. Pragian, Stewart Bay beds. Cheyne River, 76°11′23.7″N, 98°12′27.6″W. US665-6386. x1.*

**Figure 12.** Zosterophyllum *sp., axis with terminal strobili. Pragian, Stewart Bay beds. Cheyne River, 76°11′23.7″N, 98°12′27.6″W. US665-6382. x1.*

**Figure 13.** *A zosterophyll most comparable to* Zosterophyllum *sp. or* Rebuchia *sp., a dichotomous axis with terminal strobili. Pragian, Stewart Bay beds. Polar Bear Pass, 75°48′55.4″N, 98°24′38.9″W. US617-6384. x1.*

**Figure 14.** Zosterophyllum *sp., dichotomizing axis with short-stalked lateral sporangia. Pragian, Bathurst Island beds. Cheyne River tributary, 76°12′15.8″N, 98°09′24.6″W. US642-6383. x1.*

**Figure 15.** *Probable zosterophyll with bract-like structures on the axis and sporangia borne through at least two bifurcation events. Pragian, Stewart Bay beds. Cheyne River, 76°11′41.2″N, 98°10′56.3″W. US644-6378. x1.*

**Figure 16.** *A zosterophyll most comparable to either* Zosterophyllum *or* Rebuchia, *a dichotomous axis with large reniform sporangia in terminal strobili. Pragian, Stewart Bay beds. Cheyne River, 76°11′41.2″N, 98°10′56.3″W. US664-6385. x1.*

## REFERENCES

**Churkin, M., Eberlein, G.D., Hueber, F.M., and Mamay, S.H.**
1969: Lower Devonian land plants from graptolitic shale in southeastern Alaska; Palaeontology, v. 12, p. 559-573.

**de Freitas, T., Harrison, J.C., and Thorsteinsson, R.**
1993: New field observations on the geology of Bathurst Island, Arctic Canada. Part A: stratigraphy and sedimentology; in Current Research, Part B; Geological Survey of Canada, Paper 93-1B, p. 1-10.

**Dorf, E.**
1934: Lower Devonian flora from Beartooth Butte, Wyoming; Bulletin of the Geological Society of America, v. 45, p. 425-440.

**Edwards, D.**
1990: Constraints on Silurian and Early Devonian phytogeographic analysis based on megafossils; in Palaeozoic Palaeogeography and Biogeography, (ed.) W.S. McKerrow and C.R. Scotese; Geological Society Memoir 12, p. 233-242.

**Edwards, D. and Rogerson, E.C.W.**
1979: New records of fertile Rhyniophytina from the Late Silurian of Wales; Geological Magazine, v. 116, p. 93-98.

**Edwards, D., Feehan, J., and Smith, D.G.**
1983: A late Wenlock flora from Co. Tipperary, Ireland; Botanical Journal Linnean Society, v. 86, p. 19-36.

**Gensel, P.G. and Andrews, H.N.**
1984: Plant Life in the Devonian; Praeger, New York. 396 p.

**Harland, W.B., Armstrong, R.L., Cox, A.V., Craig, L.E., Smith, A.G., and Smith, D.G.**
1990: A geologic time scale; Cambridge University Press, Cambridge, 263 p.

**Harrison, J.C., de Freitas, T., and Thorsteinsson, R.**
1993: New field observations on the geology of Bathurst Island, Arctic Canada. Part B: structure and tectonic history; in Current Research, Part B; Geological Survey of Canada, Paper 93-1B, p. 11-21.

**Hueber, F.M.**
1971: Early Devonian land plants from Bathurst Island, District of Franklin; Geological Survey of Canada, Paper 71-28, 17 p.

**Larson, P.-H., Edwards, D., and Escher, J.C.**
1987: Late Silurian plant megafossils from the Peary Land Group, North Greenland; Rapports Grlands Geologiske Undersgelse, v. 133, p. 107-112.

**Mayr, U.**
1980: Stratigraphy and correlation of lower Paleozoic formations, subsurface of Bathurst Island and adjacent smaller islands, Canadian Arctic Archipelago; Geological Survey of Canada, Bulletin 306, 52 p.

**Polan, K.P. and Stearn, C.W.**
1984: The allochthonous origin of the reefal facies of the Stuart Bay Formation (Early Devonian), Bathurst Island, Arctic Canada; Canadian Journal of Earth Sciences, v. 21, p. 657-668.

**Raymond, A.**
1987: Paleogeographic distribution of Early Devonian plant traits; Palaios, v. 2, p. 113-132.

**Scotese, C.R.**
1986: Phanerozoic reconstructions: a new look at the assembly of Asia; University of Texas Institute for Geophysics, Technical Report 66, p. 1-54.

**Scotese, C.R. and McKerrow, W.S.**
1990: Revised World maps and introduction; in Palaeozoic Palaeogeography and Biogeography, (ed.) W.S. McKerrow and C.R. Scotese; Geological Society Memoir 12, p. 1-21.

**Smith, R.E.**
1980: Lower Devonian (Lochkovian) biostratigraphy and brachiopod faunas, Canadian Arctic Islands; Geological Survey of Canada, Bulletin 308, 155 p.

**Tanner, W.R.**
1982: A new species of *Gosslingia* (Zosterophyllophytina) from the Lower Devonian Beartooth Butte Formation of northern Wyoming; in Proceedings, 3rd North American Paleontological Convention, (ed.) B. Mamet and M.J. Copeland; p. 541-546.

# Surficial geology and sea level history of Bathurst Island, Northwest Territories

Jan M. Bednarski
Terrain Sciences Division, Calgary

**Abstract:** Recent field investigations have been undertaken to map the surficial geology of Bathurst and adjacent islands. Glacial geomorphology indicates that the area was covered by extensive ice caps during the last glaciation. These glaciers probably contacted the Laurentide Ice Sheet to the south, however, a larger ice mass in Penny Strait may have impinged onto northeastern Bathurst Island and coalesced with the ice caps. A survey of raised marine shorelines suggests that the magnitude of emergence was considerably less than previously thought and that the pattern of regional isobases needs revision. Marine pelecypods at elevations well above the marine limit were likely transported there by glaciers overriding pre-existing marine sediments. More work on the directions of ice movement along eastern Bathurst Island is necessary to determine the nature of these readvances.

**Résumé :** Les dépôts superficiels de l'île Bathurst et des îles adjacentes ont récemment fait l'objet de travaux de cartographie sur le terrain. La géomorphologie glaciaire indique que la région a été recouverte de vastes calottes glaciaires durant la dernière glaciation. Ces glaciers sont probablement entrés en contact avec l'inlandsis laurentidien au sud; cependant, une masse glaciaire plus étendue dans le détroit de Penny a pu empiéter sur le nord-est de l'île Bathurst et fusionner avec les calottes glaciaires. Un levé des lignes de rivage soulevées laisse supposer que l'émergence a été considérablement moins importante qu'on ne l'avait supposé et que le tracé des isobases régionales nécessite une révision. Les pélécypodes marins, observés à des hauteurs bien au-dessus de la limite marine, ont probablement été transportés jusque là par les glaciers chevauchant des sédiments marins déjà présents. Il est nécessaire de poursuivre l'étude des directions des mouvements glaciaires le long de la partie est de l'île Bathurst pour déterminer la nature de ces réavancées.

## INTRODUCTION

As part of a Mineral and Energy Resource Assessment (MERA), field investigations have been undertaken to map the surficial geology of Bathurst and adjacent islands, a total area of 20 480 km² (Fig.1). Bathurst Island is currently the focus of attention of industry, indigenous peoples, and Parks Canada, hence accurate natural resource maps are required for competent planning and implementation of land use. An understanding of the type and distribution of surficial materials and Quaternary history is a key ingredient of resource assessment. This includes regional characterization of till geochemistry and glacial dispersal relevant to mineral exploration, as well as related study of glacial and sea level history. Surficial units will also be assessed for granular resources and environmental sensitivity to disturbance. The main output of the project will be 1:250 000 scale maps of surficial geology (NTS map sheets 68G, 68H, 69A, 69B, and 79A), and digital databases of sample analyses.

Extensive areas of the Bathurst Island group were traversed during the 1995 field season by all-terrain cycles and helicopter supported traverses. Most of the smaller islands surrounding Bathurst Island were visited, with the exception of Cameron Island and the southwesternmost coastline of Bathurst Island. Preliminary investigations centred along the coastlines and heads of bays where the greatest concentrations of Quaternary sediment was found. Certain sites reported by earlier studies were also visited (Blake, 1964, 1970, 1974; Barnett et al., 1976, 1977; Edlund, 1986; Hodgson, 1989).
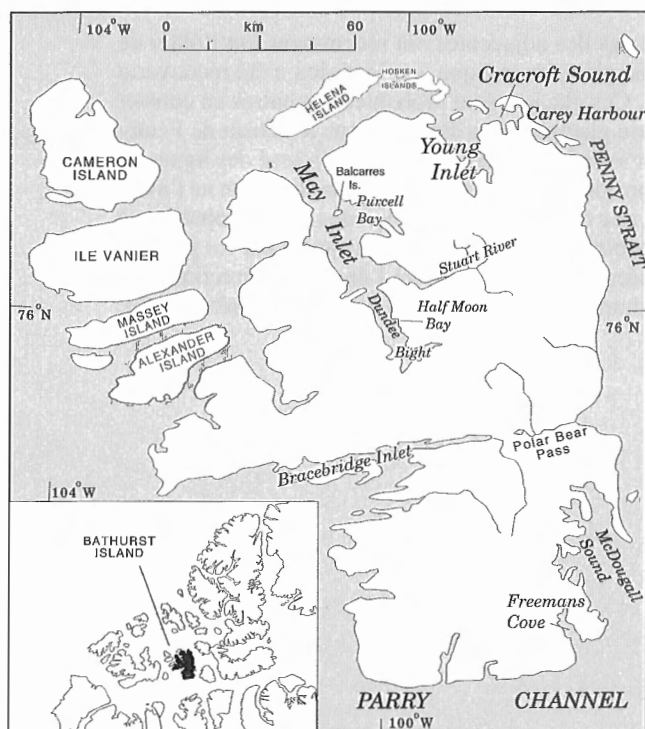


**Figure 1.** *Bathurst and adjacent islands with place names cited in the text.*

This paper describes new observations of Quaternary and sea level history and discusses the implications in the context of regional glaciation.

### Setting

Bathurst Island is the largest of a group of islands situated in the south-central Queen Elizabeth Islands, Northwest Territories (Fig. 1). Bathurst Island and the smaller islands to the west and north generally have low relief, with most areas below 200 m a.s.l. Only a few parts rise above 300 m above sea level and a maximum elevation of 412 m a.s.l. is on northwest Bathurst Island between May and Erskine inlets, in the Stokes Range. The topography varies from interior areas that are flat lying and featureless, to coastal areas that tend to be rugged and incised with steep-sided valleys. The greatest relief is in Dundee Bight, at the head of May Inlet, where truncated ridges form scarps more than 200 m above the shore. With the exception of some minor basic intrusive rocks in southeast Bathurst Island, the area is composed entirely of folded sedimentary rocks. The physiography is influenced by the underlying geological structure and related to the perpendicular intersection of the east-trending Parry Islands Fold Belt with the north-trending, cratonic Boothia Uplift on east-central Bathurst Island (Roots, 1963; Harrison et al., 1993). The majority of the Bathurst Island group is a ridged upland with broad folds underlain by the Parry Islands Fold Belt. The synclines form continuous ridges 200-275 m a.s.l., whereas, large east-trending valleys were carved into anticlinal cores. The drainage has a distinct trellis pattern with large streams flowing within main valleys and tributaries at right angles to the strike, commonly forming gorges up to 150 m deep. The topography of Bathurst Island along a 25 km zone following the eastern coast is more irregular with an indistinct northward fabric associated with the structural trend of the Boothia Uplift.

### Regional context

Bathurst Island is of particular interest to Quaternary geology because it is thought to lie just beyond the northern margin of the Laurentide Ice Sheet during the last glaciation (Late Wisconsinan). Parry Channel, bordering the southern coast of the island generally delineates the ice limit (Dyke and Prest, 1987; Dyke, 1993) except for the overlap onto southern Melville Island. Because the Queen Elizabeth Islands north of Parry Channel generally show less intense signs of glaciation, they were considered to have borne local ice caps or have been covered by a hypothesized regional ice sheet (Innuitian Ice Sheet; Blake, 1970; Dyke and Dredge, 1989; Dyke, 1993). Currently, there are no glaciers or ice caps on Bathurst Island, but semipermanent snow banks are common in protected gullies and hollows. Nonetheless, Shield provenance igneous clasts found on Bathurst Island (Barnett et al., 1976) are thought to be erratics deposited during an earlier continental glaciation.

Definite pre-Late Wisconsinan sediments on Bathurst Island contain organic material which dated >25 ka BP (Blake, 1964, 1974). This includes ice-transported shell

fragments in surface tills and pond sediments. Blake (1974) described two sites on Bathurst Island that had peat deposits >50 ka BP in age which contained plant and insect remains suggesting warmer than present conditions. The more extensive deposits, in the Stuart River valley, west-central Bathurst Island, were assigned to the "Stuart River Interglaciation".

Blake (1964) noted that the extent of postglacial emergence appears to increase from about 105 m a.s.l. in south and southwestern Bathurst Island to 120 m at the heads of inlets indenting the north coast. He noted that at the northern tip of the island postglacial shells were found at 130 m, although, in 1965, he reported postglacial shells up to 140 m a.s.l. in the northern part of the island (Blake, 1965). Blake (1964) reasoned that the increase in the elevation of the marine limit to the northwest suggested that the ice was thicker in that region and may have been part of a larger ice cap that covered the "inter-island area to the north that is now the sea" (Blake, 1964, p. 6). The concept was later expanded to the Innuitian Ice Sheet by Blake (1970).

Based on the highest elevation of surface shells of Holocene age, Hodgson (1989) noted that the marine limit on Bathurst Island rose from ≥107 m a.s.l., along the southern and southwest coast, to ≥119 m, over central Bathurst Island, to ≥150 m, in the northeast (Fig. 2). The ≥150 m sea level on northeast is based on fragments and whole valves of *Hiatella*
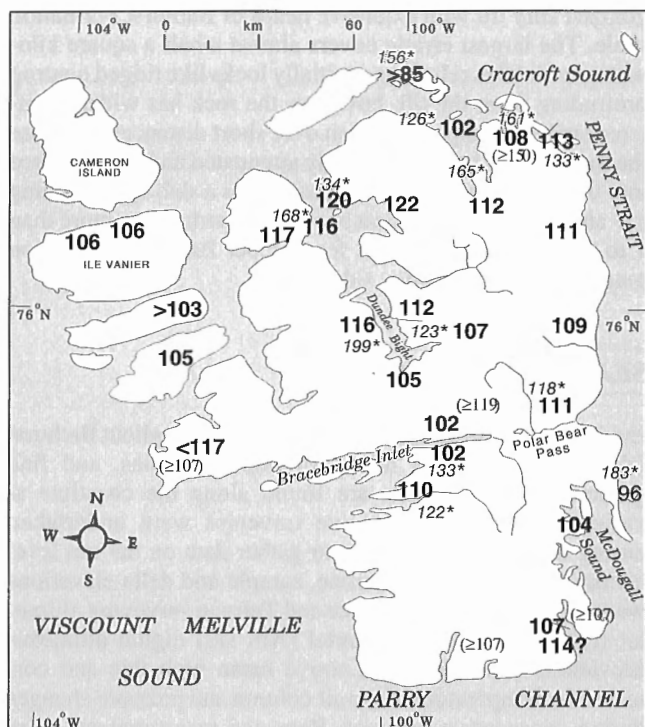
*arctica*, collected 155-145 m, in fine gravel concentrations overlying bedrock which dated 9850 ± 150 BP (GSC-4176; D.A. Hodgson, pers. comm., 1995). High Holocene-aged shell fragments were also reported near Carey Harbour (9690 ± 140 BP, GSC-251; Lowdon et al., 1967). The age of the 119 m a.s.l. shells in central Bathurst Island is 9030 ± 150 BP (GSC-386). A similar age was obtained from shells on southern Bathurst Island at 104 m a.s.l. (9070 ± 190 BP, GSC-353). Dyke et al. (1991) showed northward rising postglacial isobases over Bathurst Island (Fig. 3), however, Dyke (1993; p. 134) observed that the uplift pattern over Bathurst Island, which is immediately north of the margin of the Laurentide Ice Sheet, was "incongruous with the known or inferred pattern of glacial loading". Dyke (1993) refined the pattern of isobases over Lowther and Griffith islands in Parry Channel which further intensified the isobase pattern between Parry Channel and Bathurst Island by extending the Prince of Wales "isobase plateau" to the north. Dyke et al. (1991) suggested that the southern dip of raised shorelines in the area may reflect extensive tectonic complications of postglacial rebound. Nonetheless, the configuration of isobases north of Parry Channel can only be determined by expanding the Holocene sea level database. Dyke (1993) found that the Laurentide Ice Sheet had overridden both Lowther and Griffith islands, and did not find any evidence of southward-flowing, Innuitian ice.

## GLACIAL GEOLOGY

The Bathurst Island group, as noted above, does not show evidence of intensive glaciation compared to the islands south of Parry Channel. Most interior areas are devoid of glacial
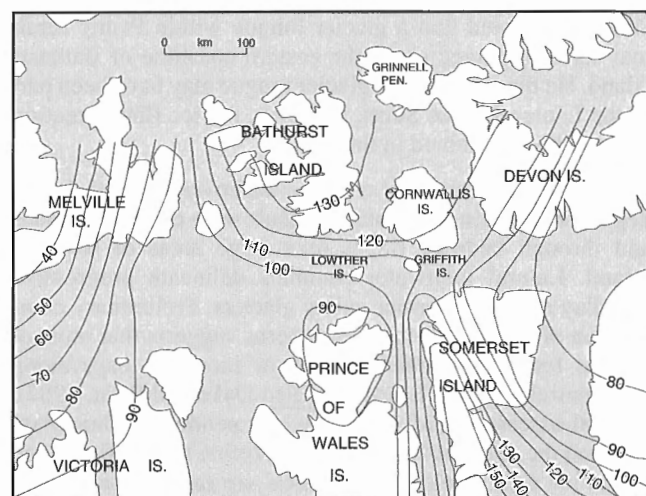


**Figure 2.** *The location and elevation of marine limit based on the highest shorelines, deltas, or washing limits are shown in bold numbers. The elevation of the highest shells within till are shown italicized with an asterisk. Elevations of the minimum marine limit elevation presented by Hodgson (1989) are shown in brackets. All elevations are in metres above sea level.*



**Figure 3.** *Isobases of the elevation (metres) of the 9.3 ka BP shoreline in the south-central Queen Elizabeth Islands, from Dyke (1993). Current field data suggests that the cell of high emergence over Bathurst Island may not exist. Instead, the isobases probably rise continually from Melville Island, across Bathurst Island, to Grinnell Peninsula on Devon Island. This implies that the very sharp inflection around Lowther and Griffith islands may not exist.*

63

deposits. Till is usually found in small patches only a few square kilometres in area at the heads of some bays and along some coastal uplands. Some upland surfaces are covered by isolated blankets of thicker till (>2 m thick) that tend to be polygonized. On northeast Bathurst Island more extensive till deposits are slightly elongated along north-south and northwest-southeast trends. Similar oriented landforms also occur in southeast Bathurst Island along McDougall Sound, but the direction of ice flow remains to be determined. Most glacial streamlining of the till is subtle and only recognizable on the airphotos.

Glacial scour of the bedrock is also limited in extent but is most pronounced where the former ice flowed parallel to strike-aligned topography. Ice scoured bedrock on the southwest side of Polar Bear Pass, west of Caledonian River, records northward flowing ice that swung westward to flow down Bracebridge Inlet. Owing to the recessive nature of the bedrock and scarcity of a protective till cover, only one exposure of striae was found. This, on the present shoreline of Balcarres Island in central May Inlet, showed a general north-south alignment. However, even these striae may have been produced by sea ice. Blake (1964) reported north-northeast-trending striae within one valley on northernmost Bathurst Island that he thought "suggested ice motion towards the north".

Extensive end moraines are absent in the study area, however small moraine segments, up to 10 m high and hundreds of metres long, can be found in lowland areas at the head of deeply indented bays in Dundee Bight. These probably mark the recession of local valley glaciers. Larger, but more subdued end moraines are found in northeastern Bathurst Island, where they crosscut the streamlined drift that trends generally north-south. The ice configuration that resulted in these moraines has yet to be determined, however, Blake (1964) suggested that a glacier tongue within Penny Strait may have impinged along the eastern coastline of Bathurst Island. He thought that the glacier tongue may have been part of the Laurentide Ice Sheet, however, the ice flow direction is yet to be determined in the area.

The best evidence for a native ice cover was left during deglaciation when meltwater channels were cut into hillsides and through bedrock ridges over large areas of Bathurst Island. Lateral meltwater channels delineate progressive upvalley retreat of former valley glaciers. Preliminary compilation of the nested channel patterns suggests that most of the ice tongues retreated to one or more ice caps along east-central Bathurst Island (see also Dyke and Prest, 1987). Careful assessment of available, and pending, radiocarbon dates on the deglacial pattern should refine the configuration of the ice caps. Meltwater channels are rare on the smaller islands northwest of Bathurst Island. Although the relic channels outline local ice cap(s) during deglaciation, this does not rule out a large, off-island, ice sheet prior to this time.

Barnett et al. (1976) noted that on Bathurst and Cornwallis islands shield provenance erratics were "widespread" in distribution and at a "variety" of elevations, but he considered them to have been deposited during a "pre-classical Wisconsin" glaciation because of the lack of Laurentide tills

and end moraines. During the 1995 field season, numerous igneous erratics of boulder to granule size were found but no igneous erratics were found on the uplands, despite extensive searching by all field parties. Only a single gneiss was found above the level of postglacial marine submergence. It was about 15 m above the marine limit in a stream bed on Ile Vanier (Fig. 1). Generally, there were more shield provenance erratics on the westernmost islands of the Bathurst Island group, but most were in stream beds at low elevations. Since most the erratics found were below the marine limit, deposition by ice rafting cannot be discounted, however, it is conceivable that, given a long enough period of time, glacially transported erratics from the Shield were either buried by felsenmeer on the uplands, or redeposited at lower elevations by hillslope processes. Consequently, Barnett et al.'s premise may be valid, although most of the granite and gneiss found were not substantially weathered.

Locally derived erratics cover the Bathurst Island group at all elevations. The most common are rounded to subangular quartzose sandstones derived from the mid-Devonian Hecla Bay Formation (Kerr, 1974), however, this formation outcrops widely, and consequently, cannot be used to infer glacial flow directions. The most spectacular erratics found during the 1995 field season were very large slabs of displaced upper Bathurst Island Formation within the Half Moon Bay anticline in Dundee Bight (Fig. 1). The eroded core of the anticline forms a broad valley that is mantled by a polygonized silty till with extensive heaps of Bathurst Formation shale. The largest erratic covers almost a half a square kilometre, with 10 m relief, and initially looks like ridged outcrop protruding from the till, however, the rock has widely scattered strike and dip orientation over short distances. Because the rock has not been extensively attenuated and incorporated into the till, it must have been plucked as a slab by overriding ice and transport must have been short, perhaps no more than 1 to 2 km to the northwest from upper Bathurst Formation outcrops along the valley side.

## SEA LEVEL HISTORY

Evidence of isostatic uplift is widespread throughout Bathurst Island and numerous raised strandlines, deltas, and fine grained marine deposits are found along the coastline at various elevations. Extensive traverses were undertaken during the 1995 field season to gather data on the sea level history of the island. Shoreline, sample and delta elevations were measured with a Wallace and Teirnan surveying altimeter (type FA-181) and a Pretel (Alti D2) digital altimeter. Elevations were measured above mean high tide and corrected for temperature of the air column and pressure changes during consecutive readings. Repeated measurements were usually within ±1 m, and rarely exceeding ±2 m. Greatest errors occurred during high winds. Over one hundred marine pelecypod, driftwood, whale bone, and narwhal bone samples, related to raised marine deposits and strandlines, were collected for eventual radiocarbon dating. This information will be used to construct emergence curves for the different parts of the study area.

To determine the marine limit in the study area, the highest raised beaches, deltas, or washing limits found on airphotos were measured on the ground. Figure 3 shows the elevation of the marine limit measured on Bathurst Island. In many areas the marine limit was not clearly defined except for a faint washing limit, with patches of fine grained sediment containing marine bivalves found below. Ice-contact deltas marking the marine limit are rare and mostly confined to the heads of bays in Dundee Bight. As noted, Cameron Island was not visited, but the marine limit on the north coast of Ile Vanier is 106 m a.s.l.. The marine limit of Ile Marc and Massey and Alexander islands in not clearly defined, but the highest definite beaches are at about 105 m a.s.l. Generally, the marine limit rises toward north-central Bathurst Island to a maximum of 122 m in Purcell Bay, May Inlet. From there, the marine limit declines to 108 m in northwest Bathurst Island and to 107 m in the southeast.

The marine limit elevations presented here are the highest geomorphic expression of a sea level in given area, irrespective of the age. Nonetheless, because uplift was ongoing during deglaciation, the maximum elevation of marine onlap depends on the magnitude of the former ice load and the date of deglaciation (minimum age of the marine limit). The diachronous nature of the marine limit means that it must be dated to properly infer glacial loading. The ages of most of these features will be determined with pending radiocarbon dates. In addition, fragments of marine shells well above the highest marine strandline are widespread on Bathurst Island (Fig. 2), these will be discussed in the following section.

## DISCUSSION

The glacial geomorphology of Bathurst Island, beyond the northern limit of the Laurentide Ice Sheet, suggests that at some point during deglaciation, the island was covered by local ice caps. Before that time, the ice caps may have been coalescent with, or part of, a larger ice mass but this is not yet known. There is some evidence of an ice-flow along Penny Strait that impinged onto the northeast coast of Bathurst Island.

If there are no tectonic complications, the configuration of former ice masses during the last glaciation may be determined by the pattern of crustal emergence. As noted above, the assumed trend in marine limit elevation suggests that the former ice load was greatest on northeast Bathurst Island, however, Dyke (1993) thought this was inconsistent with a former Innuitian Ice Sheet (cf. Blake, 1970). The oldest Holocene radiocarbon dates on shells and peat suggest that northernmost Bathurst became ice-free first (Dyke and Prest, 1987). This suggests that the marine limit in the north is higher because it is older than in the south, but Dyke (1993) thought that the delay in ice retreat was insufficient to make a significant difference in the isobase pattern. A northern uplift cell over Bathurst Island appears to be problematic (Dyke et al., 1991), however, new data from the 1995 field season, and close scrutiny of the available data, suggest the isobase pattern over Bathurst Island is in need of revision.

The geomorphologically defined marine limits presented here (Fig. 2) are considerably lower than sea levels previously presented for Bathurst Island (see "Introduction") because of several reasons discussed here. In previous work, a reasonable assumption was made that the marine limit must be higher than the elevation of the highest postglacial shells, such as the Holocene shells reported by Blake (1964) and Hodgson (1989) on northeast Bathurst Island. As noted above, the highest Holocene aged shells (GSC-4176; 9850 ± 150 BP) were collected on a hillslope from 145 to 155 m a.s.l. along Cracroft Sound (Fig. 1). The sample consisted of shell fragments and some whole valves of *Hiatella arctica* (D.A. Hodgson, pers. comm., 1995). Nevertheless, shell fragments are found right up to the summits above Cracroft Sound (>160 m a.s.l.). Moreover, during the 1995 field season, extensive traverses along the north coast did not find any strandlines at these elevations. Commonly, shell fragments were found in diamictons mantling the summits of local bluffs along Cracroft Sound and Young Inlet (Fig. 2). To this author the diamictons are till, suggesting that the shells must have been transported by the ice. This means that the elevation of the shells is irrelevant in terms of the elevation of the marine limit. Shell fragments were also found at very high elevations in other parts of Bathurst Island. For example, Blake (1964) reported *Hiatella arctica* in till at 145 m a.s.l., south of Bracebridge Inlet (GSC-212, 35 900+1400/-1200). Moreover, during the 1995 field season, undated shells were found in till at 183 m a.s.l. in southeast Bathurst Island, at 199 m a.s.l. along western Dundee Bight, and at 156 m a.s.l. on the top of east Hoskin Islands (Fig. 2). Some of these samples include complete valves. Unquestionably, individual fragments should be dated with AMS to determine if the shells are truly Holocene and not a mix of pre- and postglacial ages. It is likely that previously reported Holocene dates must include some Holocene shells. If the shells are indeed Holocene, there must have been an early Holocene glacial readvance that picked up the shells and deposited them above the marine limit. The streamlined till on northeastern Bathurst Island could indicate such an advance to the north. Hodgson (1994) documented several major glacial readvances along the retreating margin of the Laurentide Ice Sheet into western Parry Channel between 11 ka and 9 ka BP. These readvances need not have been climatically controlled, but caused by local instability of the ice margin in contact with high sea levels.

The Dyke et al. (1991) used 15 radiocarbon dates on raised marine shells, driftwood, and terrestrial peat to construct two emergence curves for south and central Bathurst Island. The curves were then used to construct isobase maps of the central Arctic which depicted the cell of greater uplift over Bathurst Island that Dyke (1993) considered problematic (see above), although Dyke (1993) also noted that the isobase pattern north of Parry Channel is poorly constrained. In fact, the fieldwork reported here, suggests that isobase pattern may be considerably different than drawn by Dyke et al. (1991). The critical upper part of Dyke et al.'s central Bathurst Island emergence curve is based a Holocene shell date on northeast Bathurst Island (GSC-251; 9690 ± 140, at 137 m a.s.l.). As was discussed earlier, a glacial readvance may have redeposited

Holocene shells in this area. Moreover, a major problem exists with the location and elevation of the sample, as with many of the early GSC dates, because of inaccuracies in the original topographic base maps. For example, given the latitude and longitude of the former site, the nearest land with that elevation is over 1 km to the west, so it is practically impossible to check the elevation. Moreover, the area was revisited during the 1995 field season and shells were found in a surface diamicton up to 133 m, well above the highest strandlines in the area. The second critical date defining Dyke's emergence curve comes from Dundee Bight, 75 km southwest of the first site (GSC-386; 9030 ± 150, at 119 m a.s.l.). In this case, the recorded latitude and longitude plot on the eastern coast of Dundee Bight, in an area below 30 m a.s.l., not on a 119 m a.s.l. beach as reported. In 1995, the highest beach measured in this area was only 112 m, over 1 km upslope. Similar problems arise in locating the highest three radiocarbon-dated samples for the southern Bathurst Island emergence curve (Dyke et al., 1991). In fact, one of the samples is located in the middle of Freemans Cove, over 2 km from any land high enough. Nevertheless, the elevation of the highest beaches measured in 1995 is similar to what has been previously reported, namely 107 m a.s.l. Given the problems with the location and elevation of the early samples, it is clear that they should be treated with caution, particularly in constructing emergences curves.

In conclusion, geomorphological evidence suggests that the marine limits over Bathurst Island are lower than previously thought and the cell of high emergence depicted by Dyke et al. (1991) and Dyke (1993) may not exist. Holocene shells previously used to define a northward rise in marine limit may have been redeposited during a glacial readvance. Nevertheless, isobases may rise northeastward across Penny Strait, where the marine limit on western Grinnell Peninsula is 131 m a.s.l. (A.S. Dyke, pers. comm., 1995). Of course, this can be substantiated only with dated shorelines. Secondly, it may be that the tectonically created "isobase plateau" over Prince of Wales Island (Dyke, et al., 1991) extends onto Bathurst Island. Certainly, the western boundary of the cratonic Boothia Uplift extends northward, from Prince of Wales Island, onto eastern Bathurst Island (Harrison et al., 1993). Finally, the nature of the last glaciation of Bathurst Island, with respect to adjacent ice masses, can only be resolved by future fieldwork attempting detailed reconstruction of ice flows and ice-marginal chronology.

## ACKNOWLEDGMENTS

## REFERENCES

**Barnett, D.M., Dredge, L.A., and Edlund, S.A.**
1976: Terrain inventory: Bathurst, Cornwallis, and adjacent islands, Northwest Territories; Report of Activities, Part A; Geological Survey of Canada, Paper 76-1A, p. 201-204.
1977: Surficial geology, Bathurst and adjacent islands, District of Franklin; Geological Survey of Canada, Open File 0479, maps, scale 1:125 000.

**Blake, W., Jr.**
1964: Preliminary account of the glacial history of Bathurst Island, Arctic Archipelago; Geological Survey of Canada, Paper 64-30, 8 p.
1965: Surficial geology, Bathurst Island; Geological Survey of Canada, Paper 65-1, Report of Activities, p. 2-3.
1970: Studies of glacial history in Arctic Canada. I. Pumice, radiocarbon dates, and differential postglacial uplift in the eastern Queen Elizabeth Islands; Canadian Journal of Earth Sciences, v. 7, p. 634-664.
1974: Studies of glacial history in Arctic Canada. II. Interglacial peat deposits on Bathurst Island; Canadian Journal of Earth Sciences, v. 11, p. 1025-1042.

**Dyke, A.S.**
1993: Glacial tectonics and sea level history of Lowther and Griffith Islands, Northwest Territories: a hint of tectonics; Géographie physique et Quaternaire, v. 47, p. 133-145.

**Dyke, A.S. and Dredge L.A.**
1989: Quaternary geology of the northwestern Canadian Shield; in Chapter 3 of Quaternary Geology of Canada and Greenland, R.J. Fulton (ed.); Geological Survey of Canada, Geology of Canada, no. 1, (also Geological Society of America, The Geology of North America, v. K-1), p. 189-214.

**Dyke, A.S. and Prest V.K.**
1987: Late Wisconsinan and Holocene retreat of the Laurentide Ice Sheet; Geological Survey of Canada, Map 1702A, scale 1:5 000 000.

**Dyke, A.S., Morris, T.F., and Green, D.E.C.**
1991: Postglacial tectonic and sea level history of the central Canadian Arctic; Geological Survey of Canada, Bulletin 397, 56 p.

**Edlund S.A.**
1986: Surficial materials, Bathurst Island area and Byam Martin Island, District of Franklin, N.W.T.; Geological Survey of Canada, Open File 1275, map, scale 1:250 000.

**Harrison, J.C., de Freitas, T., and Thorsteinsson, R.**
1993: New field observations on the geology of Bathurst Island, Arctic Canada: Part B, structure and tectonic history; in Current Research, Part B; Geological Survey of Canada, Paper 93-1B, p. 11-21.

**Hodgson, D.A.**
1989: Introduction (Quaternary geology of the Queen Elizabeth Islands); in Chapter 6 of Quaternary Geology of Canada and Greenland, R.J. Fulton (ed.); Geological Survey of Canada, Geology of Canada, no. 1, (also Geological Society of America, The Geology of North America, v. K-1), p. 443-459.
1994: Episodic ice streams and ice shelves during the retreat of the northwesternmost sector of the late Wisconsinan Laurentide Ice Sheet over the central Canadian Arctic Archipelago; Boreas, v. 23, p. 14-28.

**Kerr, J.W.**
1974: Geology of the Bathurst Island group and Byam Martin Island, Arctic Canada (Operation Bathurst Island); Geological Survey of Canada, Memoir 378, 152 p.

**Lowdon, J.A., Fyles, J.G., and Blake, W., Jr.**
1967: Geological Survey of Canada radiocarbon dates VI; Radiocarbon v. 9, p. 156-197.

**Roots, E.F.**
1963: Physiography; in Geology of the north-central part of the Arctic Archipelago Northwest Territories (Operation Franklin), (ed.) Fortier, Y.O. et al., Geological Survey of Canada, Memoir 320, p. 580-585.

# C-band radar signatures of lithology in arctic environments: preliminary results from Bathurst Island, Northwest Territories

Paul Budkewitsch[1], Marc A. D'Iorio[2], and J. Chris Harrison
GSC Calgary, Calgary

**Abstract:** A variety of sedimentary rock types exposed on Bathurst Island provides a rich test site for examining the effect of radar imaging parameters on radar backscatter. Two bright radar units are examined. One unit corresponds to carbonate rocks of the Eids and Blue Fiord beds, whereas the other corresponds to a thick sequence of quartz arenites belonging to the Hecla Bay Formation.

Radar backscatter signatures are not unique indices for lithological mapping. They are, however, good indicators of surface roughness, which can be diagnostic of the weathering style of particular rock types in arctic environments. The tone and texture of the radar images define geological radar units and their distribution reveals a pattern strongly correlated to mapped geological formations and regional structures. In some cases, radar brightness and textural variations can be correlated to specific stratigraphic members. Previously unmapped fault and fold structures are also inferred from the radar data.

**Résumé :** Les différents types de roches sédimentaires affleurant sur l'île Bathurst font que ce coin de pays constitue un site d'essai propice à l'identification des meilleurs paramètres pour obtenir des images sur la rétrodiffusion radar dans le cadre de travaux géologiques. Deux unités ressortant bien sur les images radar sont analysées; il s'agit des roches carbonatées des couches d'Eids et de Blue Fiord, de même que d'une épaisse séquence d'arénite quartzique de la Formation d'Hecla Bay.

Les signatures de rétrodiffusion radar ne sont pas des indices uniques pour la cartographie lithologique. Elles sont cependant de bons indicateurs de la rugosité de surface, qui peut être symptomatique de l'altération de certains types de roches dans les milieux arctiques. Le ton et la texture des images radar permettent de définir les unités géologiques selon les ondes radar; quant à la répartition des unités, elle révèle un motif qui correspond bien aux formations géologiques et aux structures régionales cartographiées. Dans certains cas, la brillance des images radar et leur variation texturale peuvent être corrélées à des membres stratigraphiques spécifiques. À partir des données radar, il est en outre possible d'inférer la présence de failles et de plis qui ne figurent pas sur les cartes actuelles.

---

[1] MIR Télédétection, Longueuil, Quebec
[2] Canada Centre for Remote Sensing, Ottawa, Ontario K1A 0Y7

## INTRODUCTION

In preparation for the availability of data from RADARSAT, Canada's polar-orbiting radar-satellite, studies have been initiated by the Canada Centre for Remote Sensing (CCRS) to evaluate the potential of radar data in a variety of applied disciplines. Objectives of the present study are to evaluate the radar imaging parameters that are best suited for examining lithological units and recognizing geological structures in arctic environments. For the user community, these results will ultimately provide guidelines for choosing among the 25 beam modes and positions offered by RADARSAT which are best suited for specific applications (Denyer et al., 1993; Corbley and Engel, 1995).

Numerous studies investigating radar sensor parameters appropriate for geological studies have been carried out, but mainly in temperate (see Singhroy et al., 1993), tropical (e.g., Sabins, 1983; Ford and Casey, 1988), or semiarid environments (e.g., Blom and Daily, 1982; Blom et al., 1987; Blom, 1988; Arvidson et al., 1993). Preliminary results are presented that include description of some of the terrain features which control the radar backscatter in synthetic aperture radar (SAR) images acquired over Bathurst Island, Northwest Territories.

Radar remote-sensing systems are active microwave transmitters and receivers. SAR processing of the radar backscatter (the amount of radar energy returned to the sensor) results in a digital radar image of the area imaged where pixel brightness is a function of both the amplitude and phase of the backscatter signal. The radar backscatter from a parcel of ground is controlled by a number of factors. Dielectric constant of the ground material has an influence on the amount of backscatter, however, the variation for dry rocks and soils is too small to fully account for the range of backscatter observed (Ulaby et al., 1986). The other factors that strongly affect backscatter are: (I) the presence of moisture, (ii) compactness or bulk density of the material, (iii) local orientation of the surface with respect to the sensor, and (iv) the millimetre- to decimetre-scale microtopography, or "surface roughness", as it is referred to in the remote sensing literature (Schaber et al., 1976; Ulaby et al., 1986)

## GEOLOGICAL SETTING
## OF BATHURST ISLAND

Bathurst Island (Fig. 1) forms the eastern part of the Parry Islands Fold Belt and is bordered to the east by fault structures related to the Cornwallis Fold Belt (Boothia Uplift). The structure and stratigraphy of the Phanerozoic rocks on Bathurst Island has been described by Kerr (1974) and published as a 1:250 000 scale geological map. The style of deformation in the Parry Islands Fold Belt is the result of a long history of deformation (Harrison, 1995) dominated by a complex sequence of faults and associated folds. The eastern margin of Bathurst Island exhibits evidence for an early (Lower Devonian) phase of deformation along north-trending structures (Harrison et al., 1993). Much of the island is characterized by gently west- to southwest-plunging open synclinal folds spaced about 10 to 15 km apart and separated

by thrust- and normal-faulted anticlines. These second-phase structures are largely attributed to post-Middle Devonian (Famenian) deformation (Harrison et al., 1993). The transition zone between these folds and a third phase (mid-Tertiary) of near orthogonal north-trending deformation on the east side of the island is characterized by Type-1 (Ramsay, 1967) fold interference patterns.

The sedimentary succession consists of a series of shallowing-upward sequences that consist of deep water shales and siltstones to platformal carbonates and nonmarine sandstones (de Freitas et al., 1993). Thus, a wide variety of sedimentary rock types occur on Bathurst Island, making the areas suitable for examining the effects of lithological control on radar backscatter. In most regions, outcrop is not directly exposed, but the presence of monolithic pebble, or cobble fields (felsenmeer) imply derivation through frost heave from near surface bedrock. The style of cryogenic fragmentation and displacement of rock appears to be characteristic of the underlying lithology.

Topography of Bathurst Island is relatively subdued and does not exceed 350 m above sea level. Broad valleys are separated by flat-topped ridges of low relief. Narrow ravines incise the flanks of the ridges and link together in the valleys to form an extensive seasonal drainage network. The island lies in the zone of continuous permafrost and lakes or standing water are quite rare, except along Polar Bear Pass, a valley east of Bracebridge Inlet (Fig. 1, 2).

## REMOTE SENSING AND FIELD DATA

Preliminary findings from optical Landsat-TM data (bands 4, 5, 7) and satellite ERS-1 radar data reveal a strong spatial correlation between radar units and the lithological units and
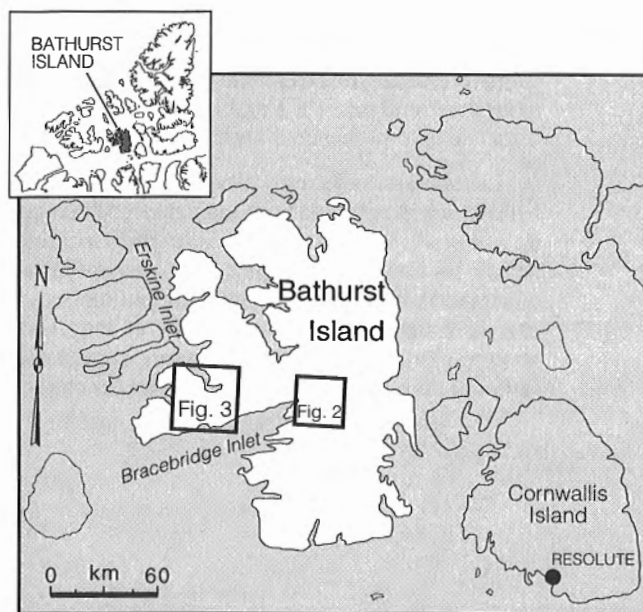


*Figure 1. Bathurst Island in the Arctic Archipelago. Location of the two study sites discussed (Fig. 2, 3) are outlined.*

structures outlined on the geological map of Kerr (1974). Airborne radar was collected by CCRS in April 1995, coincident with the airborne radar programme carried out for sea-ice investigations in the vicinity.

One important aspect of cold-temperature data acquisition is that no ground moisture (liquid phase water) is present. Any pore water present in the surface material is frozen, and thus, does not affect the dielectric constant of surface material as greatly as liquid water. Clouds and even several decimetres of dry snow are easily penetrated with C-band radar without significant attenuation (Ulaby et al., 1986). This part of the arctic receives very little precipitation and snow thickness due to drifting does not usually exceed 1 m on Bathurst Island (Miller, 1993). Thus, radar data obtained for this study offer an excellent opportunity to investigate the radar backscatter response to ground surface roughness, as related to weathering and rock type in arctic environments.

## Radar data acquisition

The CCRS airborne SAR is a C-band (wavelength of 5.6 cm) imaging-radar system that operates in nadir, narrow-swath and wide-swath modes (Livingstone et al., 1987, 1988). Wide-swath mode data with an azimuth resolution of 10 m and range resolution of 20 m are used in this study. The swath width is made up of 4096 pixels (15 m pixels), for total ground distance of about 60 km. Radar incidence angles increase from 45° in the near-range to 85° in the far-range. Three east to west flight lines acquired in April 1995 provided almost full coverage of Bathurst Island.

Part of the eastern side of the island was imaged in narrow-swath mode along north-south flight transects. Narrow-swath operation provides a greater resolution at 6 m in both the range and azimuth directions. However the swath width is reduced to about 20 km. Radar incidence angles are from 45° in the near-range and reach 76° in the far-range.
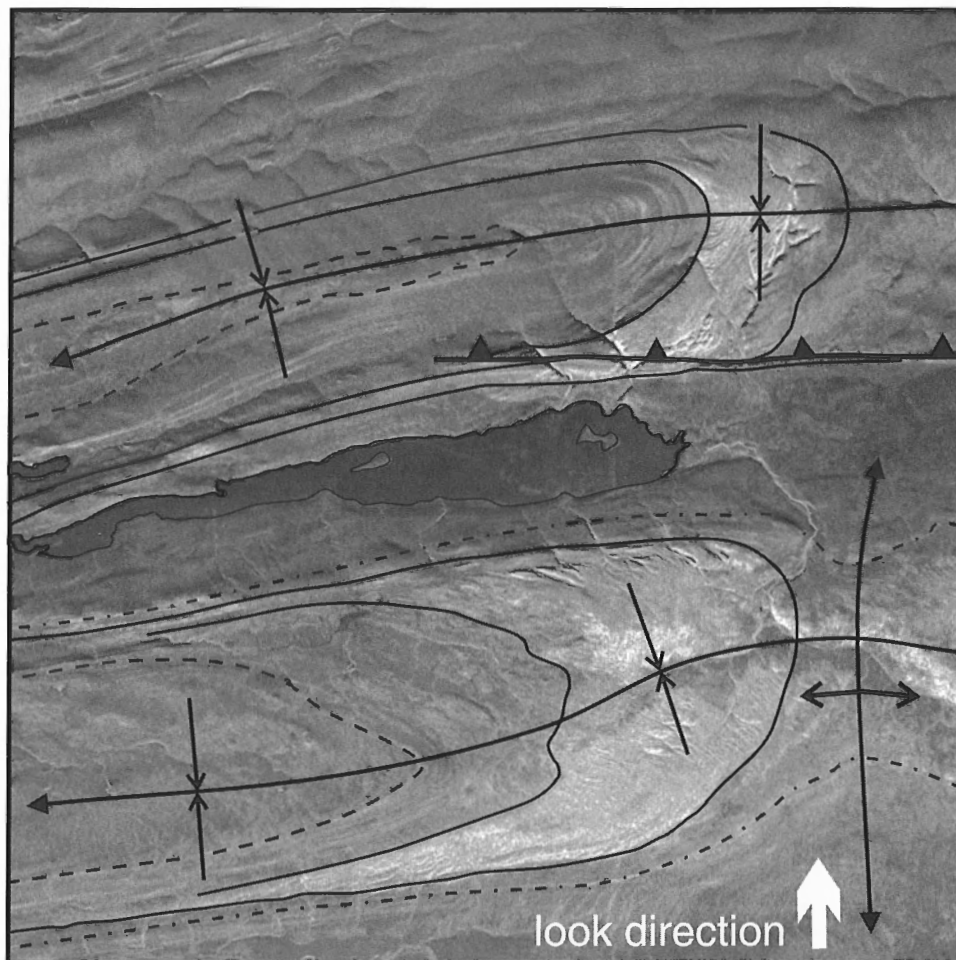


*Figure 2. Bright radar units of the Eids and Blue Fiord beds (outlined with solid lines) exposed in the hinge zone of two synclines near Bracebridge Inlet. Near-range is along the bottom; far-range is at the top. Area shown is about 30x30 km.*

## Field data

Field data gathered in July 1995 focused on identifying distinct radar units by their tonal and textural expression on the images. Representative sites of the radar units were examined in the field in order to verify the terrain features associated with the radar signature. Certain rock types often develop a characteristic degree of surface roughness, however, surface roughness or radar backscatter can not be uniquely correlated to specific lithologies. Surface roughness parameters were estimated from the mean size of loose rock fragments, percentage of ground coverage, and measurements of roughness using a chain method described by Saleh (1993). Most formations were examined for these roughness characteristics. Preliminary results of field observations from two radar units that exhibit high backscatter and broadly correspond to a carbonate unit (Eids and Blue Fiord beds) and a quartz arenite unit (the Hecla Bay Formation) are reported. The sizes of rock fragments indicated below represent one standard deviation below and above the mean, rounded to the nearest centimetre.

## Radar expression of the Eids and Blue Fiord beds

Two bright, arcuate radar units examined at the head of Bracebridge Inlet correspond to exposures of the Eids and Blue Fiord beds in the hinges of west-plunging synclines (Fig. 2). This part of the sequence is moderately bedded and has been redefined by Harrison et al. (1993) and de Freitas et al. (1993) as part of the Blue Fiord beds. Wide areas represented by these rocks are exposed as a felsenmeer of fragments about 4 to 8 cm across and a similar vertical relief. Weathered rock fragments tend to be larger and more equant in the western part of the bright radar unit where they are partly silicified and dominated by coral and crinoid fossil fragments.

The Eids beds, which underlie the Blue Fiord, are well laminated marls and petroliferous shales (Harrison et al., 1993). This part of the bright radar unit (Fig. 2) is more commonly represented by a felsenmeer of thin platelets, 2 to 6 cm across, which are either stacked flatly upon one another or subvertically imbricated. In the field, the carbonate
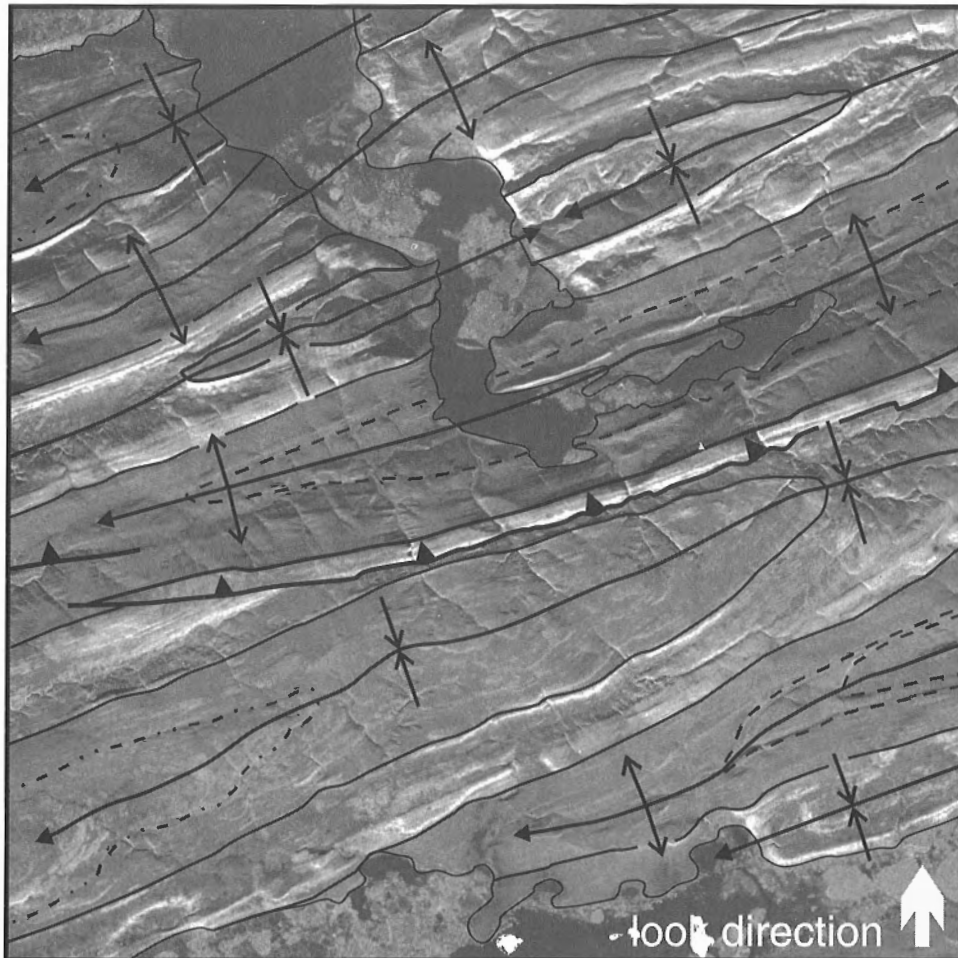


*Figure 3. A series of gently plunging anticlines and synclines near Erskine Inlet. Outlined radar unit (solid lines) corresponds to quartz arenites of the Hecla Bay Formation. Near-range is along the bottom; far-range is at the top. Area shown is about 35x35 km.*

felsenmeer form large hummocks, tens of metres long and a few metres high which appear to be caused by selective erosion along less resistant bedding planes. On the SAR images, slight radar shadowing due to the topographic changes creates braid-like features, which is more characteristic of the Eids than the Blue Fiord beds. Differences between the Eids and Blue Fiord are more apparent on narrow-swath SAR images (higher resolution) where the Blue Fiord appears to have a slightly higher backscatter than the Eids, likely due to the larger fragments that form the Blue Fiord felsenmeer. In aerial photographs or Landsat-TM images, the two units are very difficult to distinguish and often not discernible at all because of their compositional similarity.

The Eids and Blue Fiord beds are easily distinguished from dark radar units, above and below, which correspond to limy siltstones and mudrocks (the Bird Fiord Formation and Stuart Bay beds of de Freitas et al. (1993)). These rocks are much more fissile and erode recessively such that few outcrops or felsenmeer of the siltstones or mudrocks are encountered. Generally the terrain is composed of sand and mud deposits and a few perched rock fragments derived from the underlying bedrock. As a result, this terrain is relatively flat and smooth and exhibits a much lower backscatter than the units previously described.

### Radar expression of the Hecla Bay Formation

Bright radar units shown in the vicinity of Erskine Inlet (Fig. 3) correspond to resistant ridges that are composed of quartz arenites belonging to the Hecla Bay Formation. The ridges correlate well to the lower member of the Hecla Bay Formation, described by Kerr (1974) as a massive, well cemented quartzite. In the field, the bright zones correspond to block fields consisting of large (7 to 31 cm) subequant, angular cobbles or 2 to 5 cm thick slabs of orthoquartzite. The ridges are consistently radar bright, but include one distinct dark band (and a few minor ones) that runs parallel to the ridge for several kilometres (Fig. 3). These bright and dark bands likely correspond to mappable members of the Hecla Bay Formation.

The radar unit overlying the bright, folded ridges has a distinct coarse (mottled) texture that corresponds to the upper member of the Hecla Bay Formation. This texture is best observed where the unit is almost flat-lying, such as near hinge areas of synclines (Fig. 3). The upper unit is a poorly cemented, fine grained orthoquartzite that disintegrates quite readily, leaving sandy flats and some well rounded (1 to 9 cm) friable pebbles. These areas have relatively low backscatter and appear dark on radar images. Resistant parts of the upper member remain exposed as small hills or hoodoos (Kerr, 1974), which accounts for the bright areas that yield the mottled texture for this unit. The mottled radar unit terminates against a second bright radar unit that appears as a resistant ridge on images. This unit is much thinner than the underlying one and marks the onset of a well cemented quartz arenite, corresponding to a locally mappable member in the lower part of the Beverley Inlet Formation.

South of Erskine Inlet (Fig. 3), a thrust fault (not present on Kerr's map) is inferred from the relationships of the radar units. The lateral continuity of the bright radar unit (lower Hecla member) is abruptly truncated against itself in the western part of the image. In the centre and east, the truncated margin of the bright unit can be seen to cut across the mottled radar unit (upper Hecla member), thinning the unit in a manner consistent with thrust faulting along a north-dipping fault plane.

## DISCUSSION AND CONCLUSIONS

Radar signature variations examined on Bathurst Island correspond to large changes in surface roughness of the terrain that are largely controlled by lithology, but not uniquely related to a specific lithology. High radar backscatter occurs from terrain characterized by felsenmeer consisting entirely of rock fragments from a few centimetres to almost 0.5 m in size. Weathering of thick-bedded, resistant rock types, such as reefal carbonates and well cemented arenites, release blocks of these dimensions from the underlying bedrock. In contrast, fissile and poorly cemented sandstone, siltstone, and shale erode more deeply and are frequently covered by fine debris. The latter have smooth ground surfaces and are dark on SAR images. Thus, radar data can provide important information for understanding the relationship between different terrain types and underlying lithology.

In arctic environments where mechanical weathering dominates, radar remote sensing is able to map variations in terrain surface roughness. In some cases, changes in surface roughness correspond to lithological transitions recognized in the field. This provides supporting evidence that fabric (e.g., fossiliferous vs. laminated) differences between carbonates of similar composition can be differentiated in radar data on the basis of how they weather (i.e., their surface roughness).

Radar units can serve as useful guides for delineating lithological contacts where surface roughness and density of rock fragments are characteristic surface expressions of the rock units under study. This technique shows particular promise for regional investigations over wide areas where gradual changes, or subtle continuities are difficult to trace across several aerial photographs. Discontinuities across strata (such as the fault in Fig. 3) are also more easily identified.

The high quality (high resolution) of optical aerial photography guarantees that detailed features of interest will always be best discerned from these images. Even the relatively high 6 m spatial resolution of airborne SAR is not adequate for delineation or identification of smaller features visible in aerial photographs. Airborne (or satellite) SAR and aerial photography in tandem, however, provide complementary information at small and large scales that are effective to aid geologists for mapping structures and stratigraphic units and enable rapid recognition of these features across wide areas.

## CONTINUING WORK

Airborne SAR collected at various incidence angles and look-directions (orthogonal to flight direction) together with ERS-1 satellite data is the subject of current investigations and much uncertainty about the geological information content remains to be discovered in arctic regions. The purpose of further work is to learn more about resolution and viewing geometry to the lithological and rock fabric information that can be maximized from advantageous imaging parameters represented in these data sets. The purpose of the field roughness measurements is to better quantify the surface roughness and to examine the relationship between roughness and lithology for the purpose of mapping. In addition to general brightness of a unit, radar-image textural variations (e.g., Haralick, 1979) can provide a classification basis for supporting the continuity of a radar unit for the purpose of lithological mapping.

This radar geology project involves other researchers at the Canada Centre for Remote Sensing who are involved with interferometric SAR (e.g., Livingstone et al., in press) and SAR coherence images (Vachon et al., 1995). Integration of other geological data sets with SAR is another aspect of this work that will be examined.

## ACKNOWLEDGMENTS

## REFERENCES

**Arvidson, R.E., Shepard, M.K., Guinness, E.A., Petroy, S.B., Plaut, J.J., Evans, D.L., Farr, T.G., Greeley, R., Lancaster, N., and Gaddis, L.R.**
1993: Characterization of lava-flow degradation in the Pisgah and Cima volcanic fields, California, using Landsat Thematic Mapper and AIRSAR data; Geological Society of America Bulletin, v. 105, p. 175-188.

**Blom, R. and Daily, M.**
1982: Radar image processing for rock-type discrimination; IEEE Transactions on Geoscience and Remote Sensing, v. 20, p. 343-351.

**Blom, R.G.**
1988: Effects of variation in look angle and wavelength in radar images of volcanic and aeolian terrains, or now you see it, now you don't; International Journal of Remote Sensing, v. 9, p. 945-965.

**Blom, R.G., Schenck, L.R., and Alley, R.E.**
1987: What are the best radar wavelengths, incidence angles, and polarizations for discrimination among lava flows and sedimentary rocks? A statistical approach; IEEE Transactions on Geoscience and Remote Sensing, v. GE-25, p. 208-213.

**Corbley, K.P. and Engel, P.**
1995: Ordering RADARSAT data products: a guide for commercial users; Geocarto International, v. 10, no. 3, p. 92-96.

**de Freitas T., Harrison, J.C., and Thorsteinsson, R.**
1993: New field observations on the geology of Bathurst Island, Arctic Canada: Part A, stratigraphy and sedimentology of the Phanerozoic succession; in Current Research, Part B; Geological Survey of Canada, Paper 93-1B, p. 1-10.

**Denyer, N., Raney, R.K., and Shepherd, N.**
1993: The RADARSAT SAR data processing facility; Canadian Journal of Remote Sensing, v. 19, no. 4, p. 311-316.

**Ford, J.P. and Casey, D.J.**
1988: Shuttle radar mapping with diverse incidence angles in the rainforest of Borneo; International Journal of Remote Sensing, v. 9, p. 927-943.

**Haralick, R.M.**
1979: Statistical and structural approach to texture; Proceedings of the IEEE, v. 67, no. 5, p. 786-804.

**Harrison, J.C.**
1995: Melville Island's salt-based fold belt, Arctic Canada; Geological Survey of Canada, Bulletin 472, 331 p. (+ Map 1844A, scale 1:250 000, 12 sheets).

**Harrison, J.C., de Freitas, T., and Thorsteinsson, R.**
1993: New field observations on the geology of Bathurst Island, Arctic Canada: Part B, structure and tectonic history; in Current Research, Part B; Geological Survey of Canada, Paper 93-1B, p. 11-21.

**Kerr, J.W.**
1974: Geology of Bathurst Island Group and Byam Martin Island, Arctic Canada; Geological Survey of Canada, Memoir 378, 152 p. (+ Map 1350A, scale 1:250 000, 2 sheets).

**Livingstone, C.E., Gray, A.L., Hawkins, R.K., Olsen, R.B., Halbertsma, J.G., and Deane, R.A.**
1987: CCRS C-band airborne radar: system description and test results; Proceedings of the 11th Canadian Symposium on Remote Sensing, June 22-25, Waterloo, Ontario, p. 503-518.

**Livingstone C.E., Gray, A.L., Hawkins, R.K., and Olsen, R.B.**
1988: CCRS X/C Airborne Synthetic Aperture Radar: an R and D tool for the ERS-1 timeframe; Aerospace and Electronic Systems Magazine, v. 3, no. 10, p. 15-21.

**Livingstone C.E., Gray, A.L., Hawkins, R.K., Vachon, P., Lukowski, T.I., and Lalonde, M.**
in press: The CCRS airborne SAR systems: radar for remote sensing research; Canadian Journal of Remote Sensing.

**Miller, F.R.**
1993: Peary Caribou calving and postcalving periods, Bathurst Island complex, N.W.T., 1991; Canadian Wildlife Service (Environment Canada Publication), Technical Report Series, no. 166, 99 p.

**Ramsay, J.G.**
1967: Folding and Fracturing of Rocks; McGraw-Hill, N.Y., 568 p.

**Sabins, F.F.,Jr.**
1983: Geologic interpretation of Space Shuttle radar images of Indonesia; American Association of Petroleum Geologists, Bulletin, v. 67, p. 2076-2099.

**Saleh, A.**
1993: Soil roughness measurement: chain method; Journal of Soil and Water Conservation, v. 48, p. 527-529.

**Schaber, G.G., Berlin, G.L., and Brown, W.E.**
1976: Variations in surface roughness within Death Valley, California - geologic evaluation of 25-cm-wavelength radar images; Geological Society of America Bulletin, v. 87, p. 24-41.

**Singhroy V., Slaney, R., Lowman, P., Harris, J., and Moon, W.**
1993: RADARSAT and Radar Geology Applications in Canada; Canadian Journal of Remote Sensing, v. 19, no. 4, p. 338-351.

**Ulaby, F.T., Moore, R.K., and Fung, A.K.**
1986: Microwave Remote Sensing: Active and Passive, Volume III: From Theory to Applications; Artech House, Norwood, MA, p. 1065-2162.

**Vachon, P.W., Gray, A.L., and Geudtner, D.**
1995: ERS-1 SAR repeat-pass interferometry: temporal coherence and implications for RADARSAT; Proceedings of the 17th Canadian Symposium on Remote Sensing, June 13-15, Saskatoon, Saskatchewan, p. 803-808.

# Regional gravity survey of Ellesmere and Axel Heiberg islands, Northwest Territories

D.B. Hearty[1], D.A. Seemann, P. Maye[2], and R. Jackson[3]
GSC Victoria, Sidney

**Abstract:** During the period May-July, 1995, a regional gravity survey was conducted on Ellesmere Island and adjacent Axel Heiberg Island. This multi-agency project completes one of the last major voids in the regional gravity coverage of Canada. The 1349 newly acquired gravity stations will not only meet the needs of the Canada/United States (CANUS) Defence Plan but will also contribute to an improved geoid. During the survey, a joint GPS project was also undertaken with the National Survey and Cadastre of Denmark. The GPS derived co-ordinates will be used in future horizontal and/or vertical motion studies across Nares Strait. Canadian geoscientists will use the gravity data to help resolve the ongoing controversy regarding plate reconstructions in the area. A preliminary comparison of the gravity field and the regional geology suggests a complex relationship: although anomalies parallel some geological boundaries they are discordant with others.

**Résumé :** Entre mai et juillet 1995, un levé gravimétrique régional a été réalisé sur l'île d'Ellesmere et sur l'île adjacente Axel Heiberg. Ce projet auquel ont participé plusieurs organismes comble l'une des principales dernières lacunes de la couverture gravimétrique régionale du Canada. Les 1 349 nouvelles stations gravimétriques répondent non seulement aux besoins du plan de défense du Canada et des États-Unis, mais contribuent également à améliorer la détermination de la forme du géoïde. Durant le levé, un projet conjoint faisant appel au SPG a en outre été entrepris avec l'organisme national des levés et du cadastre du Danemark. Les coordonnées établies à l'aide du SPG serviront à étudier les déplacements horizontaux et verticaux futurs dans le détroit de Nares. Les géoscientifiques canadiens utiliseront les données gravimétriques pour résoudre la controverse actuelle portant sur les reconstitutions tectoniques dans la région. Une comparaison provisoire du champ gravimétrique et de la géologie régionale laisse entrevoir un tableau complexe, les anomalies étant parallèles à certaines limites géologiques, mais discordantes par rapport à d'autres.

[1] Geodetic Survey Division, Geomatics Canada, 615 Booth St., Ottawa, Ontario K1A 0E9
[2] Mapping and Charting Establishment, Department of National Defence, Ottawa
[3] GSC Atlantic, Dartmouth

## INTRODUCTION

In the period 1991-1994, a new phase of a long withstanding co-operative program of "enhanced" gravity surveys was initiated in the Canadian Cordillera in response to Canada-United States (CANUS) Defence Plan requirements for gravity data. Logistics and field operations during the three surveys (referred to as OP BOUGUER91/92/93) were carried out by military personnel from the Mapping and Charting Establishment (MCE), Department of National Defence (DND). The Geological Survey of Canada (GSC) was responsible for training in gravity operations and for monitoring the quality of measurements and final data. The surveys, which were funded by the U.S. Defence Mapping Agency (US DMA) and the GSC in the ratio 4:1, acquired 5185 gravity stations and essentially completed the regional gravity coverage of the Cordillera.

Upon completion of the Cordilleran surveys, the largest gravity void remaining in Canada was over Ellesmere and Axel Heiberg islands and adjoining Nares Strait in the Canadian Arctic (Fig. 1). In 1995, a multi-agency international project was undertaken to complete the regional gravity coverage in these areas. The project was sponsored by the Mapping and Charting subcommittee of the Canada-United States Military Cooperation Committee and was funded largely by US DMA, MCE, and Geodetic Survey Division (GSD) with contributions from GSC Victoria (Sidney),

Canadian Hydrographic Service (CHS), and the Polar Continental Shelf Project (PCSP). This report describes the land portion of the survey (details are described in an internal DND report by P. Maye, 1995) and presents some preliminary observations on the computed Bouguer anomalies.

## ELLESMERE-AXEL HEIBERG REGIONAL GRAVITY SURVEY (OP BOUGUER95)

### Planning

In early 1994, MCE arranged for 300 drums of fuel to be positioned via sea-lift (annual supply of provisions to northern communities), 200 drums to Thule Air Force Base for delivery via Hercules aircraft to Alert, and 100 drums to Eureka. A reconnaissance survey was undertaken in August 1994 involving personnel from MCE, GSC, and the Danish National Survey and Cadastre (KMS). Using a chartered de Havilland Twin Otter aircraft based out of Resolute, the survey crew visited Alert, Eureka, and Tanquary Fiord on Ellesmere Island and Thule and Qaanaaq on Greenland (Fig. 1). As part of the survey, critical ties were conducted between gravity base stations at these locations (absolute gravity stations at Resolute, Alert, and Thule) in order to strengthen the gravity network between the two countries and to confirm instrument calibrations at higher latitudes.

The OP BOUGUER95 survey was planned and laid-out using a 12 km grid yielding some 1250 stations, however due to some extra infilling, 1349 stations were actually observed (Fig. 2a, b). A marine component of the survey (Nares Strait) was planned and conducted separately using GSC, KMS, and CHS personnel. The marine survey is not discussed here but the preliminary data acquired in it have been included in the gravity compilation shown in Figure 3. One of the more time consuming tasks in the planning involved plotting the position of the 1250 proposed stations (as well as existing stations) on 1:250 000 NTS maps: given that the survey area encompassed 26 NTS map sheets and four copies of each were needed. The paper work was also daunting as 16 separate land use permits, clearances and licences were required to carry out the field survey and to cache fuel. Prior to the survey the field crew underwent rigorous training (by GSC) on the proper handling of gravimeters while MCE provided instruction on the GPS receivers and data processing techniques.

### Survey technique

Two Bell 206L helicopters from Canadian Helicopters (chartered through PCSP) were outfitted with Ashtech L1/L2 dual frequency GPS antennas mounted on top of the vertical tail fin. The height difference between the antenna and the ground was accurately measured and used to correct GPS derived elevations. As the field crew usually read the gravimeters at the nose of the helicopter there was an additional horizontal offset. This offset was more difficult to correct as the azimuth of the helicopter varied from station-to-station, and, for a variety of reasons, it was not always possible to observe at the nose.
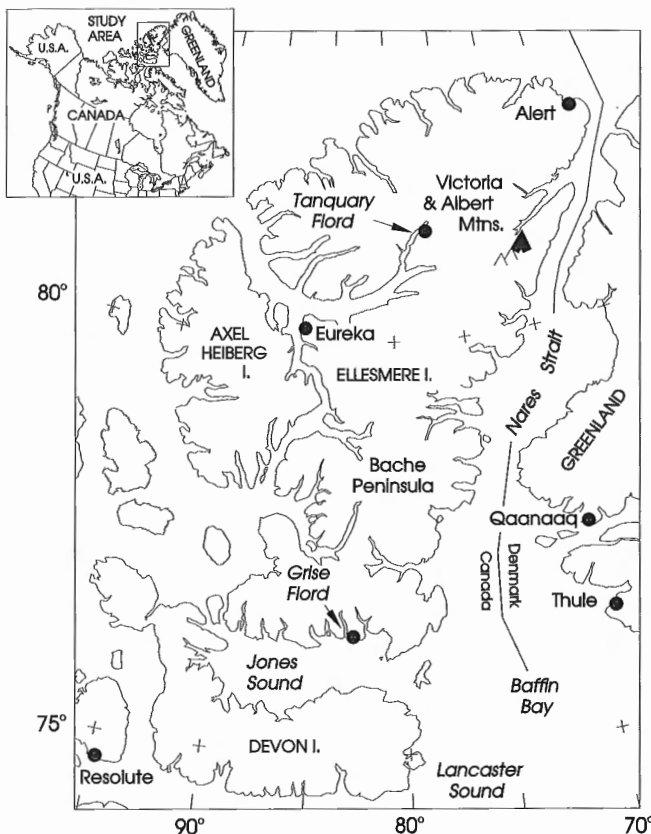


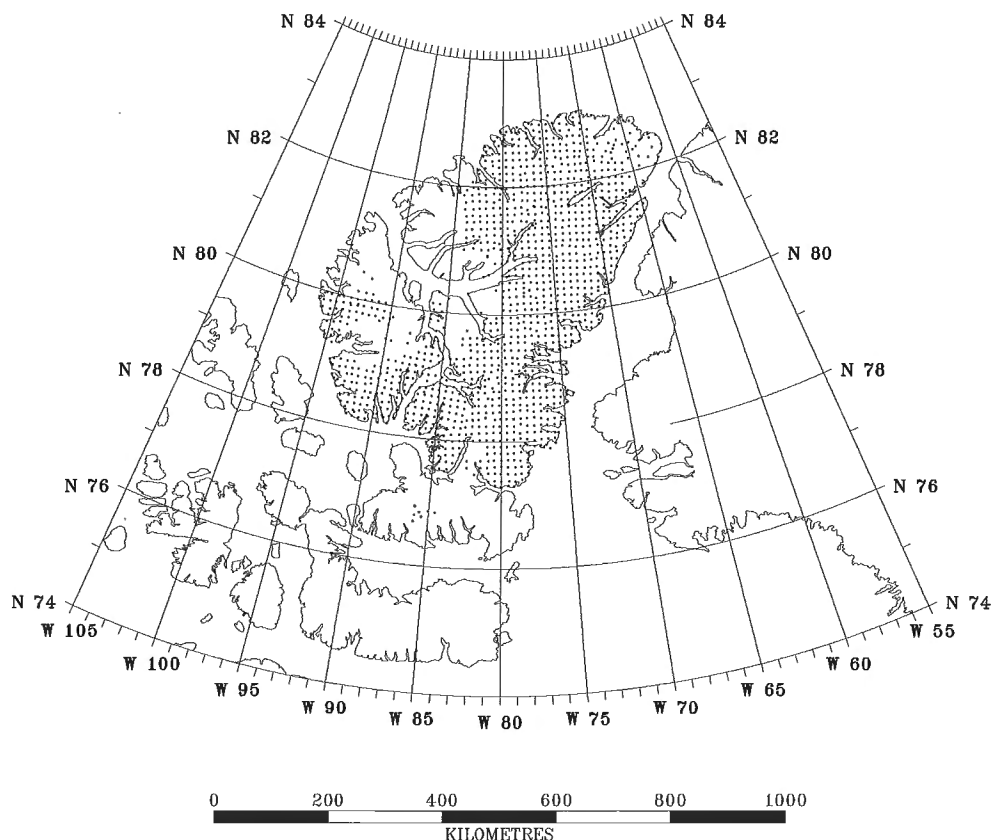**Figure 1.** *Index map of the survey area.*

**Figure 2a.** *Distribution of the 1349 gravity points acquired during OP BOUGUER95. The blank and/or sparse areas on Ellesmere and Axel Heiberg islands were previously covered by gravity surveys conducted in 1967 and 1987.*



**Figure 2b.** *Captain Phil Maye at a gravity station in the Victoria and Albert Mountain Range northeast of the Agassiz Ice Cap, Ellesmere Island.*

Daily traverses included between 24 and 32 stations per helicopter. Weather conditions, which were the single largest influence on productivity, necessitated flexibility in traverse routing. On the other hand, when the weather was favourable, full advantage was taken of the almost continuous daylight to increase productivity, albeit resulting in some extremely long work days.

During a traverse, the pilot (using the aircraft GPS receiver) would enter the way-point of the desired station. Upon reaching his destination, he would search for an ice free landing spot within a 1 km radius of the predetermined station co-ordinates. The extent of some of the ice-fields and glaciers often prevented the pilot from finding such a site. More then 300 stations were unfortunately positioned on the ice. The Bouguer anomaly values computed at these stations are not very accurate as the Bouguer correction was computed assuming a rock density of 2670 kg/m$^3$. Clearly, the greater the thickness of ice, the larger the inherent error in the computed Bouguer anomaly.

75

## GPS data collection

At least one (often two) GPS bases stations were operating during the gravity traverses. Typically one base station was set up at Alert or Eureka, and the other deployed (on a daily basis) in the immediate survey area, usually over a geodetic monument or at a fuel cache. The Ashtech Z-12 GPS receiver installed within the helicopter was generally switched "on" upon leaving the base and remained so until the traverse was completed. At a gravity station, the station number was entered into the receiver and tracking initiated. The sample duration was set to 90 epochs at a 5 second sampling rate (7.5 minutes of recording). Unlike previous OP BOUGUER surveys which used a "rapid static" method of positioning and required 15 minutes of data, the "on-the-fly" technique, used in this survey, greatly increased production. Once the data were processed using the Ashtech PRISM software, the resultant co-ordinates displayed accuracies in the ±1 m range, which was well within the ±3 m requirement.

## Gravity survey

Three gravity base stations were used during the survey, Alert, Eureka, and Tanquary Fiord. Gravity traverses always started and ended at a base station. Secondary bases established at the larger fuel caches sites were visited each time a helicopter refuelled (usually after 8 stations). During the survey, gravity stations were generally not repeated, however, repeat readings were observed at the fuel cache locations. The repeat readings not only provided a check on the performance of the gravimeter, but, also on the skill of the observer. Of the 133 repeat measurements (10% of the total stations) the mean difference was 0.067 mGal with a standard deviation of ±0.087 mGal which was well within acceptable limits.

GSD or GSC personnel maintained the five Lacoste and Romberg model G meters throughout the survey. They also performed the gravity computations: gravity observations were reduced using the inhouse software PCGRAV. Bouguer anomalies were calculated using the International Gravity
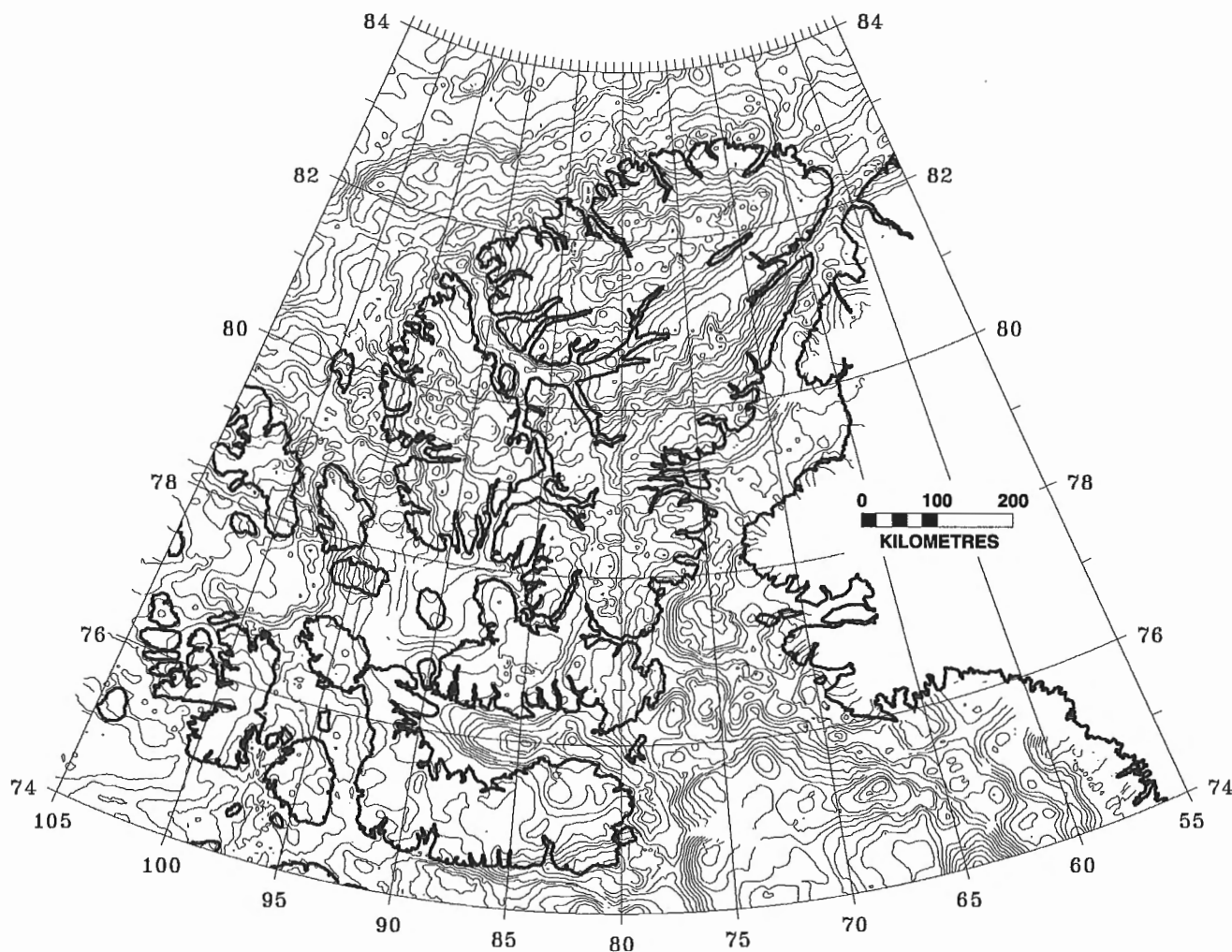


**Figure 3.** *Gravity map (Bouguer on land, Free Air offshore). The gravity compilation contains 19 700 points and includes existing and recently acquired data (including the 1995 Nares Strait survey). Contour interval is 10 mGal.*
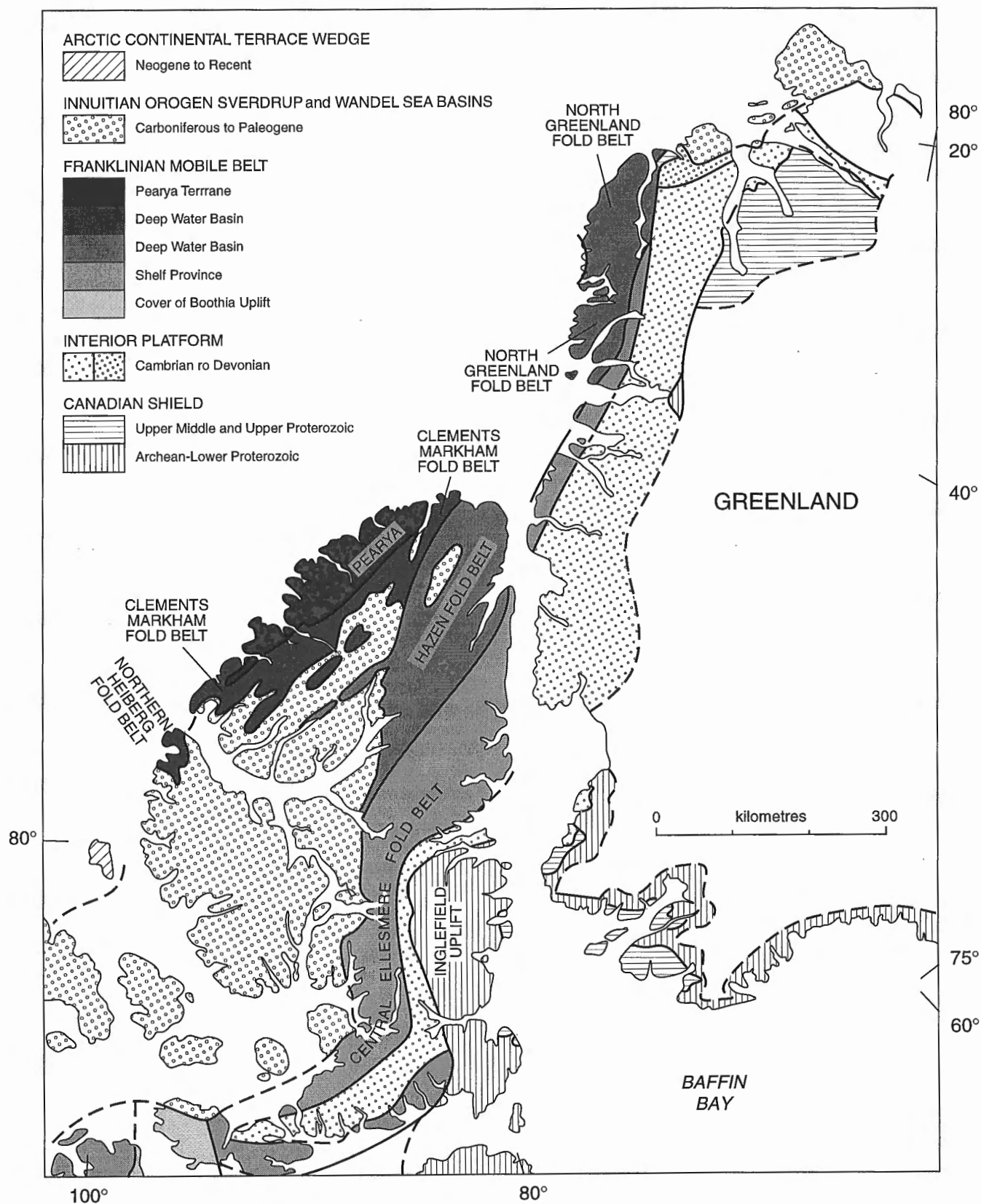
***Figure 4.*** *Geology map simplified from Trettin (1991).*

Standardization Network 1971 and the Geodetic Reference System 1967. A standard density of 2670 kg/m$^3$ was used in the Bouguer correction. Station distribution and gravity values were plotted daily, and stations with anomalous readings were revisited.

The distribution of the OP BOUGUER95 stations is shown in Figure 2a. The newly acquired data have been merged with existing data to produce the gravity plot (Bouguer on land, Free Air offshore) shown in Figure 3. The reader is cautioned that the data are preliminary and subject to change (terrain corrections have yet to be applied to Bouguer anomalies and geoidal height corrections have yet to be applied to station elevations).

## CORRELATION OF THE GRAVITY FIELD WITH REGIONAL GEOLOGY

### Preliminary observations

The following is a preliminary comparison of the gravity anomaly contours (Fig. 3), physiography, and the regional geology (Fig. 4).

A series of local gravity minimum is located in Nares Strait, Jones Sound, and Lancaster Sound. The largest amplitude negative anomaly (-150 mGal) is in Nares Strait. In contrast, in northern Baffin Bay and along the polar margin the anomalies are positive.

A prominent negative gravity gradient (1.7 mGal/km) follows Nares Strait from the Bache Peninsula to the northern end of Ellesmere Island. The maximum lows (-155 mGal) are coincident with the shelf province of the Franklin Mobile Belt (Fig. 4). South of Bache Peninsula this relationship is not maintained; specifically, the Franklinian Mobil Belt continues to the south but the gravity contours are no longer linear. In the region of Nares Strait and Ellesmere Island, beginning at the strait and moving inland, there are 3 parallel anomalies, a low, a central high and another low. The first low, already described, follows the coast. The parallel high (>-10 mGal) trends across the Hazen Fold Belt of Early Cambrian to Early Devonian age into the Sverdrup Basin of Carboniferous to Paleogene age. The second gravity minimum (<-110 mGal) is entirely within the area mapped as Sverdrup Basin sequence.

Centred on Axel Heiberg Island there are lows that trend in a radically different direction than those observed on Ellesmere Island. Here the gravity minimum strike approximately northwest to southeast.

Summarizing, in the survey area there is not a simple relationship between the gravity anomalies, the bathymetric features, and/or the mapped geological boundaries. The new gravity data were compared with the published gravity map of the Innuition Orogen (Sobczak, 1991). The contours on northern Ellesmere Island that were not supported by data are now confirmed and redefined by the new information.

## CANADA-GREENLAND GPS PROJECT

As part of the OP BOUGUER95 field program, a GPS fiducial network was set up with sites on both sides of Nares Strait. During the first recording session (24 hour duration) Danish surveyors occupied 4 stations situated along the coast of Greenland while Canadian surveyors (from the Geodetic Survey) occupied sites at Resolute and Grise Fiord and MCE personnel manned Alert and Eureka. Three other GPS sessions were similarly conducted (using different station combinations) during the gravity survey. The 15 new stations will secure a consistent GPS datum between the Canadian and Greenland base networks and will be integrated with additional GPS ties to triangulation stations and tied to tide gauge bench marks. In addition, they will be used to help define the geoid in the region, provide a base for future crustal motion surveys, and provide constraints for climate and earth rheology models.

## ANCILLARY BENEFITS FROM THE SURVEY

During the course of the survey, gravity and GPS measurements were observed at 21 geodetic points. These data will provide an independent check on the published orthometric heights of the points.

The Canadian geoid model, GSD95, provides geoid heights along a regular grid at a 10 km interval over the whole of Canada. Computation of an accurate geoid height is achieved by using Stokes's integral equation, but it requires a dense set of gravity measurements (Mainville et al., 1992). The new gravity data will be used by the Geodetic Survey Division (GSD) to improve the accuracy of the Canadian geoid model and will influence the 428 544 points which currently make up the model.

During a one week period, while the survey was based at Alert, park wardens from the Ellesmere Island National Park Reserve often accompanied survey crews recording animal sightings and collecting biological specimens. Similarly, a wildlife technician from the Wildlife Division, Northwest Territories Renewable Resources also accompanied one of the helicopters (during a 10 day period while the survey was based in Eureka) observing and recording caribou sightings. When an observer was not able to accompany the survey crew, the gravity operator and/or pilot kept records of wildlife movements. These data will be incorporated in wildlife monitoring programs.

## SUMMARY

The new gravity and GPS data acquired during OP BOUGUER95 is the result of a multi-agency international effort. The survey, which was mainly funded by DMA and conducted by military personnel from MCE, completes the

largest remaining gravity void on the Canadian landmass. Although the data are preliminary, some of the larger gravity anomalies, trends and gradients can be correlated with the regional geology. The numerous observed discordancies between the Bouguer data and the mapped geology suggest that the geology may be more complex than previously realized.

## ACKNOWLEDGMENTS

## REFERENCES

**Mainville, A., Forsberg R., and Sideris, M.**
1992: Global Positioning System testing of geoids computed from geopotential models and local gravity data - a case study; Journal of Geophysical Research, v. 97, no. B7, p. 11137-11147.

**Sobczak, L.W.**
1991: Gravity, Innuition Orogen and Arctic Platform; in Geology of the Innuition Orogen and Arctic Platform of Canada and Greenland, (ed.) H.P. Trettin; Geological Survey of Canada, Geology of Canada, no. 3, Figure 5A.1, scale 1:5 000 000 (in pocket).

**Trettin, H.P.**
1991: Tectonic Framework; Chapter 4 in Geology of the Innuitian Orogen and Arctic Platform of Canada and Greenland, Trettin H.P. (ed.) Geological Survey of Canada, Geology of Canada no. 3, p. 59-66.

# New showings and new geological settings for mineral exploration in the Arctic Islands

J.C. Harrison and T. de Freitas

GSC Calgary, Calgary

**Abstract:** Significant occurrences of breccia-related and replacement sphalerite and galena have been discovered in Lower Devonian (Emsian) dolostone of the lower Blue Fiord Formation on southeastern Bathurst Island. Bitumen, hydrothermal dolomite, calcite spar and marcasite(?) are important accessory components near and within the showings. Exploration potential for Mississippi Valley-type lead-zinc deposits exists within this and other stratigraphic intervals both locally and throughout the central and eastern Arctic Islands. Other potential targets in the Arctic Islands include epigenetic vein and sedimentary-exhalative lead-zinc deposits in lower Paleozoic graptolitic shale, redbed-related copper in upper Paleozoic strata, and kimberlites.

**Résumé :** D'importantes occurrences de sphalérite et de galène de remplacement associées à des brèches ont été découvertes dans les dolomies du Dévonien inférieur (Emsien) de la partie inférieure de la Formation de Blue Fjord (partie sud-est de l'île Bathurst). À proximité des indices et à leur site même, le bitume, la dolomie hydrothermale, la calcite et la marcasite(?) constituent d'importantes composantes accessoires. Des gisements de plomb-zinc de type Mississippi-Valley pourraient être découverts dans cet intervalle et dans d'autres, tant à l'échelle locale que dans tout le centre et l'est de l'archipel arctique. Parmi les autres cibles potentielles de l'archipel arctique, il faut d'abord mentionner les gisements filoniens épigénétiques et exhalatifs sédimentaires à minéralisation de plomb-zinc, logés dans des shales graptolitiques du Paléozoïque inférieur, mais aussi les gisements de cuivre encaissés dans des couches rouges du Paléozoïque inférieur et les kimberlites.

## INTRODUCTION

Promising developments in mineral exploration in coastal northern Labrador underscore the remaining potential for new discoveries in coastal areas of northern Canada. Two producing zinc-lead mines in Canada's Arctic Islands benefit from feasible access to maritime export of mine concentrate in spite of limitations imposed by a short shipping season. Access to tidewater and the increasing use of Polar class icebreakers capable of reaching far into the Arctic Ocean will provide strong incentives for an expanded interest in the resource potential of the Arctic Islands. This paper describes several unreported base metal showings discovered in 1995 during the course of a regional bedrock mapping project by the Geological Survey of Canada (GSC). The showings are located less than a 15 minute walk from sea level on eastern Bathurst Island and are almost within sight of Cominco's Polaris zinc-lead mine on Little Cornwallis Island. This paper also provides some additional recommendations for the exploration of both sediment-hosted ore deposits and the kimberlitic suite of igneous rocks in the Arctic Islands.

## MARKHAM POINT AREA SHOWINGS

### Location

The newly discovered showings of sphalerite and galena are located between 9 and 12 km northwest of Markham Point on the southeastern coast of Bathurst Island, and 34.7 km northwest of the Polaris minesite (Fig.1, 2). The distance from the principle showing to the coast is approximately 900 m. However, occurrences of zinc and lead sulphides are scattered along a northward-trending belt ranging up to 1700 m north from tidewater near the head of McDougall Sound. The showings lie entirely on crown land. The southern boundary of the Polar Bear Pass National Wildlife Area lies 2.8 km north of the northern limit of known zinc mineralization. Similarly, the northern boundary of Nunavut land claim settlement region RB-32/68 E, H lies 4.8 km to the south.

### Stratigraphy

Paleozoic stratigraphy of Bathurst Island and of the showing area is illustrated in Figures 3 and 4. Sulphide mineralization lies in the lower part of the Lower to basal Middle Devonian
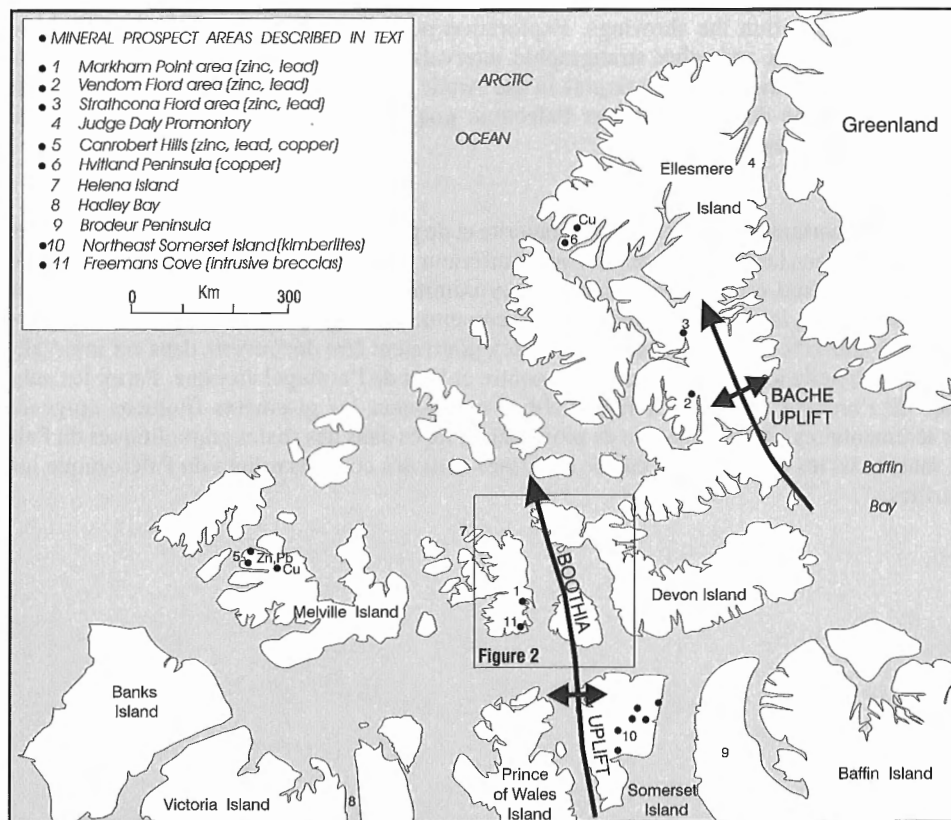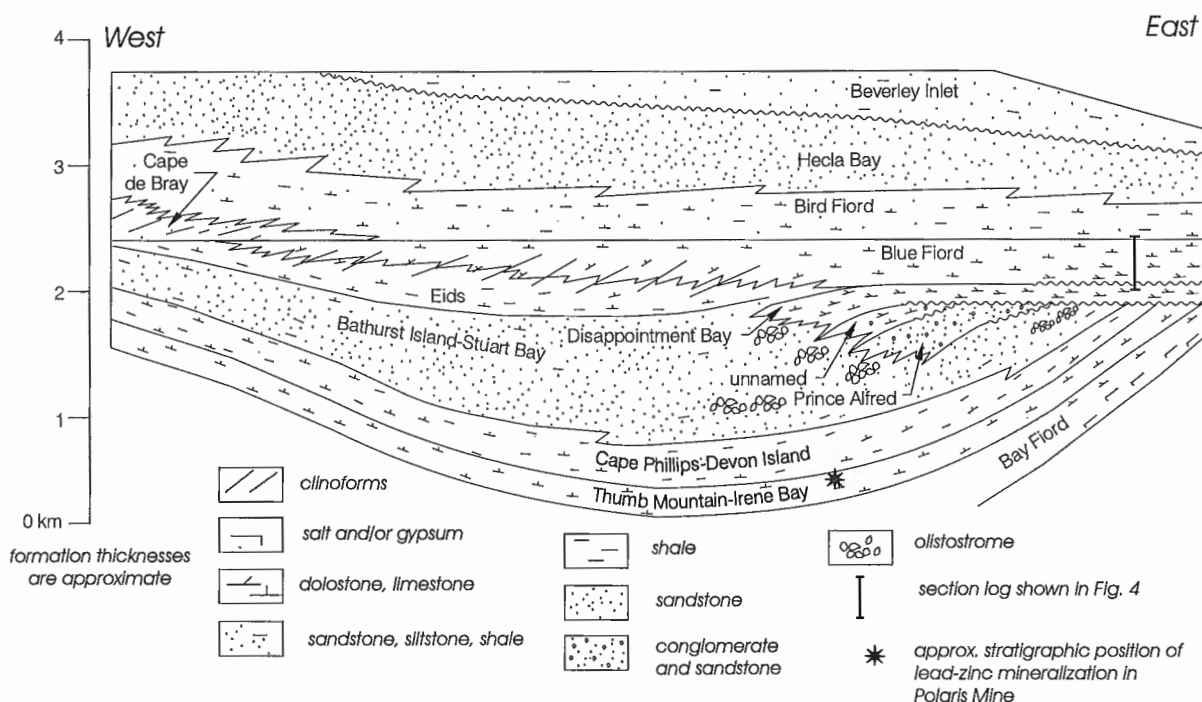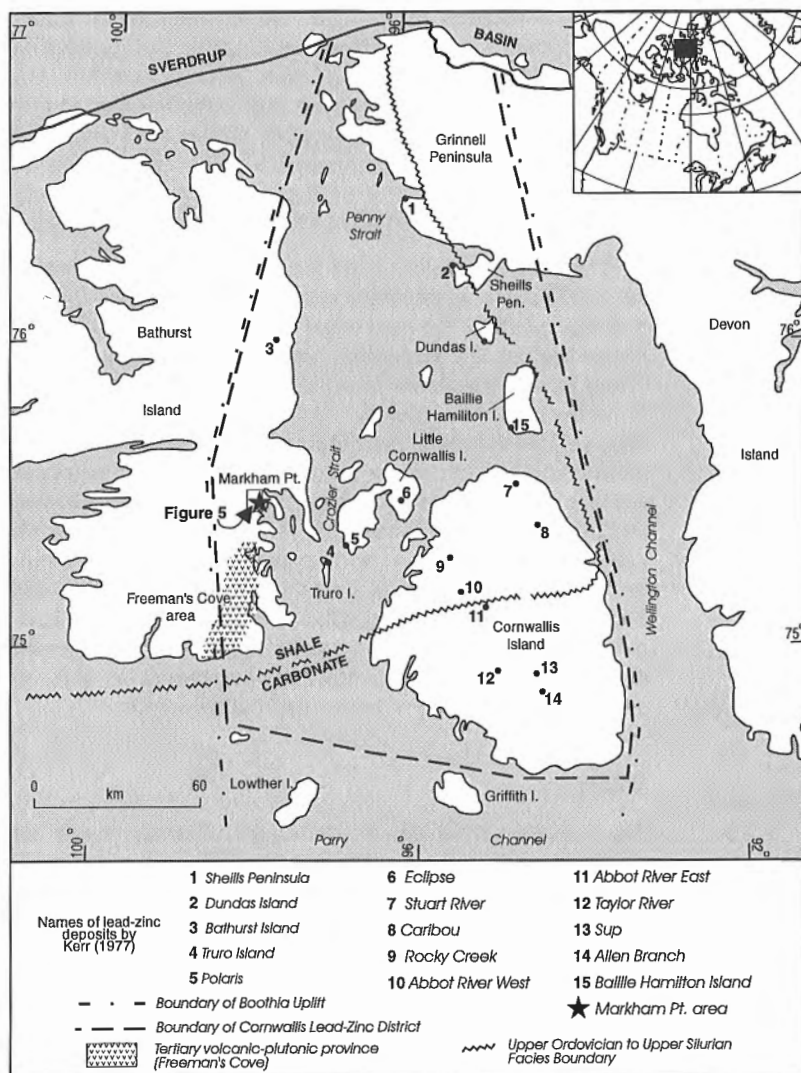


*Figure 1. Location map of the Canadian Arctic Islands displaying key mineral prospect areas and selected geographic localities referred to in the text.*

Blue Fiord Formation (Emsian to lower Eifelian). On eastern Bathurst Island, the Blue Fiord Formation disconformably overlies yellow weathering dolostone of the Disappointment Bay Formation (Emsian) and is in turn overlain conformably by calcareous sandstone, siltstone, and limestone of the Bird Fiord Formation (Eifelian). The Blue Fiord Formation grades to the west into the slope facies limestone of the Eids Formation which on Bathurst Island contains both Emsian and

Eifelian conodonts (McGregor and Uyeno, 1972). Other strata exposed in the Markham Point area include graptolitic and tentaculitid shales of the Upper Silurian (Ludlow and Pridoli) Devon Island Formation and fluvial-deltaic quartz sandstone of the Middle Devonian (Givetian) Hecla Bay Formation. The Upper Ordovician Thumb Mountain Formation, host unit for the Polaris lead-zinc deposit, is entirely concealed by younger strata in this part of Bathurst Island.

The Blue Fiord Formation has been measured by one of us (TdeF) along an unnamed eastward-flowing river located 3 to 4 km south of the base metal sulphide showings (Fig. 5). In this section, the formation is approximately 333 m thick. Three locally mappable informal members are recognized. From the base these include: 1) 51 m of thick bedded, moderate yellowish brown, petroliferous dolostone with common biomoldic porosity, minor limestone, and several metres of arenaceous dolostone at the base; 2) 183 m of medium- and thick-bedded, pale grey and pale yellowish-grey, wavy laminated fenestral dolostone with abundant bird's eye and pinpint porosity, interbeds of limestone in the upper part; and 3) 99 m of thick and massive bedded pale brown stromatoporoidal limestone. The showings are confined to the upper part of the lower informal member in an interval approximately 0 to 25 m below the middle member.

*Structure*

The Markham Point area of southeastern Bathurst Island lies along the western flank of the Boothia Uplift (Okulitch et al., 1991; Harrison et al., 1993). The latter is a major northward-trending basement-involved uplift extending 1000 km from Boothia Peninsula (in the south) to Grinnell Peninsula on western Devon Island (Fig. 1). West of Markham Point, the Blue Fiord Formation is widely exposed in uplifted panels throughout what Kerr (1974) has called the Southeast Bathurst Fault Zone (Fig. 5). Individual fault strands trend variously between N14°E and N26°W. The Markham Point segment of the fault zone lies within the hinge region of a northward-plunging regional anticline. Parasitic anticlines and synclines are also present including a faulted eastward-inclined anticline, the hinge culmination of which coincides with all known mineralization. The oldest exposed strata include Disappointment Bay and Devon Island formations. Blue Fiord and Bird Fiord formations are exposed to the east and west on the regional fold limbs. Two principal fault strands within the regional fold hinge enclose a downdropped lenticular-shaped inlier of Hecla Bay Formation and Bird Fiord Formation strata. Sphalerite and galena showings lie in the upthrown lower part of the Blue Fiord Formation immediately west of the Hecla Bay Formation inlier (Fig. 5). The showings occur in outcrop, talus and stream bed boulders derived from adjacent flat to very gently west-dipping strata located 130 to 260 m west of one N22°W-striking inlier boundary fault. Showings are distributed parallel to this fault over a distance of 1930 m. A second, parallel, subsidiary fault places a panel of east-dipping upper Blue Fiord limestone in tectonic contact with mineralized lower Blue Fiord dolostone.
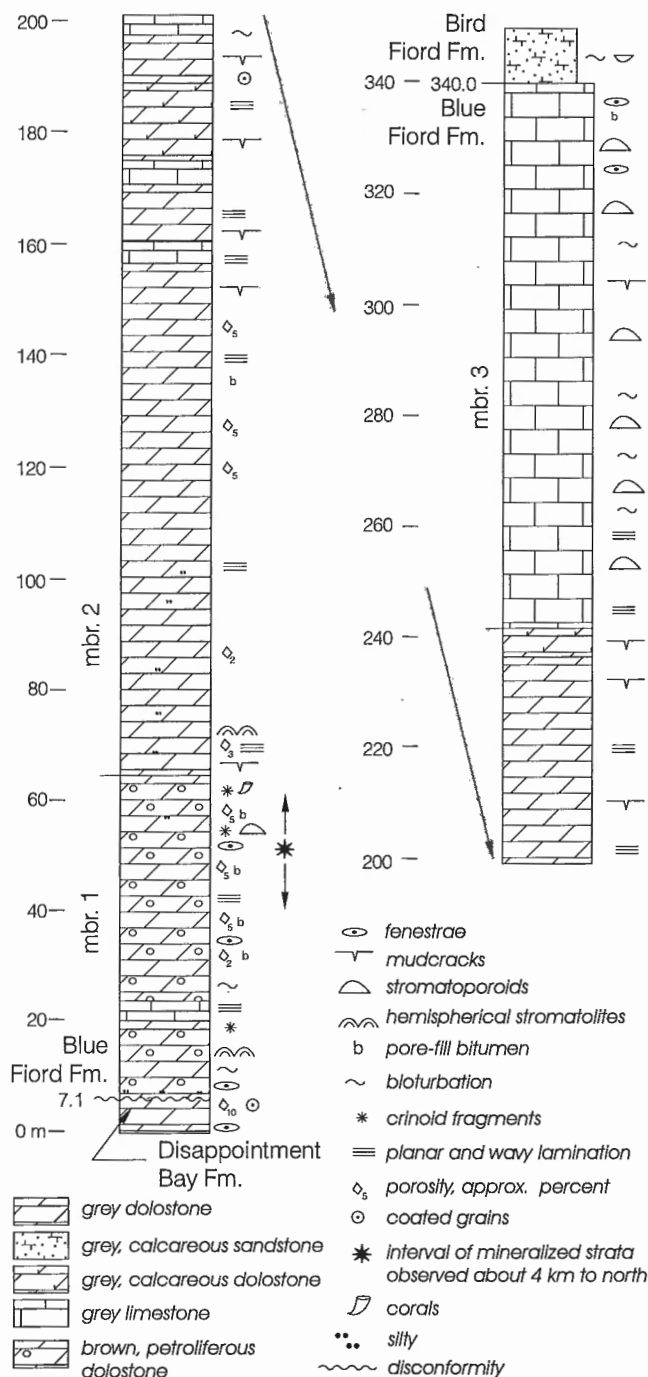


*Figure 4. Measured section of Blue Fiord Formation along an unnamed river located approximately 10 km west of Markham Point on eastern Bathurst Island (see Fig. 5 for location).*

The structural interpretation of this area favours extensional reactivation of one or more thrusts detached on the Bay Fiord evaporite. However, nothing is known about the dip direction of these faults.

## Description of showings

Base metal sulphide mineralization has been exposed by stream bank incision into a 30 m high, east-facing escarpment of Blue Fiord dolostone. Exposures in the lower 20 m of the escarpment are assigned to the informal lower member. The principle showing is located in an interval of brecciation 12 to 15 m above stream level on the northwest bank of an unnamed southeastward-flowing stream near latitude 75°30.06'N, longitude 98°04.50'W. Mineralized breccia extends parallel to bedding and parallel to the creek bed for about 10 m. The full extent of mineralization is obscured by talus both up-and downstream, and uphill to the north. Comparable mineralization has not been located on the south bank of the creek. Sulphide mineralization lies primarily in the matrix of the brecciated host dolostone (Fig. 6a, b) and includes colour-zoned bright yellow, pale yellowish-brown to brownish-orange varieties of medium- to coarse-grained sphalerite (estimated 3 to 10% of rock volume) with lesser
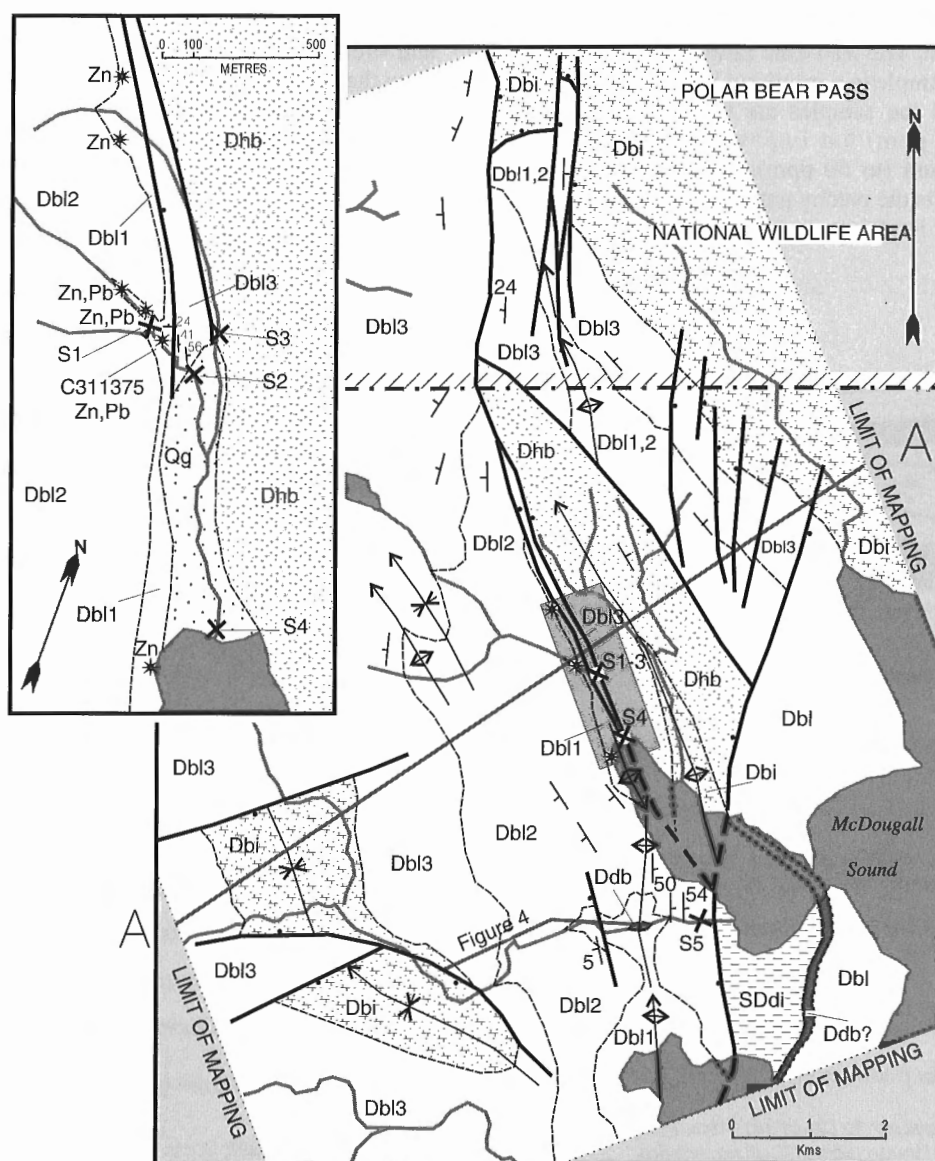


**Figure 5.** *Geology and simplified cross-section of the Markham Point area. The map has been drafted directly from Canadian government air photograph A16203-71 and contains unrectified scale distortions. Inset: local geology of the Markham Point area lead-zinc showings.*

galena. Other matrix components include spar calcite (10 to 25% of rock volume), dolomite, bitumen, a little iron sulphide (probably marcasite), and comminuted rock fragments.

Five grab samples from this showing were selected for multi-element analysis. Methods of analysis included initial pulverization to -150 mesh. Procedures for lead, zinc, silver and barium assay involved total digestion of a 0.5 g sample in a mixture of hydrofluoric, nitric and perchloric acid, dissolution of the dried residue in hydrochloric acid, dilution to volume, and atomic absorption spectroscopic (AAS) analysis. A modified procedure for copper, nickel, cobalt, cadmium, manganese, and iron analyses included partial digestion and dissolution of a 0.5 g sample in nitric and hydrochloric acid prior to AAS. Results are provided in Table 1. Grades of combined zinc and lead range from a little less than 2% to a maximum of 11.3%. The lead-zinc ratio ranges from 1.2 in the highest grade sample to a minimum of 0.01 in two lower grade samples. All the samples are relatively enriched in cadmium (to 290 ppm) but impoverished in silver (to 0.9 ppm) and barium (to 60 ppm). The variable grade of sample assay reflects the patchy pattern of sulphide distribution within the host breccias.

Brecciation is spatially associated with a north-striking fault traceable through talus immediately east of the showing. Tectonic breccias without sulphide mineralization also occur in the downthrown middle member dolostone immediately east of this fault. Composition of fragments in mineralized breccia are similar to those in footwall strata, exposed at 3 to 12 m below the showing. These underlying strata locally dip to the north at 24° in beds 50 to 150 cm thick. Dominant lithology is a moderate yellowish-brown petroliferous crinoidal dolowackestone with 5 to 10% biomoldic and vuggy porosity (Fig. 6c). The two-holed crinoid *Gasterocoma bicaula* (Emsian/Eifelian age range) is common. Pore space in tabulate colonial corals, is lined with coarse white calcite spar (5 to 15% of rock volume) and intercrystalline bitumen.

Other occurrences of sphalerite and galena occur in talus and stream bed boulders over a distance of 300 m upstream from the mineralized breccia outcrop. (Mineralized boulders have also been carried at least 60 m downstream.) In these boulders, the sulphides occur as widely scattered patches (to ca. 15 cm each) within vuggy brown dolostone. Brecciation is generally absent and pores are infilled with sphalerite and lesser intergrown galena, calcispar, dolospar, bitumen and
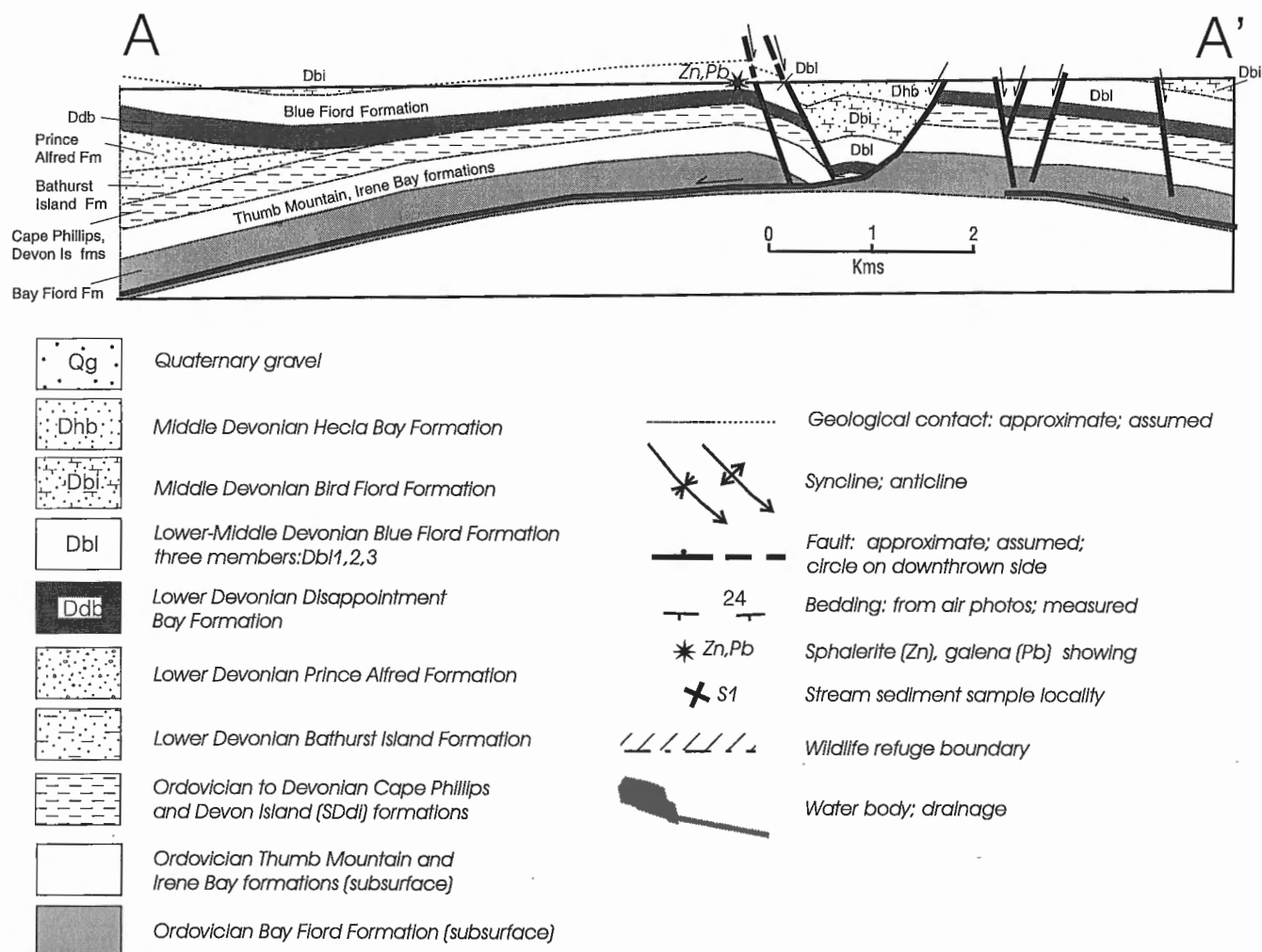


*Figure 5. Legend.*
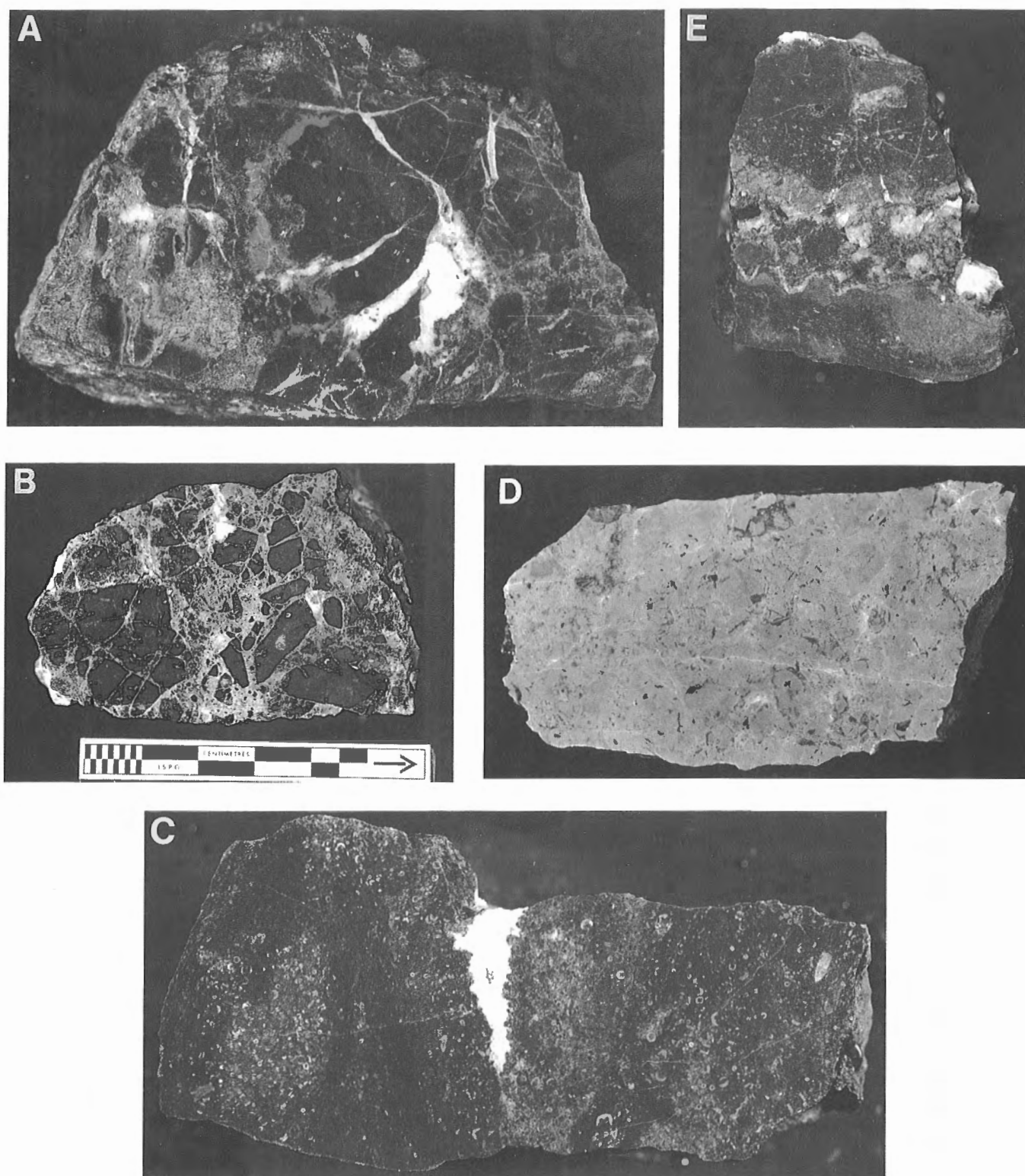
**Figure 6.** Photographs of hand specimens. Counterclockwise from upper left: **A)** brecciated crinoidal dolostone with matrix of spar calcite, bitumen and sphalerite (ISPG photo 4522-12); **B)** brecciated dolostone with matrix of calcite, sphalerite and comminuted rock fragments (ISPG photo 4522-2); **C)** hostrock crinoidal dolostone (ISPG photo 4522-17); **D)** caprock fenestral dolostone (ISPG photo 4522-10); **E)** crinoidal dolostone with haloes of lighter coloured hydrothermal dolomite surrounding spar calcite and bitumen fracture fill (ISPG photo 4522-3).

minor marcasite. Sphalerite replacement of large colonial corals is common. Sphalerite textural varieties include coarse grains, colour zoned coarse euhedra (to 5 mm) and small rosettes of larger sphalerite crystals. Sulphides have also invaded the host rock. The upstream limit of sulphides (near lat. 75°30.14′N, long. 98°05.01′W) coincides with the upper exposed limit of the brown dolostone host rock. The upper 10 m of the escarpment lacks sulphides. This obvious caprock is a pale grey fenestral dolostone with estimated 0 to 5% poorly connected pinpoint and bird's eye pore space locally lined with calcite and minor amounts of bitumen (Fig. 6d).

Three other occurrences of sphalerite have been discovered in this study area. Tiny (centimetre-scale) patches of sphalerite occur in brown petroliferous dolostone talus at two sites 660 and 860 m north of the main mineralized breccia showing. Similar small patches of sphalerite occur in a calcite-veined, bitumen-rich dolostone outcrop at sea level, 1030 m south of the breccia showing. Veinlets, centimetre-scale vugs and decimetre-scale masses of transported bitumen, along with secondary hydrothermal(?) dolomite and calcite, are especially well developed in other coastal exposures up to at least 1980 m south of the main breccia showing (Fig. 6e). Bitumen is common in all the vuggy brown dolostones in the Markham Point area but is not a universal characteristic of the lower member of the Blue Fiord Formation on eastern Bathurst Island.

### Stream sediment samples

Five stream sediment samples were collected in the immediate vicinity of the showings (Fig. 5). Sample S1 was collected amongst boulders containing obvious patches of sphalerite and galena approximately 120 m upstream from the breccia showing and 180 m downstream from the highest occurrence of sulphide mineralization. Sample S2 was collected 60 m downstream from the breccia showing, also amongst mineralized stream boulders. Sample S3 was collected 170 m east of the breccia showing on a tributary draining the north end of the mineralized belt. Sample S4 was collected from the delta 930 m to the south and sample S5 was collected from the delta of a second river 3.6 km to the south; both distances were measured from the breccia showing.

The samples were processed and analyzed for nine elements using the atomic absorption spectrometry technique as described by Friske et al. (1994). Results are provided in Table 2. Care must be taken in interpreting these results as the sample population is statistically inadequate and at this time

**Table 1.** Multielement analyses for selected rock samples collected at latitude 75°30.06′N, longitude 98°04.50′W in the Markham Point area, southeastern Bathurst Island.

| Sample No. | Cu ppm | Pb ppm | Zn % | Ag ppm | Ni ppm | Co ppm | Mn ppm | Fe % | Cd ppm | Ba ppm |
|---|---|---|---|---|---|---|---|---|---|---|
| C311375-1 | 11 | 168 | 1.73 | .6 | 3 | <2 | 108 | .25 | 35 | 25 |
| C311375-2 | 12 | 483 | 2.78 | .7 | 4 | <2 | 102 | .4 | 115 | 30 |
| C311375-3 | 10 | 6.2% | 5.10 | .9 | 2 | 2 | 110 | .2 | 290 | 20 |
| C311375-4 | 10 | 395 | 6.45 | .5 | 3 | <2 | 113 | .15 | 200 | 60 |
| C311375-5 | 11 | 207 | 2.24 | .6 | 4 | <2 | 113 | .2 | 55 | 25 |

**Table 2.** Multielement analyses for selected stream sediment samples collected in the Markham Point area, southeastern Bathurst Island.

| Sample No. | Location | Cu ppm | Pb ppm | Zn ppm | Ag ppm | Ni ppm | Co ppm | Mn ppm | Fe % | Cd ppm |
|---|---|---|---|---|---|---|---|---|---|---|
| S1 | 75°30.10′N, 98°03.95′W | 12 | 6 | 104 | .3 | 6 | 2 | 104 | .15 | .4 |
| S2 | 75°30.07′N, 98°04.38′W | 11 | 7 | 71 | .2 | 7 | 2 | 121 | .25 | .2 |
| S3 | 75°30.10′N, 98°04.15′W | 14 | <2 | 46 | .2 | 18 | 9 | 300 | 1.50 | .2 |
| S4 | 75°29.65′N, 98°03.41′W | 9 | 2 | 58 | .3 | 5 | 3 | 125 | .50 | .3 |
| S5 | 75°28.48′N, 98°01.53′W | 15 | 5 | 31 | .2 | 13 | 4 | 190 | .65 | <.2 |

cannot be compared with geochemical values likely to be encountered away from mineralized bedrock in the Bathurst Island area. Nevertheless, metal values are all significantly less than the anomalous limits for copper (70 ppm), lead (74 ppm), and zinc (180 ppm) as determined by industry for these elements in sediments collected from streams draining lower Paleozoic carbonate formations of central Ellesmere Island (Gibbins, 1985).

## Interpretation

Discovery of lead and zinc sulphide mineralization near tidewater in the Markham Point area of eastern Bathurst Island provides valuable new opportunities for exploration within a well established mining district. These showings are the first to be located in rocks unequivically younger than the Disappointment Bay Formation and may contain the most significant known concentration of sphalerite and galena from strata above the top of the Thumb Mountain Formation. These showings lay to rest the idea that mineralizing brines in the Polaris mine area predate the widespread sub-Disappointment Bay disconformity (Kerr, 1974; Randell and Anderson, 1990). Rather, these showings support the evidence provided by paleomagnetic studies and unpublished Rb-Sr ages that indicate a probable late Devonian age for mineralization (Symons and Sangster, 1992; Randell, 1994), coincident with either the Ellesmerian Orogeny (post-middle Famennian to pre-late Viséan), or the peak of foredeep sediment loading in this part of the Ellesmerian foreland (Givetian–Frasnian), which may have preceded the Ellesmerian Orogeny by 10 to 20 Ma (Skibo et al., 1991). Specific guides for exploration are described below.

The full extent of mineralization within the lower informal member of the Blue Fiord Formation needs to be assessed, especially where this prospective horizon is sealed by an impervious dolostone caprock. The coincidence of migrated hydrocarbons and sulphide mineralization within local closure on one parasitic anticline is undoubtedly significant. This relationship implies that the geological concepts and exploration philosophy guiding the search for oil and gas should also be employed for economic concentrations of lead and zinc in this area. Thus, areas of closure on other parasitic anticlines have good exploration potential. Vertical stacking of metallogenic horizons is also possible. In this respect, assessment should be made of the concentration of metal sulphides in the upper Thumb Mountain Formation below the Markham Point showings and at this stratigraphic level within other local anticlines.

The importance of faulting to mineral concentration remains ambiguous. Clearly, there is a concentration of sulphides in fault-related breccias; brecciation resulting from either dolomitization or the tensile space created on the extending bends of curvilinear faults. Less obvious is the extent to which faults in the Markham Point area provide channel ways or seals for migrating brines. Either brines migrated parallel to bedding into this faulted and brecciated anticline, or they migrated up (or along) a fault-parallel zone of brecciation and then spread out laterally below an impervious caprock. Alternatively, these breccia zones may be the

locus for convergence of separate fluid migration pathways: one for metallogenic brines, another for sulphate-bearing brines.

There is a need to prospect the lower Blue Fiord Formation throughout its known distribution including eastern and southern Bathurst Island, the Cornwallis Island area, the smaller offshore islands, Grinnell Peninsula, and southern Ellesmere Island. Large areas of southern and eastern Bathurst Island are now known to have been erroneously included by Kerr (1974) in the Disappointment Bay Formation and should in fact have been mapped variously as Blue Fiord Formation, Prince Alfred Formation, or an unnamed Lower Devonian carbonate formation that lies between the Prince Alfred and Disappointment Bay formations (Fig. 3). Resource potential in all these areas remains significant and inadequately prospected. The extent to which stream sediment sampling will help in this search remains to be proven.

## OTHER SHOWINGS AND SETTINGS

### Other MVT targets

Other settings and regions of the Arctic Islands remain to be properly explored for Mississippi Valley-type (MVT) deposits. (Summary description of MVT and other ore deposit types is provided by Eckstrand, 1984.) The largest area extends in a 50 km wide belt from Grinnell Peninsula on western Devon Island to Judge Daly Promintory on northern Ellesmere Island (Fig. 1); a prospective strike length of 900 km (Trettin et al., 1991; de Freitas et al., 1993). Potential carbonate traps are provided by: 1) the upper Thumb Mountain Formation below an Irene Bay Formation seal; 2) reef and forereef facies Allen Bay Formation (Late Ordovician to mid-Silurian) below Cape Phillips Formation or Devon Island Formation seals; 3) the Goose Fiord Formation below Eids Formation or Vendom Fiord Formation seals; and 4) Blue Fiord Formation traps below intraformational seals (as in the Markham Point area). Potential sources of sulphur are provided by thick and widespread evaporites of the Baumann Fiord Formation. Gypsum and anhydrite also occur locally in the lower Bay Fiord, Vendom Fiord, and Blue Fiord formations.

Particularly significant is the west side of the Bache Uplift between Irene Bay and Makinson Inlet within Vendom Fiord and Strathcona Fiord map areas (NTS 49D, E). The geological history of this area is similar to that of Boothia Uplift and there are indications of migrated hydrocarbons, barite, fluorite, hydrothermal(?) dolomite and disseminated galena and sphalerite within Silurian shelf edge carbonate of the Allen Bay Formation (Gibbins, 1985; Harrison et al., 1994; Thorsteinsson et al., 1994; de Freitas et al., 1995).

### SEDEX targets

Settings for sediment-hosted (sedimentary-exhalative or SEDEX) lead-zinc deposits are described by Eckstrand (1984) and Sangster (1981). In the Arctic Islands, prospective strata include basin facies shale and carbonate of the

graptolitic Ordovician to Devonian Cape Phillips Formation, chert and shale of the Cambrian to Silurian Hazen Formation, the Proterozoic Arctic Bay Formation of northern Baffin Island and the Proterozoic Piling Group of central Baffin Island. Nevertheless, exploration to date in these strata has not been encouraging (Gibbins, 1985). The most promising area for SEDEX-type deposits may exist within the Ordovician to Devonian Ibbett Bay Formation in the Canrobert Hills area of northwestern Melville Island. Epigenetic sphalerite-galena-fluorite veins are described by Harrison (1995) at one locality in the Lower Devonian upper member of this formation. Basin facies phosphorite and chert with hydrothermal(?) iron sulphide and aluminite have been documented at a second locality in the medial (Upper Ordovician-Lower Silurian) member (Harrison, 1995). These showings and the associated sedimentary rocks remain only superficially prospected.

### *Redbed copper targets*

Replacement copper sulphides occur in shelf carbonates at two localities on the Hvitland Peninsula of northwestern Ellesmere Island (Fig. 1): one in a bivalve coquina of the upper Paleozoic Nansen Formation; the other in grainstone of the Upper Permian Degerböls Formation (Mayr et al., 1995). Elsewhere, stratiform redbed sandstone-hosted replacement chalcopyrite has been documented within an outlier of the Canyon Fiord Formation (Bashkirian to Sakmarian) on northwestern Melville Island (Harrison, 1995). These showings provide some indication of the potential for redbed-related copper deposits (Eckstrand, 1984) in upper Paleozoic strata throughout the Arctic Islands. The Canyon Fiord Formation includes rift-related, proximal to distal, alluvial fan, tidal flat, and shallow marine deposits and restricted marine evaporites (locally) in a belt of syndepositional horsts and grabens which extend in outcrop from Melville Island to northernmost Ellesmere Island (Davies and Nassichuk, 1991). The Canyon Fiord Formation is also exposed on Grinnell Peninsula of western Devon Island, four areas on northern Bathurst Island and on the small islands north of Bathurst, including both north and south coastal areas of Helena Island (unpublished results from 1995 field work). Redbeds of the older but similar Borup Fiord Formation (Serpukhovian-Bashkirian) exposed only on northern Ellesmere Island should also be considered prospective.

Potential sources of sulphur in the upper Paleozoic succession are provided by the Otto Fiord, Antoinette and Mount Bayley evaporite formations. Sources for metallogenic brines could include either organic-rich lacustrine shale of the Emma Fiord Formation, basinal facies shale of the Hare Fiord, Trappers Cove and Van Hauen formations, or various lower Paleozoic units in sub-Carboniferous basement (Davies and Nassichuk, 1991; Beauchamp and Henderson, 1994).

## KIMBERLITES

Although this paper deals primarily with the exploration for sediment-hosted ore deposits in Arctic Canada, the following comments are prompted by the current interest in diamond exploration and the search for the related suite of igneous rocks (Fipke et al., 1995). While much of the exploration has concentrated on the Archean shield areas, especially the Slave Province of northwestern Northwest Territories, it is now known that the productive kimberlitic rocks in the Slave are mainly early Tertiary in age (Nassichuk and McIntyre, 1995). It follows from this that areas featuring thin pre-Tertiary sedimentary cover on Archean shield rocks should receive an equal level of reconnaissance exploration activity. An inlier of probable Archean granitoid rocks at Hadley Bay on northern Victoria Island (Thorsteinsson and Tozer, 1962; Campbell, 1981) implies continuity of the Slave Province to at least 72° N. Some elevated potential for kimberlitic rocks therefore, is indicated for all of eastern Victoria Island especially those areas east of the thick Proterozoic sedimentary basins of the Shaler Mountains and southern Victoria Island. Similar potential may exist within adjacent areas of thin Paleozoic sedimentary cover including King William, Prince of Wales, and eastern Somerset islands, Brodeur Peninsula on northwestern Baffin Island and large areas of Devon Island east of Grinnell Peninsula.

The existence of kimberlite pipes on northeastern Somerset Island is well known (Mitchell, 1976; Stewart, 1987) and continues to be investigated. Less well known is the petrology and petrochemistry of the Eocene Freeman's Cove volcanic-plutonic suite on southeastern Bathurst Island. Field work by Geological Survey of Canada staff in 1995 has shown that this igneous province is even more widespread than previously indicated by the surveys of Kerr (1974) and Mitchell and Platt (1984). The majority of known intrusives have not been studied and it is very likely that many igneous bodies within the province remain to be discovered. Nevertheless, most of the obvious dykes and plugs in the area are only about 2 to 40 m wide. The predominance of rift-related phonolite, nephelinite and alkali basalt (Mitchell and Platt, 1984) is also considered geochemically unfavourable. Less well understood are the petrological characteristics and petrochemistry of various intrusive breccia and agglomerate. These semicircular bodies range to several hundreds of metres in diameter and contain a wide range of sedimentary and volcanic clasts including xenocrysts of olivine and phlogopite. Apart from those breccia bodies located by Mitchell and Platt (1984), intrusive breccias have also been recently discovered at the following GPS co-ordinates: 1) latitude 75°06.63′N, longitude 98°07.30′W; 2) latitude 75°04.64′N, longitude 98°28.08′W; 3) latitude 75°17.11, longitude 98°23.01′W; 4) latitude 75°82.18′N, longitude 98°20.95′W; and 5) latitude 75°03.93, longitude 98°29.45′W.

Indian and Northern Affairs Canada, Parks Canada, and the Geological Survey of Canada. Critical review comments by R. Thorsteinsson have improved the final manuscript.

# REFERENCES

**Beauchamp, B. and Henderson, C.M.**
1994:    The Lower Permian Raanes, Great Bear Cape, and Trappers Cove formations: stratigraphy and conodont zonation; Bulletin of Canadian Petroleum Geology, v. 42, p. 565-600.

**Campbell, F.H.A.**
1981:    Stratigraphy and tectono-depositional relationships of the Proterozoic rocks of the Hadley Bay area, northern Victoria Island, District of Franklin; Geological Survey of Canada, Paper 81-1A, p. 15-22.

**Davies, G.R. and Nassichuk, W.W.**
1991:    Carboniferous to Permian geology of the Sverdrup Basin, Arctic Islands; Chapter 13 in Innuitian Orogen and Arctic Platform of Canada and Greenland, (ed.) H.P. Trettin; Geological Survey of Canada, Geology of Canada, no. 3., p. 343-367.

**de Freitas, T.A., Harrison, J.C., and Thorsteinsson, R.**
1993:    New field observations on the geology of Bathurst Island, Arctic Canada: Part A, stratigraphy and sedimentology of the Phanerozoic succession; in Current Research, Part B; Geological Survey of Canada, Paper 93-1B, p.1-10 .
1995:    Stratigraphic controls on potential hydrocarbon and mineral accumulations of central Ellesmere Island, Canadian Arctic Islands; in Proceedings of the Oil and Gas Forum '95, (ed.) J.S. Bell, T.D. Bird, T.L. Hillier, and P.L. Greener; Geological Survey of Canada, Open File 3058, p. 175-180.

**Eckstrand, O.R.**
1984:    Canadian mineral deposit types: a geological synopsis; Geological Survey of Canada, Economic Geology Report 36, 86 p.

**Fipke, C.E., Gurney, J.J., and Moore, R.O.**
1995:    Diamond exploration techniques emphasizing indicator mineral geochemistry and Canadian examples; Geological Survey of Canada, Bulletin 423, 86 p.

**Friske, P.W.B., McCurdy, M.W., Day, S.J., Gross, H., Balma, R., Lynch, J.J., and Durham, C.C.**
1994:    Regional lake sediment and water geochemical data, southeastern Yukon; Geological Survey of Canada, Open File 2860, 44 p.

**Gibbins, W.A.**
1985:    Arctic Islands region; Chapter 4 in Mineral Industry Report 1982-83, Northwest Territories, (ed.) J.A. Brophy; Department of Indian Affairs and Northern Development, Yellowknife, p. 95-155.

**Harrison, J.C.**
1995:    Melville Island's salt-based fold belt, Arctic Canada; Geological Survey of Canada, Bulletin 472, 331 p.

**Harrison, J.C., de Freitas, T.A., and Thorsteinsson, R.**
1993:    New field observations on the geology of Bathurst Island, Arctic Canada: Part B, structure and tectonic history; in Current research, Part B; Geological Survey of Canada, Paper 93-1B, p. 11-21.

**Harrison, J.C., Thorsteinsson, R., and de Freitas, T.A.**
1994:    Phanerozoic geology of Strathcona Fiord map area (NTS 49E and part of 39F), District of Franklin, Northwest Territories; Geological Survey of Canada, Open File 2881, scale 1:125 000.

**Kerr, J.W.**
1974:    Geology of the Bathurst Island group and Byam Martin Island, Arctic Canada (Operation Bathurst Island); Geological Survey of Canada, Memoir 378, 152 p.
1977:    Cornwallis lead-zinc district's Mississippi Valley-type deposits controlled by stratigraphy and tectonics; Canadian Journal of Earth Sciences, v. 14, no. 6, p. 1402-1426.

**McGregor, D.C. and Uyeno, T.T.**
1972:    Devonian spores and conodonts of Melville and Bathurst islands, District of Franklin; Geological Survey of Canada, Paper 71-13, 37 p.

**Mayr, U., Harrison, J.C., and Beauchamp, B.**
1995:    Geological map of Carboniferous and Permian units on Hvitland Peninsula and adjacent areas, northwestern Ellesmere Island, Arctic Canada; in Current Research 1995-B; Geological Survey of Canada, p. 1-7.

**Mitchell, R.H.**
1976:    Kimberlites of Somerset Island, District of Franklin; in Report of Activities, Part A; Geological Survey of Canada, Paper 76-1A, p. 501-502.

**Mitchell, R.H. and Platt, R.G.**
1984:    The Freeman's Cove volcanic suite: field relations, petrochemistry, and tectonic setting of nephelinite-basanite volcanism associated with rifting in the Canadian Arctic Archipelago; Canadian Journal of Earth Sciences, v. 21, p. 428-436.

**Nassichuk, W.W. and McIntyre, D.J.**
1995:    Cretaceous and Tertiary fossils discovered in kimberlites at Lac de Gras in the Slave Province, Northwest Territories; in Current Research 1995-B; Geological Survey of Canada, p. 109-114.

**Okulitch, A.V., Packard, J.J., and Zolnai, A.I.**
1991:    Late Silurian-Early Devonian deformation of the Boothia Uplift; in Chapter 12, Innuitian Orogen and Arctic Platform of Canada and Greenland, (ed.) H.P. Trettin; Geological Survey of Canada, Geology of Canada, no. 3., p. 302-307.

**Randell, R.N.**
1994:    Geology of the Polaris Zn-Pb Mississippi Valley-type deposit, Canadian Arctic Archipelago; PhD. thesis, University of Toronto, Toronto, Ontario, 600 p.

**Randell, R.N. and Anderson, G.M.**
1990:    Geology of the Polaris Zn-Pb Mississippi Valley-type deposit, Canadian Arctic Archipelago; in Current Research, Part D; Geological Survey of Canada, Paper 90-1D, p. 47-53.

**Sangster, D.F.**
1981:    Three potential sites for the occurrence of stratiform, shale-hosted lead-zinc deposits in the Canadian Arctic; in Current Research, Part A; Geological Survey of Canada, Paper 81-1A, p.1-8.

**Skibo, D.N., Harrison, J.C., Gentzis, T., and Goodarzi, F.**
1991:    Organic maturity/time-temperature models of the Ellesmerian (Paleozoic) Orogeny, Melville Island, Northwest Territories; in Current Research, Part E; Geological Survey of Canada, Paper 91-1E, p. 165-175.

**Stewart, W.D.**
1987:    Late Proterozoic to Early Tertiary stratigraphy of Somerset Island and northern Boothia Peninsula, District of Franklin, N.W.T.; Geological Survey of Canada, Paper 83-26, 78 p.

**Symons, D.T.A. and Sangster, D.F.**
1992:    Late Devonian paleomagnetic age for the Polaris Zn-Pb deposit, Canadian Arctic Archipelago; Canadian Journal of Earth Sciences, v. 29, p. 15-25.

**Thorsteinsson, R. and Tozer, E.T.**
1962:    Banks, Victoria, and Stefansson islands, Arctic Archipelago; Geological Survey of Canada, Memoir 330, 83 p.

**Thorsteinsson, R., Harrison, J.C., and de Freitas, T.A.**
1994:    Phanerozoic geology of Vendom Fiord map area (NTS 49D), District of Franklin, Northwest Territories; Geological Survey of Canada, Open File 2880, scale 1:125 000.

**Trettin, H.P., Mayr, U., Long, D.G.F., and Packard, J.J.**
1991:    Cambrian to Early Devonian basin development, sedimentation and volcanism, Arctic Islands; Chapter 8 in Innuitian Orogen and Arctic Platform of Canada and Greenland, (ed.) H.P. Trettin; Geological Survey of Canada, Geology of Canada, no. 3, p. 165-238.

# AUTHOR INDEX

## NOTE TO CONTRIBUTORS

Submissions to the Discussion section of Current Research are welcome from both the staff of the Geological Survey of Canada and from the public. Discussions are limited to 6 double-spaced typewritten pages (about 1500 words) and are subject to review by the Chief Scientific Editor. Discussions are restricted to the scientific content of Geological Survey reports. General discussions concerning sector or government policy will not be accepted. All manuscripts must be computer word-processed on an IBM compatible system and must be submitted with a diskette using WordPerfect. Illustrations will be accepted only if, in the opinion of the editor, they are considered essential. In any case no redrafting will be undertaken and reproducible copy must accompany the original submissions. Discussion is limited to recent reports (not more than 2 years old) and may be in either English or French. Every effort is made to include both Discussion and Reply in the same issue. Current Research is published in January and July. Submissions should be sent to the Chief Scientific Editor, Geological Survey of Canada, 601 Booth Street, Ottawa K1A 0E8 Canada.

## AVIS AUX AUTEURS D'ARTICLES

Nous encourageons tant le personnel de la Commission géologique que le grand public à nous faire parvenir des articles destinés à la section discussion de la publication Recherches en cours. Le texte doit comprendre au plus six pages dactylographiées à double interligne (environ 1500 mots), texte qui peut faire l'objet d'un réexamen par le rédacteur scientifique en chef. Les discussions doivent se limiter au contenu scientifique des rapports de la Commission géologique. Les discussions générales sur le Secteur ou les politiques gouvernementales ne seront pas acceptées. Le texte doit être soumis à un traitement de texte informatisé par un système IBM compatible et enregistré sur disquette WordPerfect. Les illustrations ne seront acceptées que dans la mesure où, selon l'opinion du rédacteur, elles seront considérées comme essentielles. Aucune retouche ne sera faite au texte et dans tous les cas, une copie qui puisse être reproduite doit accompagner le texte original. Les discussions en français ou en anglais doivent se limiter aux rapports récents (au plus de 2 ans). On s'efforcera de faire coïncider les articles destinés aux rubriques discussions et réponses dans le même numéro. La publication Recherches en cours paraît en janvier et en juillet. Les articles doivent être envoyés au rédacteur en chef scientifique, Commission géologique du Canada, 601, rue Booth, Ottawa K1A 0E8 Canada.

Geological Survey of Canada Current Research, is released twice a year, in January and July. The four parts published in January 1996 (Current Research 1996-A to D) are listed below and can be purchased separately.

Recherches en cours, une publication de la Commission géologique du Canada, est publiée deux fois par année, en janvier et en juillet. Les quatre parties publiées en janvier 1996 (Recherches en cours 1996-A à D) sont énumérées ci-dessous et sont vendues séparément.

Part A:     Cordillera and Pacific Margin
Partie A :   Cordillère et marge du Pacifique

Part B:     Interior Plains and Arctic Canada
Partie B :   Plaines intérieures et région arctique du Canada

Part C:     Canadian Shield
Partie C :   Bouclier canadien

Part D:     Eastern Canada and national and general programs
Partie D :   Est du Canada et programmes nationaux et généraux